

## **Syncopation: Unifying Music Theory and Perception**

Song, Chunyang

The copyright of this thesis rests with the author and no quotation from it or information derived from it may be published without the prior written consent of the author

For additional information about this publication click this link.

<http://qmro.qmul.ac.uk/xmlui/handle/123456789/15132>

Information about this research object was correct at the time of download; we occasionally make corrections to records, please therefore check the published record when citing. For more information contact [scholarlycommunications@qmul.ac.uk](mailto:scholarlycommunications@qmul.ac.uk)

# **Syncopation: Unifying Music Theory and Perception**

Thesis submitted in partial fulfilment  
of the requirements of the University of London  
for the Degree of Doctor of Philosophy

**Chunyang Song**

June 2014

Department of Electronic Engineering,  
Queen Mary, University of London

I, Chunyang Song, confirm that the research included within this thesis is my own work or that where it has been carried out in collaboration with, or supported by others, that this is duly acknowledged below and my contribution indicated. Previously published material is also acknowledged below.

I attest that I have exercised reasonable care to ensure that the work is original, and does not to the best of my knowledge break any UK law, infringe any third party's copyright or other Intellectual Property Right, or contain any confidential material.

I accept that the College has the right to use plagiarism detection software to check the electronic version of the thesis.

I confirm that this thesis has not been previously submitted for the award of a degree by this or any other university.

The copyright of this thesis rests with the author and no quotation from it or information derived from it may be published without the prior written consent of the author.

Signature:

Date:

Details of collaboration and publications:

- Song C, Simpson AJR, Harte CA, Pearce MT, Sandler MB (2013) *Syncopation and the Score*. PLoS ONE 8(9): e74692.  
This work is covered in Chapter 4.
- Song C, Harte CA, Simpson AJR, Sandler MB, *Syncopation models: do they measure up?* Submitted to Music Perception in May, 2014.  
This work is covered in Chapters 3 and 5.

# Abstract

Syncopation is a fundamental feature of rhythm in music. However, the relationship between theory and perception is currently not well understood. This thesis is concerned with characterising this relationship and identifying areas where the theory is incomplete. We start with a review of relevant musicological background and theory. Next, we use psychophysical data to characterise the perception of syncopation for simple rhythms. We then analyse the predictions of current theory using this data and identify strengths and weaknesses in the theory. We then introduce further psychophysical data which characterises the perception of syncopation for simple rhythms at different tempi. This leads to revised theory and a new model of syncopation that is tempo-dependent.

# Acknowledgements

I would like to thank my supervisors Mark Sandler and Marcus Pearce for their guidance and support. I would also like to acknowledge the Joint Programme College Scholarship that funded my studies and especially Yue Chen for extending the funding to support my writing up.

Special thanks to Mark Plumbley for always making time to talk and for helping me several times with my travel to conferences and research visits. Many thanks to Tanya Gold for proof-reading my thesis and to Michael Tautschnig for advice on mathematical notation.

I would like to give my biggest thanks to Chris Harte, not only for always making the time to discuss research with me and giving me good advice, but also for being my greatest support and mentor. Without his enduring encouragement I could not possibly have the confidence and persistence to drive myself to the finish line.

I also owe a great deal of thanks to Andy Simpson, the sweetest unanticipated surprise along my Ph.D journey, for pointing me in the right direction and helping me find so much insight and passion in my work. His help really put a rocket under my research in my final year and for this I will always be very grateful.

I must also thank all the people who participated in my listening tests (in alphabetical order): Alice, Alo, Andy, Bogdan, Boris, Brecht, Chris, Dan, Dimitrios, Daniele, Elio, Emmanouil, George, Han, Holger, Jordan, Katerina, Magda, Mike, Steve and Sonia.

Many thanks also to my friends in Georgia Tech who helped me so much during my three-month research visit: Qingfen, Jiechao, Weibin, Ruofeng, Aron and Mason; and Yi for taking care of me during my trip to SMPC in Toronto.

Special thanks to my dear “104 gang”, especially Siying, Tian and Yading for their huge support and great company. I will always remember

the times when we worked together till late, and when we said we would work hard but ended up nut-chatting the whole night. I appreciate that you guys tried all sorts to help me with writing up, such as hiding my phone and working in shift to watch over me. Thanks particularly to Sonia for being my writing-up buddy and cheering every step of my progress with me.

Finally, I am very grateful to my parents and entire family members in China, and also my family in UK: grandma, grandpa, ma, pa, and all my awesome Leavening branch, for their everlasting support and love.

# Contents

<b>Abstract</b> . . . . .	<b>3</b>
<b>1 Introduction</b> . . . . .	<b>17</b>
1.1 Motivations . . . . .	18
1.2 Methodology . . . . .	21
1.3 Goals and objectives . . . . .	23
1.4 Thesis outline . . . . .	24
<b>2 Syncopation in music theory</b> . . . . .	<b>27</b>
2.1 Fundamentals of rhythm . . . . .	27
2.1.1 Rhythm . . . . .	27
2.1.2 Beat . . . . .	31
2.1.3 Meter . . . . .	31
2.1.4 Tempo . . . . .	35
2.2 Definitions for syncopation . . . . .	37
2.2.1 Violation of the regular beat salience . . . . .	37
2.2.2 Off-beat . . . . .	38
2.2.3 Transformation of meter . . . . .	40
2.2.4 Polyrythm . . . . .	41
2.3 Overview of syncopation models . . . . .	42
2.3.1 Categories of models . . . . .	43
2.3.2 Capabilities of models . . . . .	44
2.4 Summary . . . . .	45
<b>3 Review of syncopation models</b> . . . . .	<b>46</b>
3.1 Background . . . . .	46
3.1.1 Sequences . . . . .	46
3.1.2 Rhythm in continuous time . . . . .	48
3.1.3 Discrete time representation . . . . .	49
3.1.4 Metrical hierarchy . . . . .	52

3.2	Syncopation models . . . . .	55
3.2.1	Longuet-Higgins and Lee 1984 (LHL) . . . . .	55
3.2.2	Pressing 1997 (PRS) . . . . .	58
3.2.3	Toussaint 2002 ‘Metric Complexity’ (TMC) . . . . .	61
3.2.4	Sioros and Guedes 2011 (SG) . . . . .	62
3.2.5	Keith 1991 (KTH) . . . . .	65
3.2.6	Toussaint 2005 ‘Off-Beatness’ (TOB) . . . . .	66
3.2.7	Gómez 2005 ‘Weighted Note-to-Beat Distance’ (WNBD) . . . . .	67
3.3	Summary . . . . .	68
<b>4</b>	<b>Syncopation and the score . . . . .</b>	<b>70</b>
4.1	Experiment 1: Score . . . . .	70
4.1.1	Participants . . . . .	71
4.1.2	Stimuli . . . . .	71
4.1.3	Procedure . . . . .	74
4.2	Results . . . . .	75
4.2.1	6/8 is more syncopated than 4/4 . . . . .	75
4.2.2	Polyrhythms are more syncopated . . . . .	75
4.2.3	Missing down-beats result in syncopation . . . . .	77
4.2.4	Switching component order affects syncopation . . . . .	78
4.3	Discussion . . . . .	81
4.3.1	4/4 versus 6/8 . . . . .	81
4.3.2	Missing down-beats . . . . .	82
4.3.3	Possible interpretation of 6/8 as 3/4 . . . . .	83
4.3.4	Polyrhythms . . . . .	84
4.4	Summary . . . . .	85
<b>5</b>	<b>Evaluation of the models . . . . .</b>	<b>86</b>
5.1	Dataset 1 . . . . .	86
5.2	Evaluation results . . . . .	89
5.3	Discussion: strengths and weaknesses of models . . . . .	90
5.3.1	Hierarchical models . . . . .	90
5.3.2	Off-beat models . . . . .	95
5.3.3	Classification models . . . . .	97
5.3.4	General discussion . . . . .	98
5.4	Summary . . . . .	98



<b>6</b>	<b>Tempo affects syncopation</b>	<b>100</b>
6.1	Background	101
6.1.1	Tactus perception and tempo	101
6.1.2	Tempo limits of tactus and meter perception	102
6.1.3	Dynamic meter perception influenced by tempo	103
6.1.4	Hypotheses for tempo effects on syncopation	106
6.2	Experiment 2: Tempo	108
6.2.1	Participants	108
6.2.2	Stimuli	108
6.2.3	Procedure	111
6.3	Results	111
6.3.1	Syncopation is a function of tempo	111
6.3.2	Quadratic function	113
6.3.3	Polyrhythms are more resistant to tempo changes	114
6.3.4	No evidence of an effect of time-signature	117
6.3.5	Individual rhythms show different sensitivity to tempo	120
6.4	Discussion	126
6.4.1	The tempo effect on syncopation parallels the tempo effect on tactus	127
6.4.2	Adjustable tactus level and syncopation	128
6.4.3	Peak tempo of syncopation is lagged to that of tactus	129
6.4.4	Polyrhythms versus monorhythms	129
6.4.5	Possible meter induction at extremely fast tempi	130
6.4.6	Time-signature	130
6.5	Summary	132
<b>7</b>	<b>Improving syncopation modelling</b>	<b>134</b>
7.1	Best-Single Combined models (BSC)	134
7.1.1	The three-way BSC model (BSC <sub>3</sub> )	135
7.1.2	The two-way BSC model (BSC <sub>2</sub> )	135
7.2	Weighted-Multiple Combined model (WMC)	136
7.3	Validation of combined models for Dataset 1	138
7.4	Tempo-dependent models	140
7.4.1	General design	140
7.4.2	Tempo-dependent combined models	140
7.5	Validation of tempo-dependent combined models for Dataset 2	142

7.6	Discussion . . . . .	145
7.7	Summary . . . . .	146
<b>8</b>	<b>Conclusions . . . . .</b>	<b>147</b>
8.1	Thesis contributions . . . . .	147
8.2	General discussion . . . . .	148
8.3	Future work . . . . .	150
	<b>Bibliography . . . . .</b>	<b>154</b>

# List of Figures

1.1	Tested and untested relationships between theory and perception. . . . .	20
1.2	Transformation: from the music score to perception. . . . .	22
1.3	Thesis outline. . . . .	25
2.1	The equation of note-values. . . . .	29
2.2	Examples of triplets. . . . .	29
2.3	Examples of tied notes. . . . .	30
2.4	Examples of dotted notes. . . . .	30
2.5	Examples of beat groupings and the resulting beat salience. . . . .	32
2.6	Duple versus triple, simple versus compound. . . . .	33
2.7	Time-signatures and their hierarchical structures, patterns of beat groupings and beat subdivisions. . . . .	34
2.8	Metrical hierarchies projected by rhythm-patterns in a given time-signature. . . . .	36
2.9	Example of tempo indication in the beginning of the musical score. . . . .	36
2.10	Examples of syncopation aroused from violation of regular beat salience. . . . .	38
2.11	Examples of off-beat notes that followed by a rest or a tied-note on the next beat. . . . .	39
2.12	Syncopation types as defined in [Kei91]. . . . .	40
2.13	Examples of transformation of meter. . . . .	40
2.14	Examples of polyrhythms and the resulting competing metrical hierarchies. . . . .	41
2.15	Models used for predicting syncopation, which are categorised by theoretical basis and main methodology. . . . .	43
3.1	An example note sequence. . . . .	48
3.2	Example rhythm-patterns with their minimum-length time-span and velocity sequences. . . . .	50

3.3	Metrical hierarchies for different time-signatures. . . . .	54
3.4	Tree decomposition of the Son clave rhythm for the LHL syncopation measure. . . . .	57
3.5	Example calculation of the Pressing syncopation measure for the Son clave rhythm-pattern. . . . .	61
3.6	Sioros and Guedes syncopation scores and potentials for the Son clave rhythm. . . . .	64
3.7	Geometric representation of $B$ for the three rhythm patterns in Figure 3.2. . . . .	66
3.8	Illustration of the relationship between note $y_n$ and the beats from $\mu_i$ to $\mu_i + 2$ . . . . .	68
4.1	Construction of stimuli. . . . .	72
4.2	Group mean syncopation ratings for rhythm-patterns. . . . .	76
4.3	Categorical analysis. . . . .	77
4.4	Syncopation by rhythm-component. . . . .	78
4.5	Pair-wise changes in ratings when rhythm-component order was switched. . . . .	80
5.1	The example score of rhythm-pattern BCBC. . . . .	88
5.2	Group mean syncopation ratings for the extended stimuli. . . . .	88
5.3	The ranked mean ratings of entire dataset. . . . .	89
5.4	Comparisons of model predictions for 4/4 monorhythms. . . . .	92
5.5	Comparisons of model predictions for 6/8 monorhythms. . . . .	93
5.6	Comparisons of model predictions for polyrhythms. . . . .	94
5.7	Examples of rhythms with syncopation that cannot be captured by the LHL model. . . . .	94
5.8	Examples of non-syncopated rhythms that are measured as syncopated by off-beat models. . . . .	95
5.9	A specific limitation of the WNBD model. . . . .	96
6.1	Histogram of beat-tapping rates. . . . .	102
6.2	Dynamic adjustment of tactus level with change in tempo. . . . .	105
6.3	Rhythmic scores for Experiment 2. . . . .	110
6.4	Grand mean syncopation ratings as a function of tempo. . . . .	112
6.5	Peak and width of a quadratic curve. . . . .	113
6.6	Tempo effects between rhythm-categories. . . . .	115

6.7	Unpaired-subject comparisons of peaks and widths between rhythm-categories. . . . .	116
6.8	Paired-subject comparisons of peaks and widths between rhythm-categories. . . . .	117
6.9	Tempo effects between time-signatures. . . . .	118
6.10	Unpaired-subject comparisons of peaks and widths between time-signatures. . . . .	119
6.11	Paired-subject comparisons of peaks and widths between time-signatures. . . . .	119
6.12	Tempo effects on monorhythms between time-signatures. . . . .	121
6.13	Unpaired-subject comparisons of peaks and widths between time-signatures for monorhythms. . . . .	121
6.14	Paired-subject comparisons of peaks and widths between time-signatures for monorhythms. . . . .	122
6.15	Tempo effects between rhythm-patterns. . . . .	123
6.16	Unpaired-subject comparisons of peaks and widths between rhythm-stimuli. . . . .	124
6.17	Paired-subject comparisons of peaks and widths between pairs of rhythm-stimuli. . . . .	125
6.18	Hypothetical explanation for the effect of time-signature in Experiment 1. . . . .	131
7.1	Predictions of combined models for Dataset 1. . . . .	139
7.2	A tempo-dependent model. . . . .	141
7.3	Flow chart of the overall algorithm for tempo-dependent combined models. . . . .	142
7.4	Separate tempo scaling functions for monorhythms and polyrhythms.	143
7.5	Predictions of tempo-dependent combined models for Dataset 2. . . . .	144

# List of Tables

2.1	Basic note-values and the corresponding music notations. The note-values are relative to a whole-note. . . . .	28
2.2	Comparisons of the properties of syncopation models. Basis: H - Hierarchical-based, C - Classification, O - Off-beat-based, A - Autocorrelation-based. . . . .	44
6.1	Tempo (QPM) in relation to quarter-note time interval (ms).	109
7.1	Linear regression coefficients for the BSC model. . . . .	135
7.2	Linear regression coefficients for the BSC <sub>2</sub> model. . . . .	136
7.3	Coefficients of the full models of multiple linear regression.	136
7.4	Coefficients of the reduced models of multiple linear regression. . . . .	138

## List of Abbreviations

BPM	Beats Per Minute
QPM	Quarter-note Per Minute
TPM	Tones-Per-Minute
SSL	Short-short-long
s	seconds
ms	milliseconds
LHL	Longuet-Higgins and Lee's model
PRS	Pressing's model
TMC	Toussaint's Metric Complexity model
SG	Sioros and Guedes's model
TOB	Toussaint's Off-beatness model
WNBD	Weighted Note-to-Beat Distance model
KTH	Keith model
KSA	Keller and Schubert's Autocorrelation model
BSC	Best-Single Combined model
WMC	Weighted-Multiple Combined model
P&E	Povel and Essens

# Glossary of Symbols

$\in$	Set notation ‘in’ i.e. denotes membership of a set or sequence e.g. $x \in X$ , $x$ is a member of $X$ .
$\forall$	Set notation ‘For all...’
$\exists$	Set notation ‘There exists...’
$\emptyset$	The empty sequence.
$\langle \cdot \rangle$	Contents of angle brackets form a sequence.
$*$	Concatenation operator for two sequences.
$\odot$	Iterative concatenation operator for sequences.
$ \cdot $	Cardinality (length) of a sequence.
$\lceil \cdot \rceil$	Ceiling function (round up to nearest integer).
$t_{\text{org}}$	Time origin for a rhythm pattern.
$t_{\text{end}}$	End time of a rhythm pattern.
$t_{\text{span}}$	Total duration for a rhythm pattern time-span.
$t_s$	Onset time of a note with respect to $t_{\text{org}}$ .
$t_d$	Duration of note.
$\nu$	Dynamic or <i>velocity</i> of a note.
$Y$	A sequence of notes $y_n$ .
$T$	Time-span sequence, time points $t_m$
$V$	A sequence of normalised velocity values $v_m$ .
$B$	Binary sequence (each element $b_m = \lceil v_m \rceil$ )
$X$	A logic <i>don't care</i> term; considered equal to both 1 and 0 when comparing binary values.
$L$	The metric level (range 0 to $L_{\text{max}}$ ).
$W$	The sequence of metrical weights $w_L$ .
$\Lambda$	The sequence of subdivisions $\lambda_L$ .
$H_L$	The sequence of metrical weights $h_m$ for metrical level $L$ that corresponds to the time points in $T$ .
$\Psi$	The sequence of terminal nodes $\psi_i$ .



$S_M(Y)$	Syncopation prediction for $Y$ for model $M$
$\eta$	Node type, i.e. note $N$ or rest $R$ .
$\kappa$	Function used to calculate the sequence of terminal nodes in the LHL model.
$g$	Function to classify prototypes in the PRS model.
$q$	Normalisation function in the PRS model.
$f$	Recursive accumulation function in the PRS model.
$\varphi$	Metricity of a rhythm-pattern in the TMC model.
$\vartheta$	Function that calculates difference level factor for the SG model.
$\beta$	Weighting factor used in function $\vartheta$ .
$\rho, \varrho$	Functions that calculate the next and previous indices of notes in the SG model.
$u$	Function that calculates the average of the difference between a note and its neighbours in the SG model.
$\gamma$	Weighting factor used in function $u$ .
$s_m$	Syncopation value of a note in the SG model.
$\phi_m$	Syncopation potential in the SG model.
$c_n$	The highest power of two no greater than a note's duration in the KTH model.
$\sigma, \epsilon$	Functions that classify whether a note starts and/or ends off-beat in the KTH model.
$k_n$	Syncopation value for a note $y_n$ in KTH model.
$\varsigma_m$	Off-beatness of a note in the TOB model.
$\mathcal{W}(y_n)$	WNBD measure for a note $y_n$ .
$d(\cdot, \cdot)$	Distance function.
$\mathcal{T}(y_n)$	Distance of a note $y_n$ to its closest beat.
$\mu_i$	A beat position in the WNBD model.
$\Upsilon$	Tempo (QPM).
$M \sim T$	Tempo-dependent version of model $M$ .
$S_{M \sim T}(Y, \Upsilon)$	Syncopation prediction for $Y$ played at tempo $\Upsilon$ for model $M \sim T$ .
$F$	Tempo-dependent scaling function.

# Chapter 1

## Introduction

Music is a temporal phenomenon; it unfolds over time. Rhythm describes how musical events are structured in time. A key feature of musical rhythm is regularity; periodicities in rhythms are perceived by human listeners as beats. We naturally infer structure, known as meter, from these underlying periodicities. Meter allows us to anticipate future events and to engage with music, for example by dancing in time to the music. Deliberate violations of meter in music can provide a curious, often disorienting sensation known as syncopation, and can occur with even a single, carefully placed note in an otherwise regular stream. Hence, syncopation provides a channel through which we may investigate the broader nature of meter.

Syncopation is widely used in music and is even a central feature of many music styles and cultures such as Jazz, Cuban Son and African drumming. Various compositional techniques have been established to achieve an effect of syncopation, but essentially they all undermine the perception of meter by adding conflicting components onto the rhythm surface. Syncopation can enhance the complexity and richness of rhythm; it subtly teases our expectations and provides a mechanism to counter the orderly nature of music. In this thesis, we explore the factors that give rise to the perception of syncopation and test how well the established theories of syncopation can explain our observations.

## 1.1 Motivations

### The need for syncopation measurement

Syncopation is one of the fundamental rhythmic features in music and a crucial aspect of character in many music styles and cultures. Having a more complete understanding of syncopation and comprehensive models to capture syncopation perception allows us to better understand the broad aspects of music perception.

For example, the link between syncopation and beat or meter perception has been widely investigated [HO81, SK01, KR01, TS03, FR07]. Multiple approaches to modelling the way that meter is perceived and encoded from syncopated rhythm-context have been proposed [LHL84, PE85, Par94, Eck01, VL11]. It has been found that syncopation has an effect on rhythm identification [Moe12] and rhythm memorisation [FR07].

In addition to rhythm perception, the phenomenon of syncopation is also linked to more elusive and subjective feelings and responses to music. For example, one of the recent topics of debate explores whether syncopation facilitates or inhibits *groove*. Groove refers to the sensation of wanting to move some part of the body to music [Mad06]. Some evidence has suggested that adding syncopation led to stronger groove [MSD<sup>+</sup>13], whereas some evidence has suggested their relationship is inverted-U-shaped where the sensation of groove and pleasure is optimised at medium syncopation, but decreased towards the extreme ends of degree of syncopation [WCW<sup>+</sup>14]. More than that, syncopation seems to affect human emotion [KS11, Hur06] and some physiological responses, e.g. increased heart rate [Slo91].

With the development of brain sciences in recent years, there has been a growing interest in collecting neuroscientific evidence from both humans and animals when listening to music. One particular focus is in what kinds of neurophysiological responses are elicited by syncopation and how they correlate with the sensations that syncopation arouses [MFD<sup>+</sup>01, LH09, HLHW09, TK03, VOP<sup>+</sup>09]. For example, some evidence suggest that syncopation elicits brain activity associated with violating sensory expectations, and this effect is found from both adult listeners and newborn

infants which support the view that beat perception is innate [WHL<sup>+</sup>09, HLHW09]. There is also evidence suggesting the link between meter interpretation in a polymetric context and the activation of language areas [VWOR11]. These studies complement our understanding of the brain mechanisms and functions in processing rhythm.

In the field of music information retrieval, syncopation has been considered a contributory feature in the computation of rhythm similarities between rhythm-patterns [Smi10, PRBH14, PT11]. Psychological evidence has supported the relationship between syncopation and the perceptual judgement of rhythmic similarities [Lad09, Str06, SH93]. Some evidence has suggested that by involving perceptual features, instead of merely building upon lower-level rhythmic features, the computation of rhythm similarity improves the performance of rhythm classification tasks [GDPW04]. Thus a measure that captures perceptual syncopation will directly benefit the development of algorithms for estimating rhythm similarity and general rhythmic description.

In brief, syncopation interacts with a range of musical concepts and has broad effects on music perception and cognition. Investigations on these effects of syncopation need quantitative measures of syncopation that can correctly reflect human perception. This provides the major motivation for us to closely examine the existing theory and models for syncopation.

### **Lack of direct investigation on syncopation perception**

It is clear that there is a need for a reliable, validated measure of syncopation. However, current approaches have either been based on indirect perceptual measures or theoretical models that have not been formally tested. As Figure 1.1 shows, studies that investigate the link between syncopation and broad music perception and cognition rely on measures of rhythm-complexity or predictions of syncopation by theoretical models, i.e. links A - C in the figure.

For example, Fitch and Rosenfeld [FR07] controlled the degree of syncopation quantified by Longuet-Higgins and Lee's syncopation model [LHL84]

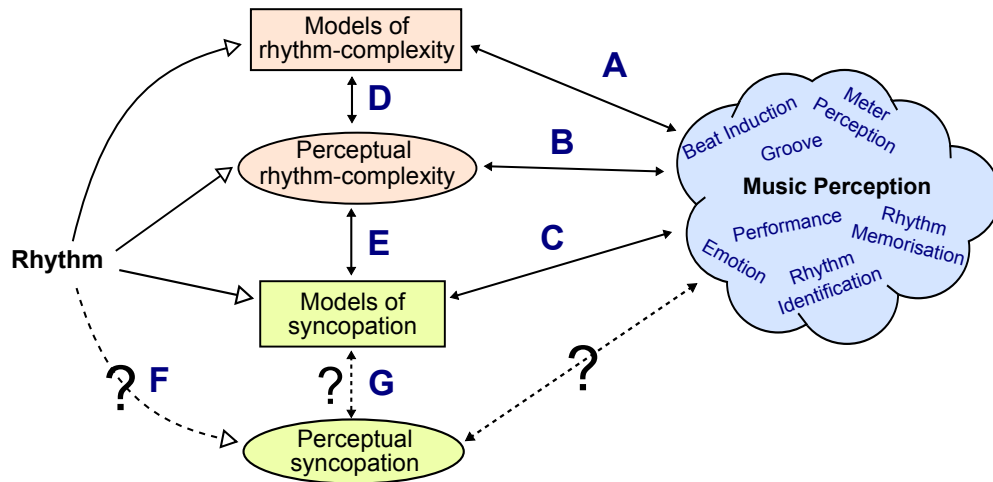


Figure 1.1: Tested and untested relationships between theory and perception. Music perception studies have been utilising indirect measures of syncopation such as rhythm-complexity, or theoretical models of rhythm-complexity and syncopation (indicated by links A - C). These models have only been tested against perceptual datasets of rhythm-complexity (links D and E). However, the relationship between syncopation perception and rhythm (link F) is still unknown. A perceptual dataset for syncopation would be valuable for the evaluation of theoretical models of syncopation and the linkage to music perception and cognition in general (link G).

(which will be discussed in detail in Sections 2.3 and 3.2.1) to test beat induction, rhythm reproduction and rhythm memorisation. Likewise, Witek et al. [WCW<sup>+</sup>14] tested the relationship between groove and predictions of syncopation generated by Longuet-Higgins and Lee’s model. Similarly, Keller and Schubert designed a model which they then used in experiments to test the effect of syncopation on emotional responses [KS11].

There has been no attempt yet to directly measure syncopation perception (Figure 1.1, link F). However, such an investigation is required in order to allow a formal and systematic evaluation of the theory and models (link G). It is therefore questionable whether current music theory or models can accurately predict the strength of syncopation as how human listeners perceive it.

The concept of syncopation has often been fused with rhythm-complexity (Figure 1.1, Links D and E) [Tou02, Thu08, SG11, Pre97, WCW<sup>+</sup>14], resulting in ambiguities in the modelling of both percepts. As illustrated

in Figure 1.1, syncopation models have previously only been evaluated against datasets of rhythm-complexity [GTT07, Thu08, SH07], such as the perceptual dataset collected by Shmulevich and Povel [SP00] that comprises perceptual ratings of rhythm-complexity for 35 rhythm-patterns.

In summary, diverse theories and modelling approaches for syncopation have been heavily used in studies in multiple disciplines, yet, they have not been proven to be entirely reliable so far. A direct investigation of syncopation perception is therefore needed to test how well the theories and models capture perception, and to clarify the confusion between syncopation and rhythm-complexity.

## 1.2 Methodology

To address the missing information on direct syncopation, we will use approaches from psychophysics to collect human data on syncopation perception. Psychophysics applies psychological methods to quantify the relationship between perception and stimulus [Ste75]. A fundamental postulate of psychophysics is that perception should have underlying objective, physical correlates which may be quantified as features of the stimulus. For example, intensity is the objective correlate of loudness (i.e. perceived intensity).

The music score is a symbolic encoding that describes the set of events comprising a piece of music. For the purposes of this thesis, we will deal only with scores that describe Western common practice art music. Before these notated events can be perceived as music by a listener, they must be rendered (e.g. by the performer) as an acoustic pressure signal that varies over time (Figure 1.2). The rendering process mediates the transformation between the score and the perception. By manipulating the score, we can find out what features of the score correspond to features of perception.

### Main method and rationale

To directly investigate the perception of syncopation, we asked musicians to provide ratings on a limited scale to indicate the perceived strength

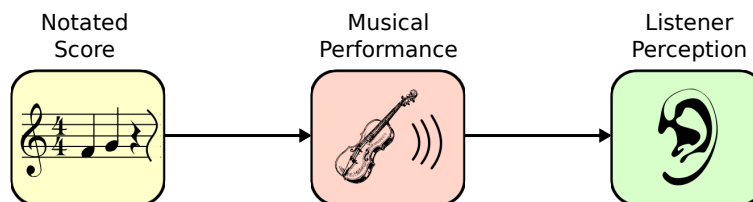


Figure 1.2: Transformation: from the music score to perception. Before the notes on the score can be perceived as music by the listener, the score must be rendered (e.g. by a performer) as an acoustic (pressure) signal which varies over time.

of syncopation elicited by designed rhythm-stimuli. This method is suitable for the purpose because the most direct method to identify human perception is by letting them describe what they have perceived (assuming it can be explicitly and accurately described). Other methods, such as measuring objective biophysical responses and behaviour, effectively separate sensation and verbalisation and are therefore viewed as *indirect methods* [BZ06].

In addition, we believe that scaled rating is the optimal approach to collect subjective measures for our task. It is easy to implement and provides well-specified and unified descriptors [BZ06]. It also allows quantifiable subjective descriptions, which suits the concept of syncopation. In contrast to other methods, such as quantifying the difference in syncopation between a pair of stimuli or ranking multiple stimuli by the degree of syncopation, scaled rating does not require comparisons between stimuli thus is simple for the listeners.

In contrast, previous studies adopted indirect methods that focus on the objective measures, such as the difficulty in rhythm reproduction [PE85, FR07], quality of rhythm recognition [FR07, Moe12], the consistency of beat synchronisation [PE85, FR07] and brain activities [HLHW09, LH09]. These methods are based on the assumed relationship between perceived syncopation and the indirect measure, but this assumption has not been verified yet.

## Experiment subjects

We selected musicians for our experiments. All of the participants had several years of music training and experience, and thus they all understand syncopation and felt confident about their perceptual ratings. Non-musicians may not have been suitable for the task because there is no guarantee that they are familiar with the concept of syncopation in the same way as musicians would be.

Another reason to choose musicians is that some evidence suggest non-musicians have a weaker ability to synchronise to the beats and organise metrical structure than musicians [CPZ08, RD07, PK90]. Hence they may be less sensitive to the perception of syncopation, because the sensation of syncopation is built upon a firm grip on mental representations of meter.

## General design of experiments

We conducted two experiments that involved collecting musicians' ratings on perceived syncopation. Experiment 1 focused on manipulation of the rhythm-score as the objective correlate of perceived syncopation. In particular, we focused on testing the effect of location and distribution of notes on syncopation. We used a monophonic, unaccented, and percussive sound in creating rhythm-stimuli, in order to rule out the potential confounding effects, such as dynamic, melodic and duration factors. A metronome was played simultaneously with rhythm-patterns to experimentally control the metrical interpretation [PE85]. Method and results will be discussed in more detail in Chapter 4.

In Experiment 2, we selected a set of syncopated rhythm-patterns from Experiment 1. These were played at different *tempi* (Section 2.1.4) to test the relationship between tempo and perceived syncopation. The method and results of this experiment will be discussed in Chapter 6.

In summary, we asked musicians to rate the degree of syncopation they perceived in response to a rendering of each rhythm-stimulus. This serves to directly investigate the perception of syncopation in a way that has not been achieved by previous approaches. It is worth mentioning here that a track of metronome is added into the rhythm-patterns to provide explicit



cues to the meter. This is a unique feature that differentiates our work from previous approaches [PE85, SP00, FR07].

### 1.3 Goals and objectives

In this thesis, we address the following two main research questions:

- Research Question 1: What are the factors in rhythm influencing on perceived syncopation?
- Research Question 2: To what extent do current theoretical models of syncopation and music theory in general capture the perception, and what elements are missing?

To find answers to these questions, our main objectives are:

- To conduct experiments that investigate the contributing factors to perceived syncopation. In particular, the rhythmic attributes that we target are: rhythm-components (i.e. micro units to form rhythm-patterns), the combinations of different rhythm-components, time-signature<sup>1</sup> and tempo.
- To review and clarify the existing theory and models of syncopation.
- To evaluate syncopation models against human perceptual data.

### 1.4 Thesis outline

The main purpose of this thesis is to provide a step towards unifying music theory with music perception in terms of syncopation. Figure 1.3 shows the overall arrangement of contents and the connections between chapters. Chapters 2 and 3 explore the theory and models of syncopation. Chapter 4 presents Experiment 1, which enables the formal evaluation of the models in Chapter 5. Chapter 6 presents Experiment 2, which, combined with findings in covered in Chapter 5, leads to the improvement

---

<sup>1</sup>In this thesis, we limit the tested time-signatures to isochronous 4/4 and 6/8 (see Section 2.1.3 for more details), and exclude non-isochronous (NI) meters [Lon04]

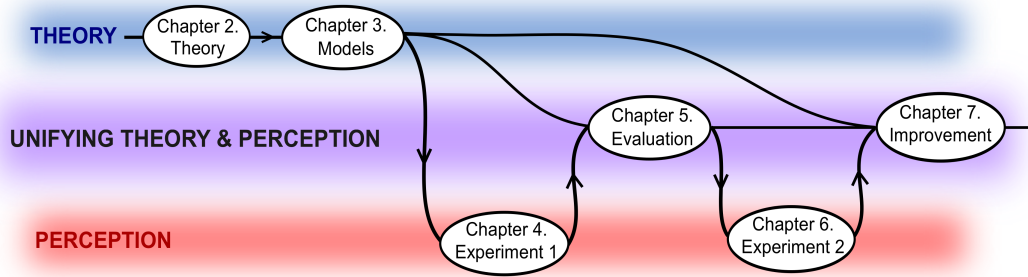


Figure 1.3: Thesis outline.

of the modelling of syncopation in Chapter 7. The following sections provide a brief overview of the individual chapters.

## Chapter 2

In this chapter, we start with presenting fundamental rhythmic concepts that are directly relevant to the understanding of this thesis, including rhythm, beat, meter and tempo. We then review how syncopation is explained in music theory and summarise the main streams of thought in the literature. Finally, we give a brief overview of the existing syncopation models and categorise them by theoretical basis.

## Chapter 3

This chapter provides a comprehensive review of syncopation models and introduces a consolidated mathematical notation that unifies the field. We first introduce some general mathematical terms and operations for representing rhythm and meter. We then describe the mechanism of each syncopation model with mathematical notations and illustrative examples.

## Chapter 4

In this chapter, we address Research Question 1 by conducting an experiment, which will be referred to as *Experiment 1*. This experiment involved manipulating rhythm-patterns by choosing different rhythm-components and time-signatures to produce audio stimuli. Using this stimuli, we collected the subjective ratings of perceived syncopation for each stimulus.

## **Chapter 5**

In this chapter, we address Research Question 2 by implementing the first formal and direct evaluation of the models described in Chapter 3 using perceptual data established from Experiment 1. Based on the evaluation results, the strengths and weaknesses of the various theoretical approaches are then identified.

## **Chapter 6**

In this chapter, we further investigate Research Question 1 to test if syncopation is tempo-dependent. We present Experiment 2, in which we collected perceptual ratings of syncopation of same rhythm-pattern played at different tempi. In the beginning of the chapter, we provide a thorough review of relevant studies in the literature. We then introduce the method for the experiment, analyse the results and finally seek connections between our observations and the findings of related studies.

## **Chapter 7**

This chapter explores ways to improve the modelling of syncopation perception. Building on the findings in Chapter 5, we consolidate the most successful elements piecemeal into new combined models. In addition, we incorporate the findings from Chapter 6 into the new models, attempting to capture the tempo-dependent nature of syncopation.

## **Chapter 8**

We conclude the thesis with a revision of the answers to the research questions. We focus on the major findings from our perceptual studies and the areas where current theory explains perception and where it falls short. We also propose research topics for the further investigation on syncopation perception.

## Chapter 2

# Syncopation in music theory

In this chapter, we review the fundamentals of rhythm, including the notions of beat, meter and tempo. We then investigate different definitions given for syncopation in music theory, and collect them into four major hypotheses. We follow this with a brief introduction of eight syncopation models from current literature, which we will cover in more detail in later chapters.









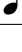
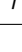
### 2.1 Fundamentals of rhythm

In order to introduce the concept of syncopation in music theory, we need to start with some musical terms that describe fundamental aspects of rhythm.

#### 2.1.1 Rhythm

The word *rhythm* has been loaded with multiple meanings, some of which are only vaguely related to each other. Some refer to rhythm as the regular recurring patterns in time that can be structured (i.e. close to meter) or grouped [LH78, LHL84, LJ83]. Some view it as the organisations of events with different perceptual emphasis, as Cooper and Meyer state: “the way in which one or more unaccented beats are grouped in relation to an accented one” [CM60, p.6]. Some propose definitions for rhythm in a broader sense, for example, the Oxford Dictionary of Music defines rhythm as “everything pertaining to the time aspect of music, as distinct from the aspect of pitch” [Ken94, p.724]. Similarly, London states that

Table 2.1: Basic note-values and the corresponding music notations. The note-values are relative to a whole-note.

Note	Rest	Note-value	American name	British name
		1	Whole-note	Semibreve
		$\frac{1}{2}$	Half-note	Minim
		$\frac{1}{4}$	Quarter-note	Crotchet
		$\frac{1}{8}$	Eighth-note	Quaver
		$\frac{1}{16}$	Sixteenth-note	Semiquaver

“rhythm involves the pattern of durations that is phenomenally present in the music” [p.4][Lon04].

Throughout this thesis, we follow the school of thought that defines rhythm in the relatively objective and broad sense [Ken94, Lon04, Gou05]: it is the sequence of durations of the musical events. Such a concept of rhythm is detached from the subjectively processed products of the patterns of event durations, such as grouping [LJ83, p.13] and periodicity [LH78]. Instead, it simply refers to the physical distributions of musical time.

### Note-values

In Western classical music theory, a sounded event is called a *note* [Ken94, p.626], and a silent event is called a *rest* [Ken94, p.722]. Each note or rest has its duration (i.e. the time between the start or *onset* and the end or *offset*). In music notation, a scored *note-value* denotes the duration of the note or rest event. Some instruments and techniques to play instruments can control the onset and offset independently, thus allowing direct control of note duration. For example, when you press a key on an organ, the sound starts and will continue sounding until the key is lifted. In contrast, a purely percussive sound, such as a side-stick on a snare drum, which has a very fast decay time, affords no control over duration. Therefore, while a note-value defines the abstract onset and offset times of an event, it does not necessarily mean the sound will actually continue for the entire

$$\begin{array}{ccccccc}
 \text{♩} & = & \text{♩} & \text{♩} & = & \text{♩} & \text{♩} & \text{♩} & \text{♩} & = & \text{♩} & \text{♩} & \text{♩} & \text{♩} & \text{♩} & \text{♩} & \text{♩} & \text{♩} \\
 \frac{1}{2} & = & \frac{1}{4} & + & \frac{1}{4} & = & \frac{1}{8} & + & \frac{1}{8} & + & \frac{1}{8} & + & \frac{1}{8} & = & \frac{1}{16} & + & \frac{1}{16} & + & \frac{1}{16} & + & \frac{1}{16} & + & \frac{1}{16} & + & \frac{1}{16} & + & \frac{1}{16} & + & \frac{1}{16}
 \end{array}$$

Figure 2.1: The equation of note-values. A half-note is equivalent in note-value to two quarter-notes, four eighth-notes or eight sixteenth-notes. The curly tails of two or more eighth-notes can be joined together by a *beam* [Tay89, p.3]; two or more sixteenth-notes can be joined together by two beams.

$$\begin{array}{ccc}
 \text{♩} = \overbrace{\text{♩} \text{♩} \text{♩}}^{\mathbf{3}} & \text{♩} = \overbrace{\text{♩} \text{♩} \text{♩}}^{\mathbf{3}} & \text{♩} = \overbrace{\text{♩} \text{♩} \text{♩}}^{\mathbf{3}} \\
 \text{(a)} & \text{(b)} & \text{(c)}
 \end{array}$$

Figure 2.2: Examples of triplets. (a) Three triplet quarter-notes are of the same length as a half-note. (b) Three triplet eighth-notes are equivalent to a quarter-note. (c) A triplet can be a group of notes and rests.

duration.

Table 2.1 lists a set of basic note-values commonly used in music notation. It should be noted that these note-values do not represent absolute time durations (e.g. seconds). Instead, they are relative durations with respect to the whole-note which is treated as the reference. For example, a half-note has a note-value of  $1/2$ , which is half the duration of a whole-note.

Each note-value shown in Table 2.1 can be divided by two to give the value on the row below (the sixteenth-note can be further divided in two, giving a thirty-second) and so on. In terms of durations, these note-values then form the relationship shown in Figure 2.1: a half-note is equivalent in note-value to two quarter-notes, four eighth-notes or eight sixteenth-notes.

The note-values in Table 2.1 are all halved to produce the row below but a note-value may also be divided by some values other than a power of two. In this case, the desired subdivision needs to be specified explicitly. For example, we commonly see a group of three equal-duration events played in the time of two, and this is known as a *triplet* figure [Ken94, p.901]. The notation convention for this is to add the number 3 above the group of events to be played as a triplet (Figure 2.2).



Figure 2.3: Examples of tied notes. (a) The final sixteenth-note is tied to the first eighth-note, which creates a single note with duration equivalent to three sixteenths. (b) An eighth-note, a half-note and a quarter-note are all tied together, forming a total duration of seven eighths.

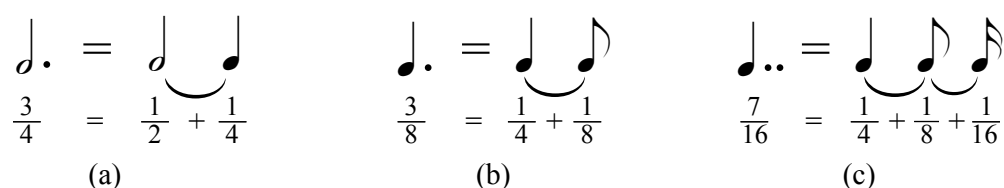


Figure 2.4: Examples of dotted notes. (a) A dotted half-note is equivalent to joining a half-note with a quarter-note (i.e. *half* of a half-note). (b) A dotted quarter-note is equivalent to an eighth-note tied to a quarter-note. (c) A double-dotted quarter-note is equivalent to a quarter-note tied to an eighth-note (half of quarter-note), then further tied to a sixteenth-note (half of the preceding eighth-note).

### Tied notes and dotted notes

In music notation, it is possible to indicate that separate musical notes (with the same pitch) should be played as a single note, by connecting them with a *tie*; the duration of this single note is equal to the sum of the note-values of individual notes [Tay89, p.33]. To illustrate, in Figure 2.3a, the curved line connecting the fourth sixteenth-note and the first eighth-note is the tie. The tied-note can also be further tied to following notes such as in Figure 2.3b.

Another notational method to extend a note-value is to add one or more dots after a note or a rest. Each dot extends the duration by half of the preceding note-value. Examples of dotted notes and their associated durations are shown in Figure 2.4.

### 2.1.2 Beat

Some musical events give rise to moments of perceptual emphasis in the musical flow; these are known as *accents* [CM60, p.7]. Accents can arise from the contrast between rest and note, a change in dynamics (e.g. soft to loud), a contrast in duration, or a change in pitch, or from a mixture of these.

Perceived accents serve as the cues for human listeners to extract an underlying periodic pattern [LJ83, p.17]. This perceived regular pattern is known as the *beat*<sup>1</sup> [Tra07], or the *pulse* [CM60, p.3]. Like the ticking of a clock, a series of beats are equally spaced in time<sup>2</sup>.

#### Tactus

The perception of beat arouses synchronised movements in the form of tapping, nodding and dancing [Lon04, pp. 9 - 12]. There can be multiple periodicities (forming multiple beat sequences) perceived from a given musical excerpt, but usually only one or two of which are primarily tracked by listeners for synchronising (e.g. tapping or dancing). This beat sequence is referred as the *tactus* [LJ83, p.21].

### 2.1.3 Meter

In some music cultures, particularly in western music, recurring patterns underlying a sequence of beats are usually strongly perceived. For example, when listening to marching music, we intuitively count the beats as ‘one-two-one-two’ or could be said to feel ‘strong-weak-strong-weak’. Likewise, when listening to waltz, the beats are naturally structured as ‘one-two-three-one-two-three’ or ‘strong-weak-weak-strong-weak-weak’. In this way, the beat groupings form higher levels of periodicity, giving rise to a multi-level structure, known as *meter* [Lon04, p.17].

---

<sup>1</sup>In this thesis, we focus only on the case of isochronous beats, as Parncutt’s notion of a layer of pulsation [Par94]

<sup>2</sup>The time intervals between successive beats are theoretically identical, but this is not always desirable in expressive musical performance where the interval may be varied by the performer for musical effect.



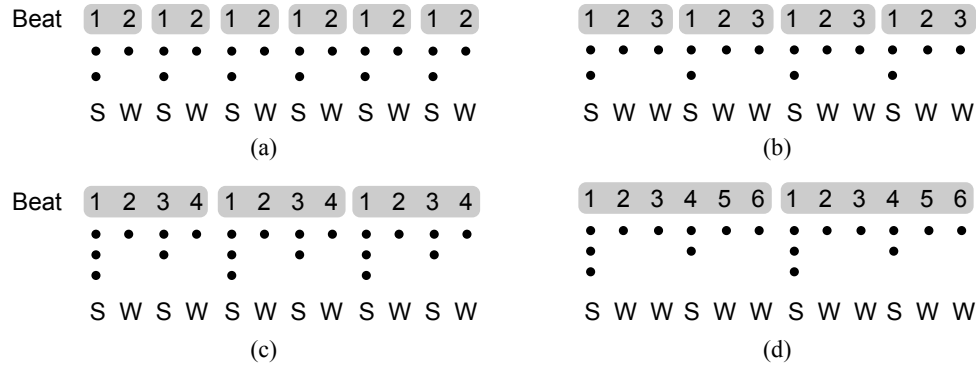


Figure 2.5: Examples of beat groupings and the resulting beat salience. The grey box indicates the group, or *bar*. S and W refer to strong and weak. (a) A two-beat grouping. (b) A three-beat grouping. (c) A four-beat grouping. (d) A six-beat grouping.

### Beat grouping and beat salience

Lerdahl and Jackendoff state that “fundamental to the idea of meter is the notion of periodic alternation of strong and weak beats” [LJ83, p.19]. The ‘strong’ or ‘weak’ here describes the perceptual beat salience. Recalling the examples of marching music and waltz, patterns of beat organisation may be illustrated in *dot notation* as in Figure 2.5a-b. Here, the two- or three-beat groupings form two levels of periodicities, and the first beat marks the coincidence of these two periodicities. If the beat at a particular level of periodicity also exists in the next larger level, it is called a *strong-beat*, otherwise is a *weak-beat*.

Additionally, the non-prime beat groupings give rise to equal size subgroups of beats (i.e. the prime factors), hence forming multi-level metrical structures. For example, the four-beat grouping in Figure 2.5c forms two groups of two beats. Likewise, the six-beat grouping in Figure 2.5d forms two groups of three beats. It is also possible to subdivide a group of six into three groups of two beat, and this gives a metrical structure with different rhythmic emphases. It should be noted that for meter to be *well-formed* [LJ83, pp.69-72], we may only group elements that are of equal length. For example, while a six-beat grouping can be two threes or three twos, it cannot be divided into a group of two and a group of four.

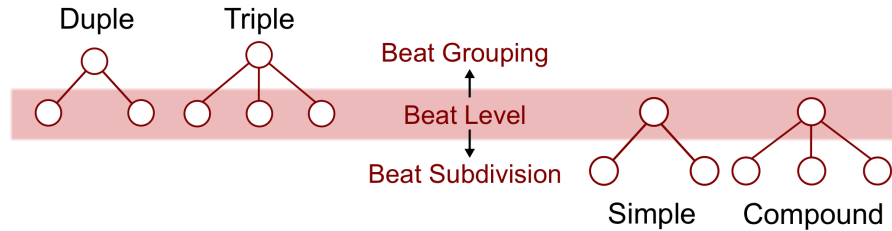


Figure 2.6: Duple versus triple, simple versus compound. Meter can be categorised by patterns of beat grouping and beat subdivision. Two-beat grouping and three-beat groupings are referred to as duple and triple respectively. Binary- and ternary-beat subdivisions are referred to as simple and compound.

## Bar

When composing, particularly when notating music, composers will generally try to choose an appropriate primary beat grouping. This serves as an indication to the performers of how to count beats, and thus how to interpret the score. Each complete cycle of this primary beat grouping is called a *bar* (or *measure*) and in musical notation is enclosed between two bar lines [Ran86, p.506] (represented by the grey boxes in Figure 2.5). The first beat in a bar is called the *down-beat*, corresponding to all the beats labelled 1 in Figure 2.5.

## Time-signature

A *time-signature* is used for notating meter in the musical score. It is usually indicated by a fraction where the denominator indicates the basic note-value counted in a bar, and the numerator indicates the number of such note-values making up the bar [Ran86]. For example, a time-signature of  $2/4$  means a bar consists of two units, each of which has a note-value of  $1/4$ , i.e. a quarter-note (Table 2.1). Similarly, a time-signature of  $6/8$  means a bar comprises six units, each of which is an eighth-note.

As shown in Figure 2.6, the basic types of beat grouping include two beats per bar and three beats per bar. These groupings are referred to as *duple* and *triple* respectively [Ran86, p.506]. Two types of beat subdivision are also distinguished: *simple* refers to a binary beat subdivision, and

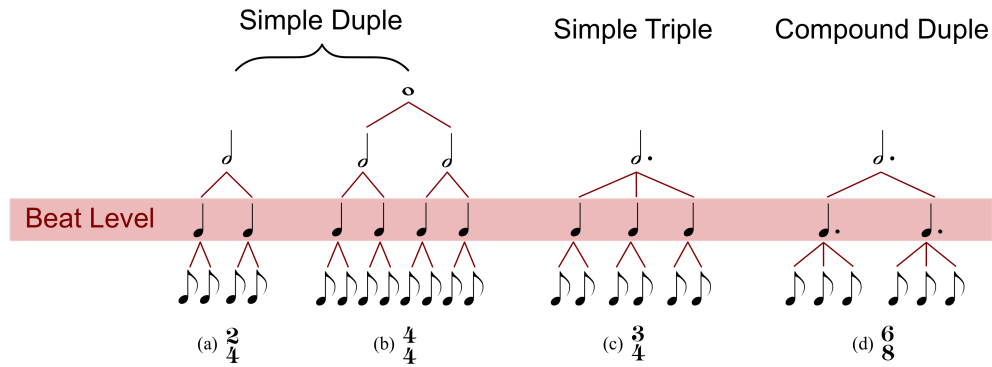


Figure 2.7: Time-signatures and their hierarchical structures, patterns of beat groupings and beat subdivisions. (a) A  $\frac{2}{4}$  time-signature. (b) A  $\frac{4}{4}$  time-signature. (c) A  $\frac{3}{4}$  time-signature. (d) A  $\frac{6}{8}$  time-signature.

*compound* refers to a ternary subdivision [Ran86, p.506].

Figure 2.7 presents four time-signatures commonly adopted in music notation, in the form of a *tree structure*. The time-signature of  $\frac{2}{4}$  and  $\frac{4}{4}$  are counted as simple-duple meters<sup>3</sup>, because both feature two-beat groupings and binary subdivisions. The time-signature of  $\frac{3}{4}$  features a three-beat grouping and binary subdivision, therefore is known as a simple-triple meter. In contrast, in  $\frac{6}{8}$  time, a two-beat grouping and ternary-beat subdivision constitute a compound-duple meter.

There is a common misinterpretation that the denominator in the fraction of time-signature refers to the note-value of the beat, and the numerator indicates the number of beats. This may be true for simple meters, but cannot work for compound meters [Lon04, p.18]. Take  $\frac{6}{8}$  for example (Figure 2.7d), the beat level is carried by dotted notes with note-value  $\frac{3}{8}$ , instead of the eighth-notes with note-value  $\frac{1}{8}$ .

### Metrical levels

So far, we have discussed the origin of meter, which manifests in the higher levels of periodicities structured from the fundamental periodicities (i.e. beats) in a rhythm sequence. We have also introduced concepts related to

<sup>3</sup>As a special case of duple meter,  $\frac{4}{4}$  is sometimes termed *quadruple meter* for its four-beat recurrence.

meter, including bar, time-signature, and categories of metrical structure in terms of patterns of beat grouping and beat subdivision. But why do we need to know these? What is meter for? Essentially, meter is used for providing a framework to structure rhythm. Borrowing from London, the relationship between rhythm and meter can be described thus: “meter is a mode of attending, and rhythm is that to which it attend” [Lon04, p.4].

Earlier, in Figure 2.7, we employed tree diagrams to present the metrical structure of different time-signatures. Throughout this thesis, we refer to each (horizontal) layer in the tree as a *metrical level*, representing the units in this level of periodicity. Each node in the tree is referred as a *metrical position*.

Different rhythms in the same time-signature are fitted into in the same framework of meter, but they may project different sets of metrical levels. As shown in Figure 2.8, the three one-bar rhythm-patterns are in a time-signature of 2/4 but have different number of metrical levels. Defined by the time-signature, their bar levels all locate at the half-note level, and all beat levels locate at the quarter-note level. However, the lowest metrical level for the three rhythms are different, because it is carried by the shortest note-values presented in the rhythm. This leads to the concept of *tatum*, which is formally defined in [Bil93, p.22] as “the regular time division that most highly coincides with all note onsets”<sup>4</sup>. Therefore the tatum levels for three rhythms in Figure 2.8 are the a) quarter-note level, b) eighth-note level and c) the sixteenth-note level. Finally, *tactus* is the periodicity that human listeners naturally tap to or dance to (Section 2.1.2). Which metrical level will be selected as *tactus* depends on *tempo*. In the following section, we introduce the concept and notation of tempo in music, and we will continue to review the relationship between *tactus* and tempo in Chapter 6.

---

<sup>4</sup>It should be noted that there is not always a tatum solution for all types of music; hardanger fiddle music for example [Lon04]

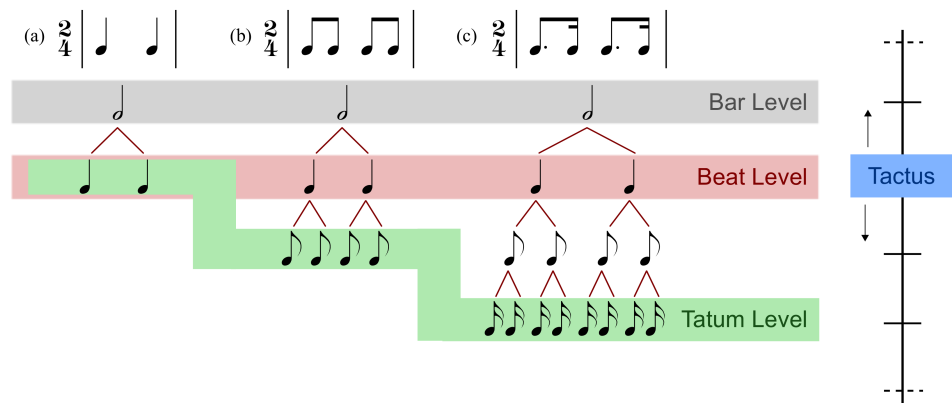


Figure 2.8: Metrical hierarchies projected by rhythm-patterns in a given time-signature. Metrical hierarchy is presented as a tree structure as in Figure 2.7. The bar level and beat level are determined by the time-signature, and are indicated in grey and pink respectively. The tatum level, indicated in green, is the smallest metrical level. Any level could be selected as the tactus, indicated in blue.

### 2.1.4 Tempo

Tempo describes the speed of a musical excerpt. Before the invention of the metronome, composers would indicate the speed of a piece of music using Italian musical terms (e.g. *allegro* means fast, quick and bright, *Moderato* means moderately). These terms would be interpreted by the musician in order to perform to piece. With the invention of metronome, it became possible for composers to specify precisely what speed the music should be played at by linking a note-value to a specific beat rate, with a metronomic indication. This is defined as the rate per unit of time of a given metrical level [Ran86, p.873]. Figure 2.9 shows an example of tempo indication in beginning of a musical score. By convention in musical notation, the tempo is indicated in beats per minute, where the beat is defined by a certain note-value.

A number of concepts are closely linked to tempo in the perceptual domain, such as the pulse rate that people would tap or dance to, called the *tactus rate* (Section 2.1.2). It is also related to the notion of *preferred tempo* (or *indifference interval*) that refers to the rate when music sounds neither too fast nor too slow but just right [QW06, MJH<sup>+</sup>06, Fra63]. In



Figure 2.9: Example of tempo indication in the beginning of the musical score. The tempo of a music excerpt, shown here in red by the metronomic indication, is indicated to be 120 beats per minute (BPM), counting each quarter-note as a beat. Therefore, each quarter-note has a duration of 0.5 seconds.

this thesis, we will refer to *tempo* only as the defined beat rate in the music notation (Figure 2.9), as opposed to the subjective judgement of tempo.

## 2.2 Definitions for syncopation

So far, we have introduced the concepts of beat and meter. From the composer’s or performer’s perspective, they serve as the fundamental structure for various interesting rhythm-patterns to be built upon. From the listener’s perspective, they are the underlying precepts extracted from the temporal patterns in the music. Sometimes, however, composers or performers may deliberately set up rhythm-patterns to undermine the established meter structure, and create a situation where the meter may not be readily perceived from the rhythm surface for listeners. This phenomenon is known as *syncopation*.

The classic definition of syncopation is the “momentary contradiction of the prevailing meter or pulse” [Ran86, p.861]. Music theorists have attempted to explain the effect of syncopation using a range of prototypical rhythm configurations. Thus, we see diverse opinions of the scopes of syncopation in terms of rhythmic instances. In the following sections, we are going to review the definitions and explanations of syncopation in music theory, and try to classify the main schools of thought on the subject.

(a) Rest on strong-beat - "loud rest"                      (b) Tied-note on strong-beat

(c) Accent on weak-beat and missing strong-beat                      (d) Loud rest and accented weak-beat

Figure 2.10: Examples of syncopation aroused from violation of regular beat salience. (a) A rhythm-pattern that has rests (indicated in red) placed on the down-beats (i.e. strong-beats). (b) The note on the second strong-beat (indicated in red) is tied to the previous note, causing an absence on the down-beat. (c) The rhythm-pattern contains an onset and agogic (durational) accent on the second weak-beat, and absence of note on the following strong-beat. (d) The reggae drum-pattern in “Stir It Up” by Bob Marley. It is also a mixture of missing down-beat and accented weak-beat.

### 2.2.1 Violation of the regular beat salience

A metrical structure is inbuilt with allocations of metrical weight (strong or weak) at each beat position (see Section 2.1.3). All explanations of syncopation share the consensus that it involves the violation of the regular succession of strong- and weak-beats, by creating an absence of sounded note on the strong-beats, and/or by shifting accents to notes on the weak-beats (Figure 2.10 provides some rhythm examples to demonstrate these two effects). The majority of sources refer syncopation to both occasions [Ran86, Ken94, Hur06, LHL84, HO06, Tem99, Tem01], with the exception of Cooper and Meyer who exclude the occasion of accented weak-beats from the scope of syncopation [CM60, p.100].

Huron [Hur06, pp. 295-297] specifies five types of syncopation affected by accenting weak-beats in different ways (see Section 2.1.2). These are: onset syncopation (due to note/rest positions), dynamic syncopation (sounding notes loudly on weak-beats), agogic syncopation (placing longer

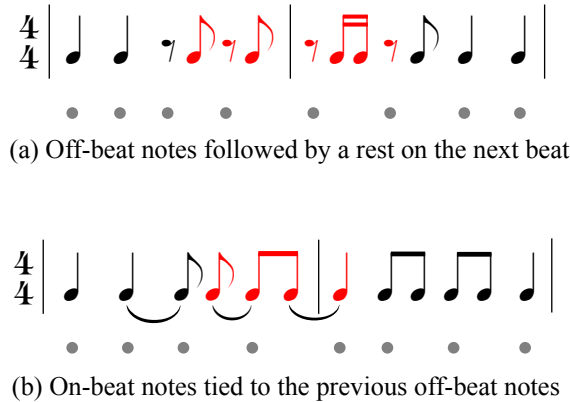


Figure 2.11: Examples of off-beat notes that followed by a rest or a tied-note on the next beat. Two short pieces of rhythm in 4/4 are presented. The grey dots indicate the beat location. In (a), there are four notes (in red) enter between the beats and the following beat is placed with a rest note. In (b), two notes occur off-beat and are tied by the notes on the following beat. Both are thought to arise syncopation [CM60, LHL84, HO06].

notes on weak-beats), harmonic syncopation (changes in pitch/harmony on weak-beats) or mixed syncopation (a combination of the above).

### 2.2.2 Off-beat

When a note is placed on the beat, it is called *on-beat*; otherwise it is *off-beat*. Off-beat events are thought to cause a shift of the emphasis away from the strong-beats, hence producing syncopation. However, theories diverge here where some state that only an off-beat event followed by an unfilled beat gives rise to syncopation, while some do not.

Cooper and Meyer were exponents of the idea that syncopation is aroused from shifting the note on the beat backward in time (i.e. move it to be earlier). They defined syncopation as “a tone which enters where there is no pulse on the primary metric level (the level on which beats are counted and felt) and where the following beat on the primary metric level is either absent (a rest) or suppressed (tied)” [CM60, p.100]. Examples are shown in Figure 2.11. Longuet-Higgins and Lee [LHL84] expressed the same notion, which was then formalised in their mathematical model, the mechanisms for which will be further discussed in Section 3.2.1.



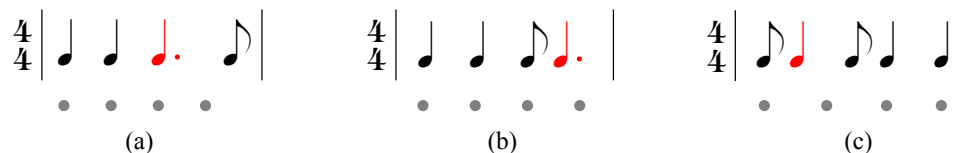


Figure 2.12: Syncopation types as defined in [Kei91]. Grey dots indicate beats. (a) presents *hesitation*, where a note (in red) ends off-beat; (b) presents *anticipation*, where the note starts off-beat; and (c) presents syncopation, where it both starts and ends off-beat.

In contrast, some believed that an off-beat event would result in syncopation regardless of the rhythmic context it is in. For instance, Keith stated that “syncopation occurs when events start or end *off the beat*” [Kei91], specifying three types of syncopated event, named *hesitation*, *anticipation* and *syncopation* (examples of which are shown in Figure 2.12). The degree of syncopation is differentiated by the rhythmic context in which the off-beat event is placed, and is thought to increase from hesitation to anticipation then to syncopation. Nevertheless, they are all regarded as manifestation of syncopation, whereas hesitation is not defined as a form of syncopation by other theorists [CM60, LHL84].

A similar notion can be found in [Tou05, GMRT05], where capturing off-beat events is the major focus in the modelling of syncopation. Gómez et. al [GMRT05] posit that the sense of syncopation is aroused by the effect of imbalance, and that this is a result of lopsided placing of the off-beat events. The essence of their syncopation model, the *Weighted Note-to-Beat Distance* model, is that the strength of syncopation is inversely related to the distance of each note to its nearest beat, i.e. the closer the note is to the beat, while it is still off-beat, the higher syncopation it gets.

### 2.2.3 Transformation of meter

Some theories state that syncopation can be aroused by a sudden transformation of the fundamental character of the meter [Ran86, Ken94]. For example, a change of feel from duple to triple, as affected by alteration of accents in the rhythm (Figure 2.13a) or a change of time-signature in the score (Figure 2.13b). The transformation of meter can give rise to

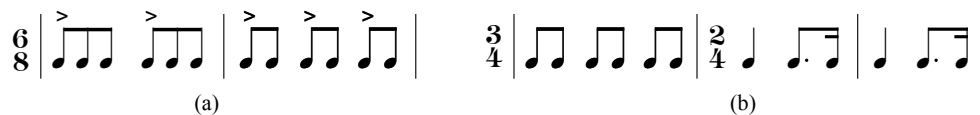


Figure 2.13: Examples of transformation of meter.

the effect of shifting the bar line, and may cause one of the weak-beats to function as a strong-beat [Ran86].

### 2.2.4 Polyrhythm

A large set of rhythms that result in a sense of competing meters is *polyrhythms* (or *cross-rhythms*). Polyrhythm has been defined as “the simultaneous use of two or more rhythms that are not readily perceived as deriving from one another or as simple manifestations of the same meter” [Ran86, p.669]. A common use of polyrhythm in composition is a triplet over a binary subdivision of the beat, e.g. Figure 2.14a. This type of polyrhythm is often referred as 3:2 polyrhythm or *hemiola*<sup>5</sup> [Ken94, p.398]. Another example is 4:3 polyrhythm, shown in Figure 2.14b, where the periodicities of four events (from the eighth-notes) and three (from the triplet) cannot resolve to a single grouping of events. Krebs [Kre99] described this phenomenon as *metric dissonance*, aroused by conflicting periodicities.

From the perspective of meter, polyrhythms present the situation where two (or more) different metrical hierarchies have to co-exist at the same time. In other words, one metrical hierarchy that is only allowed a single type of subdivision at each level cannot capture the conflicted groupings in a polyrhythm. For example, in Figure 2.14a, the rhythm-pattern on the top line suggests that the bar should be equally subdivided into three (i.e. three groups of two eighth-note beats), whereas the bottom line suggests a subdivision of the bar by two (i.e. two groups of three eighth-note beats). These two different groupings of eighth-note in the bar cannot be resolved into one metrical hierarchy. Similarly, in Figure 2.14b, the tree

<sup>5</sup>More specifically, this is known as *vertical* hemiola. The alternative, *horizontal* hemiola, refers to the transformation from duple to triple [Ran86, p.389], e.g. Figure 2.13a.

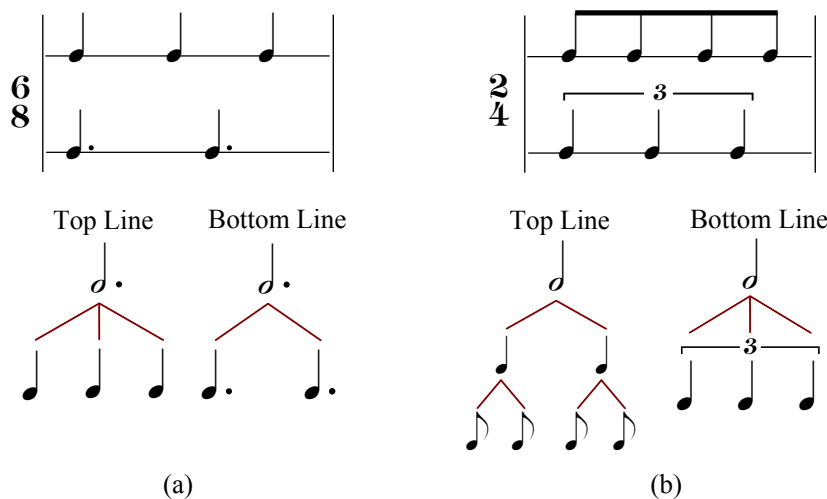


Figure 2.14: Examples of polyrhythms and the resulting competing metrical hierarchies. (a) A 3:2 polyrhythm (often referred to as a hemiola). (b) A 4:3 polyrhythm.

structure of the eighth-notes rhythm-pattern on the top line fits the metrical hierarchy implied by the scored time-signature 2/4 (two groups of two). However, the triplet pattern on the second line suggests a separate hierarchy with a subdivision of three that cannot fit with groupings of four.

In the literature, there appears to be no clean cut between syncopation and polyrhythm. Many theorists do not treat polyrhythm as a form of syncopation [Ran86, Ken94, LHL84, Lon04, CM60, HO06, Pre97], while some think polyrhythms strongly challenge metric construals, therefore feature syncopation [HO81, GMRT05]. London [Lon04] described polyrhythm as a “full-blown metric ambiguity”, whereas syncopation was a “short-term mismatch” between meter and rhythm. Indeed, compared to the effects aroused by emphasising weak-beats over strong-beats or by a sudden change of time-signature, polyrhythms produce a more constant mismatch between rhythm and meter; this seems to violate the widespread notion that the effect of syncopation is “momentary” [Ran86]. We have chosen to follow the broader interpretation of syncopation ( i.e. that it includes polyrhythms), in our experiment design in Chapter 4.

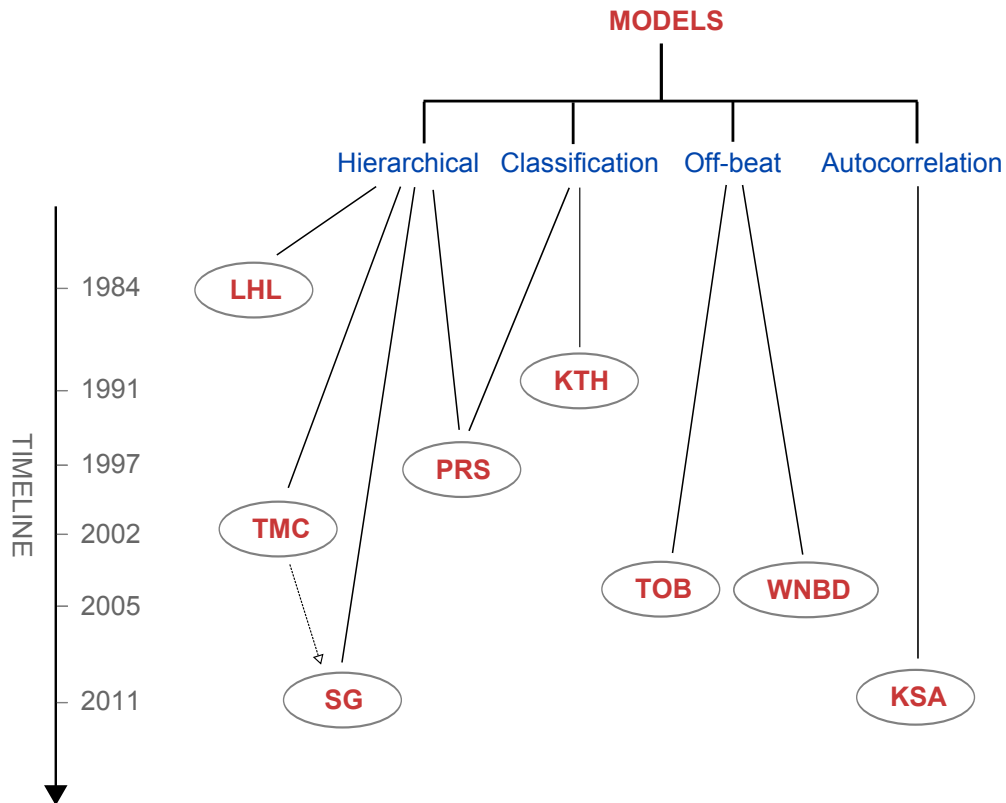


Figure 2.15: Models used for predicting syncopation, which are categorised by theoretical basis and main methodology.

## 2.3 Overview of syncopation models

Ambiguity in the definition of syncopation has led to a number of different models [LHL84, GMRT05, SG11, Tou05, Kei91, KS11], representing multiple competing hypotheses. Additionally, models of *rhythm complexity* [Pre97, Tou02] have also been applied to syncopation prediction in a number of previous studies in the literature [GTT07, Thu08] and as a result we include them in this thesis as well.

### 2.3.1 Categories of models

Figure 2.15 presents the models in categories for syncopation and the development of these models tracing back to 1984. In general, hypotheses for these syncopation models fall into four broad categories: *hierarchical*, *off-beat*, *classification* and *autocorrelation*.

Hierarchical models are designed to capture the violation of the regular succession of beat salience or metrical weights (Section 2.2.1 and 2.2.2). Four models fall into this category: Longuet-Higgins and Lee’s model (LHL) [LHL84], Pressing’s model (PRS) [Pre97], Toussaint’s Metric Complexity model (TMC) [Tou02] and Sioros and Guedes’s model (SG) [SG11] that is developed from TMC.

Another approach is to classify individual notes or rhythm sequences into a number of pre-determined syncopation types. We will refer to this category of modelling hypothesis as classification models. Keith’s model [Kei91] (KTH) and the PRS model adopted this approach.

Off-beat models ignore metrical hierarchy and instead attempt to capture note onsets that fall in between strong-beat positions (Section 2.2.2). Two models fall into this category: Gómez et al.’s Weighted Note-to-Beat Distance (WNBD) [GMRT05] and Toussaint’s off-beatness measure (TOB) [Tou05].

Finally, Keller and Schubert’s autocorrelation-based model [KS11] (KSA) differs from the other categories, and we refer to this approach as an autocorrelation model. This model measures the accent strength (the sum of durational and melodic accents weights [Dix01, MPF09, Par94, Tho82]) of each musical event in a rhythmic sequence, then calculates the two-beat-autocorrelation coefficients. The hypothesis is that the more different events separated by two beats are in terms of accent strength, the greater the violation of metric structure is, hence resulting in higher syncopation.

### 2.3.2 Capabilities of models

The various models for syncopation represent different hypotheses in terms of rhythmic features that contribute to syncopation and therefore possess different capabilities in the modelling. Table 2.2 summarises the eight models in terms of category and the musical features that they can capture.

All the models use temporal features (i.e. onset time point and/or note duration) in the modelling. The SG model also process dynamic information of musical events in rhythms (i.e. dynamic accents), and the KSA model takes account of temporal, dynamic and melodic information

Table 2.2: Comparisons of the properties of syncopation models. Basis: H - Hierarchical-based, C - Classification, O - Off-beat-based, A - Autocorrelation-based.

Model	Basis	Onset	Duration	Dynamics	Melody	Mono	Poly	Duple	Triple
LHL	H	✓				✓		✓	✓
KTH	C	✓	✓			✓	✓	✓	
PRS	H,C	✓				✓		✓	✓
TMC	H	✓				✓		✓	✓
TOB	O	✓				✓	✓	✓	✓
WNBD	O	✓	✓			✓	✓	✓	✓
SG	H	✓		✓		✓		✓	✓
KSA	A	✓		✓	✓	✓		✓	

of musical events.

In this thesis, we will use the term *monorhythm* to refer to any rhythm-pattern that is *not* polyrhythmic. All the models can measure syncopation of monorhythms, but only the KTH, TOB and WNBD models can deal with polyrhythms.

Finally, all the models can deal with rhythms (notated) in a duple meter, but only six models can cope with rhythms in a triple meter. They are the LHL, PRS, TMC, TOB, WNBD and KSA models.

## 2.4 Summary

In this chapter, we have reviewed the theoretical underpinnings of rhythm and introduced the definitions for syncopation and how it is explained in the music theory literature. We have explained the note-values that are used in western music notations, and demonstrated the construction of rhythm-patterns from combinations of notes and rests with various note-values. We have also discussed the concepts of beat, meter, and tempo. Based on these fundamental elements of rhythm, we have outlined four main schools of thought on the manifestation of syncopation, and introduced eight theoretical models of syncopation from literature to provide a broad picture of the state of the art.

# Chapter 3

## Review of syncopation models

In this chapter, we take a step further in reviewing the models of syncopation. In order to provide an explicit representation of the models, we consolidate the notations into mathematical equations, and walk through examples to assist readers in understanding the mechanisms of these models. By doing this, we benefit from unambiguous explanations of the models (as opposed to describing models in prose), and a smoother step towards programming codes of models implementation.

In the chapter, we introduce and define some relevant mathematical terms and operations. Then, we apply these mathematical notations in formalising some rhythmic concepts we mentioned in Chapter 2. Finally, we review each of the seven well-known syncopation models in depth by providing unified representation of mathematical equations.

### 3.1 Background

In order to review the models in detail, we will first define some general mathematical terms and operations with which we will represent rhythm and meter. A key to the set notation symbols we use can be found in the Glossary of Symbols.

#### 3.1.1 Sequences

We use the term *sequence* to refer to a finite, ordered set that may contain duplicated elements. A sequence  $Q$  of individual elements  $q_n$  will be

notated

$$Q = \langle q_0, q_1, \dots, q_{|Q|-1} \rangle \quad (3.1)$$

where  $|Q|$  denotes cardinality (the number of elements in a set) of  $Q$ .

We define a concatenation operator<sup>1</sup>  $*$  on two sequences  $Q$  and  $\acute{Q}$  giving a new sequence  $\hat{Q}$  such that

$$\begin{aligned} \hat{Q} &= Q * \acute{Q} = \langle q_0, q_1, \dots, q_{|Q|-1} \rangle * \langle \acute{q}_0, \acute{q}_1, \dots, \acute{q}_{|\acute{Q}|-1} \rangle \\ &= \langle \hat{q}_0, \hat{q}_1, \dots, \hat{q}_{|Q|+|\acute{Q}|-1} \rangle \end{aligned} \quad (3.2)$$

where each element  $\hat{q}_n$  of the new sequence is defined as

$$\hat{q}_n = \begin{cases} q_n & \text{for } 0 \leq n < |Q|, & q_n \in Q; \\ \acute{q}_{n-|Q|} & \text{for } |Q| \leq n < |Q| + |\acute{Q}|, & \acute{q}_{n-|Q|} \in \acute{Q}. \end{cases} \quad (3.3)$$

To illustrate, if  $\langle \Delta \rangle$  and  $\langle \blacktriangledown \rangle$  are sequences then

$$\langle \Delta \rangle * \langle \blacktriangledown \rangle = \langle \Delta, \blacktriangledown \rangle.$$

Using the concatenation operator, we can define a repetition operation  $Q^\alpha$  where  $\alpha$  specifies the number of times to repeat sequence  $Q$  such that

$$Q^\alpha = \begin{cases} \emptyset, & \text{if } \alpha = 0; \\ \bigodot_{a=0}^{\alpha-1} Q, & \text{otherwise.} \end{cases} \quad (3.4)$$

where  $\bigodot$  denotes the iterated concatenation operator<sup>2</sup>. We may apply this operation to the result of our earlier example to repeat it three times:

$$\langle \Delta, \blacktriangledown \rangle^3 = \langle \Delta, \blacktriangledown, \Delta, \blacktriangledown, \Delta, \blacktriangledown \rangle.$$

We also define a subdivision operation  $Q||_\lambda$  for  $|Q| \bmod \lambda = 0$ , whereby a sequence of elements may be split to form a sequence of  $\lambda$  equal-length sub-sequences:

$$Q||_\lambda = \langle \langle \cdot \rangle_0, \langle \cdot \rangle_1, \dots, \langle \cdot \rangle_{\lambda-1} \rangle = \bigodot_{a=0}^{\lambda-1} \langle \langle \cdot \rangle_a \rangle \quad (3.5)$$

<sup>1</sup>The concatenation operator has signature  $*$  :  $\mathbb{S} \times \mathbb{S} \rightarrow \mathbb{S}$  where  $\mathbb{S}$  is the set of all possible sequences.

<sup>2</sup> $\bigodot$  is to  $*$  as  $\sum$  is to  $+$ .



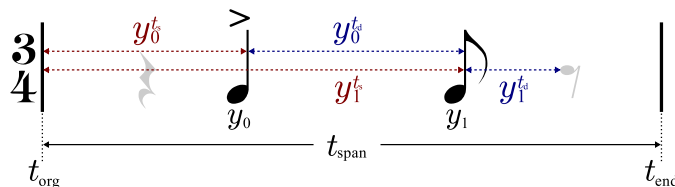


Figure 3.1: An example note sequence.

Two note events  $y_0$  and  $y_1$  occur in the time-span between time origin  $t_{\text{org}}$  and end time  $t_{\text{end}}$ . The time-span duration  $t_{\text{span}}$  is three quarter-note periods. The rests at the start and end of the bar are not explicitly represented as objects in their own right here but as periods where no notes sound.

where the  $a^{\text{th}}$  sub-sequence  $\langle \cdot \rangle_a$  takes the form

$$\langle \cdot \rangle_a = \bigodot_{\theta=0}^{\Theta-1} \langle q_{\theta+a\Theta} \rangle \quad \text{where} \quad \Theta = \frac{|Q|}{\lambda}, \quad q_{\theta+a\Theta} \in Q. \quad (3.6)$$

As an example, we may subdivide our repeated example from above into two sub-sequences

$$\langle \Delta, \nabla, \Delta, \nabla, \Delta, \nabla \rangle \|_2 = \langle \langle \Delta, \nabla, \Delta \rangle, \langle \nabla, \Delta, \nabla \rangle \rangle.$$

### 3.1.2 Rhythm in continuous time

The term *time-span* has been defined as the period between two points in time, including all time points in between [LJ83]. To represent a given rhythm, we must specify the time-span within which it occurs by defining a reference time origin  $t_{\text{org}}$  and end time  $t_{\text{end}}$ , the total duration  $t_{\text{span}}$  of which is

$$t_{\text{span}} = t_{\text{end}} - t_{\text{org}} \quad (3.7)$$

A single, *note* event  $y$  occurring in this time-span may be described by the tuple  $(t_s, t_d, \nu)$  as shown in Figure 3.1, where  $t_s$  represents start or *onset* time relative to  $t_{\text{org}}$ ,  $t_d$  represents note duration in the same units and  $\nu$  represents the note *velocity* (i.e. the dynamic; how loud or accented the event is relative to others), where  $\nu \geq 0$ .

This allows us to represent an arbitrary rhythm as a sequence of notes  $Y$ , ordered in time

$$Y = \langle y_0, y_1, \dots, y_{|Y|-1} \rangle. \quad (3.8)$$

We will use superscript notation to index individual elements of tuples so  $y_n^{t_s}$  for example will represent the onset time for the  $n^{\text{th}}$  note in  $Y$ .

Rests, time periods where there is an absence of sounded notes in music, are as important as the note events themselves. The representation detailed here allows a rest to occur at the start of the rhythm where  $y_0^{t_s} \geq 0$  i.e. the first note starts after  $t_{\text{org}}$ , a rest may occur in between notes where  $y_n^{t_s} + y_n^{t_d} < y_{n+1}^{t_s}$  and there may also be a rest at the end of the pattern if the final note finishes sounding before the end of the time-span i.e.  $y_{|Y|-1}^{t_s} + y_{|Y|-1}^{t_d} \leq t_{\text{span}}$ .

### 3.1.3 Discrete time representation

So far,  $t_s$  and  $t_d$  have been considered to be continuous variables in time. However, for the purposes of music theory it often serves to quantise them such that they are given as integer multiples of some discrete time unit  $\Delta t$ . Discretising time in this way, we may represent the time-span of  $Y$  as a sequence  $T$  comprising  $|T|$  equally spaced time points:

$$T = \bigodot_{m=0}^{|T|-1} \langle m\Delta t \rangle = \langle t_0, t_1, \dots, t_{|T|-1} \rangle. \quad (3.9)$$

where

$$|T| = \frac{t_{\text{span}}}{\Delta t}. \quad (3.10)$$

With the exception of Keith [Kei91], the syncopation models reviewed here only take account of note onsets ignoring notated duration. We may therefore choose  $\Delta t$  (and thus  $|T|$ ) for a given time-span sequence dependent upon onset times of notes in  $Y$ ; the choice of value being arbitrary provided that every note onset  $y_n^{t_s}$  can be precisely expressed as an integer multiple  $m\Delta t$  where  $m < |T|$ . For any particular sequence  $Y$ , there will be a minimum-length time-span sequence  $T_{\text{min}}$  for which

$$T_{\text{min}} = \arg \min_T |T| \quad (3.11)$$

where

$$T \in \{\hat{T} : \forall y_n \in Y, \exists t_m \in \hat{T} : t_m = y_n^{t_s}\} \quad (3.12)$$

$$\begin{array}{c}
 Y \quad \frac{4}{4} \left| \begin{array}{cccc} \text{♩} & \text{♩} & \text{♩} & \text{♩} \end{array} \right| \\
 \downarrow \\
 T_{\min} \left| \begin{array}{cccc} \times & \times & \times & \times \end{array} \right| \\
 \downarrow \\
 V_{\min} \langle \quad 1, \quad 0.8, \quad 1, \quad 0.8 \quad \rangle
 \end{array}$$

(a)

$$\begin{array}{c}
 Y \quad \frac{4}{4} \left| \begin{array}{ccccccc} \text{♩} & \text{♩} & \text{♩} & \text{♩} & \text{♩} & \text{♩} & \text{♩} \end{array} \right| \\
 \downarrow \\
 T_{\min} \left| \begin{array}{cccccccccccc} \times & \times & \times & \times & \times & \times & \times & \times & \times & \times & \times & \times \end{array} \right| \\
 \downarrow \\
 V_{\min} \langle \quad 0, \quad 0, \quad 0, \quad 1, \quad 0, \quad 0, \quad 0, \quad 0, \quad 0, \quad 0, \quad 1, \quad 0 \quad \rangle
 \end{array}$$

(b)

$$\begin{array}{c}
 Y \quad \frac{4}{4} \left| \begin{array}{ccccccc} \text{♩} & \text{♩} & \text{♩} & \text{♩} & \text{♩} & \text{♩} & \text{♩} \end{array} \right| \\
 \downarrow \\
 T_{\min} \left| \begin{array}{cccccccccccc} \times & \times & \times & \times & \times & \times & \times & \times & \times & \times & \times & \times \end{array} \right| \\
 \downarrow \\
 V_{\min} \langle \quad 1, \quad 0, \quad 0, \quad 1, \quad 0, \quad 0, \quad 1, \quad 0, \quad 0, \quad 0, \quad 1, \quad 0, \quad 1, \quad 0, \quad 0, \quad 0 \quad \rangle
 \end{array}$$

(c)

Figure 3.2: Example rhythm-patterns with their minimum-length time-span and velocity sequences. Each of the rhythm-patterns above is a single bar in 4/4 meter and we will assume a tempo of 120 quarter-note BPM (i.e. 2 beats per second). Example (a) contains four equally spaced quarter-notes with the first and third notes accented (refer to Section 2.1.2), so  $|T_{\min}| = 4$  with  $\Delta t$  of half a second. Example (b) contains both quarter-notes and quarter-note triplets thus  $|T_{\min}| = 12$  with  $\Delta t = 1/6$ s and (c) the *Son* clave rhythm contains an onset in the fourth 16<sup>th</sup> note position so  $|T_{\min}| = 16$  with  $\Delta t = 1/8$ s.

i.e.  $T_{\min}$  is the shortest possible time-span sequence for which the start time  $y_n^{t_s}$  of every note in  $Y$  has a corresponding time point  $t_m$ .

With the time resolution of  $T$  determined, we may represent the notes

in  $Y$  as a sequence  $V$  of sampled velocity values

$$V = \bigodot_{m=0}^{|T|-1} \langle v_m \rangle \quad (3.13)$$

where

$$v_m = \begin{cases} \frac{y_n^\nu}{\max(y^\nu: y^\nu \in Y)}, & \exists y_n \in Y : y_n^{t_s} = m\Delta t; \\ 0, & \text{otherwise.} \end{cases} \quad (3.14)$$

i.e. each element  $v_m$  in  $V$  corresponds to the velocity at time point  $t_m$  in  $T$ . The value of  $v_m$  is the normalised velocity  $y_n^\nu$  of a note in  $Y$  if an onset is present at  $m\Delta t$  or zero where there is none. Figure 3.2 shows example minimum-length time-span sequences for three one-bar rhythm-patterns and their associated minimum-length velocity sequences. The rhythm-pattern shown in Figure 3.2a is represented with  $V_{\min} = \langle 1, 0.8, 1, 0.8 \rangle$ . An equally valid velocity sequence could be produced with values  $|T| = 8$  and  $\Delta t = 0.25\text{s}$  giving  $V = \langle 1, 0, 0.8, 0, 1, 0, 0.8, 0 \rangle$ , but every second element is redundant in this case.

In Figure 3.2a, two notes are accented, therefore velocities in  $V$  vary in magnitude (in our example, between arbitrary values of 0.8 or 1). In some cases, we are concerned with whether a note onset is present at a particular time point rather than what its velocity value is, so we will introduce a binary sequence  $B$  of bits  $b_m$  given by

$$B = \langle b_0, b_1, \dots, b_{|B|-1} \rangle = \bigodot_{m=0}^{|T|-1} \langle \lceil v_m \rceil \rangle, \quad v_m \in V \quad (3.15)$$

where  $\lceil \cdot \rceil$  denotes the ceiling function. Thus, for the rhythm-pattern in Figure 3.2a  $B = \langle 1, 1, 1, 1 \rangle$ . In Figure 3.2b and c, no dynamics or accents are shown, so all notes are assumed to be of the same velocity, thus  $B$  will be equal to  $V$ .

A useful property of this binary sequence representation is that simple combinational logic can be employed to analyse the matching of rhythm-patterns by specifying *masking* sequences [Lew72]. For example, a binary sequence  $B$  with onsets in every position (as in Figure 3.2a) would be

matched by the expression  $\langle 1 \rangle^{|B|}$ ; a sequence containing  $|B|$  ones. Likewise, a sequence with no onsets (i.e it contains only a rest) would be equivalent to  $|B|$  zeros which may be written  $\langle 0 \rangle^{|B|}$ . We may express a mask pattern that contains a single onset at the very start of the time-span followed by rests as  $\langle 1 \rangle * \langle 0 \rangle^{|B|-1}$ . We also utilise the digital logic notion of a *don't care* notated as X. This type of value can be used in a mask pattern to signify that both 1 and 0 can be matched in that position. For example, if we want to match any rhythm-pattern that starts with a rest, we could express this as the mask pattern  $\langle 0 \rangle * \langle X \rangle^{|B|-1}$  (the sequence shown in Figure 3.2b would match this pattern).

### 3.1.4 Metrical hierarchy

The previous section defined the atomic representation of note events in time. As listeners however, the way we perceive the grouping of those events is of huge importance in the analysis of syncopation. An isolated note event cannot be syncopated; for syncopation to exist, it is necessary for the listener to have already developed a sense of meter. In Section 2.1.3, we have introduced the concept of isochronous-meter from the perspective of music theory. The following sections formalise the mathematical expression of this type of meter, especially metrical level and metrical weight.

#### Metrical level

Each metrical level in a metrical hierarchy represents a level of periodicity in the rhythm sequence, such as bar level, beat level or tatum level. Here we will define a metrical level index  $L \in [0, L_{\max}]$  with index 0 being the top level, i.e. the root node in the tree. Throughout this thesis, we set the bar level as the top level in the metrical hierarchy, and the lowest level as the tatum level (with the atomic period determined by  $\Delta t$ ).

The metrical hierarchy may be described with a sequence of subdivisions  $\Lambda = \langle \lambda_0, \lambda_1, \dots, \lambda_{L_{\max}} \rangle$  such that in each level  $L$ , the value  $\lambda_L$  specifies how nodes in the level above (i.e.  $L-1$ ) should be split to produce the current level. Analysing down to  $L_{\max} = 2$ , a single bar in 4/4 simple-duple

meter has subdivisions  $\Lambda = \langle 1, 2, 2 \rangle$  as shown in Figure 3.3a. The simple-triple meter 3/4 and compound-duple 6/8 both have six eighth-notes in a bar but their subdivisions are different; the 3/4 meter has three groups of two  $\Lambda = \langle 1, 3, 2 \rangle$  whereas the 6/8 has two groups of three  $\Lambda = \langle 1, 2, 3 \rangle$  (Figure 3.3b and c).

### Metrical weight

Events at different metrical positions vary in perceptual salience or *metrical weight* [PK90]. These weights may be represented as a sequence  $W = \langle w_0, w_1, \dots, w_{L_{\max}} \rangle$ . As mentioned in Section 2.1.3, the prevailing hypothesis for the assignment of weights in the hierarchy is that a time point that exists in both the current metrical level and the level above is said to have a *strong* weight compared to time points that are not also present in the level above [LJ83]. As Figure 3.3 shows, the left-most child of any node is considered to be a *strong* position and takes the weight of its parent while the remaining child nodes are considered to be *weak*, weighted with  $w_L$  according to the current metrical level. The choice of values for the weights in  $W$  can vary between different models but the assignment of weights to nodes is common to all.

We define a sequence  $H_L$  which contains the metrical weights at a given level in the hierarchy. The initial sequence for  $L = 0$  is built as follows

$$H_0 = \langle w_0 \rangle^{\lambda_0} \quad \text{for } \lambda_0 \geq 1. \quad (3.16)$$

$H_L$  for all subsequent levels may be calculated from sequence  $H_{L-1}$ :

$$H_L = \bigodot_{h_j \in H_{L-1}} \langle h_j \rangle * \langle w_L \rangle^{\lambda_L - 1} \quad \text{for } L > 0, \lambda_L \geq 2. \quad (3.17)$$

For example, using equations 3.16 and 3.17, a 6/8 meter as shown in Figure 3.3c with metrical weights  $W = \langle w_0, w_1, w_2 \rangle$  and subdivisions  $\Lambda = \langle 1, 2, 3 \rangle$  would yield

$$\begin{aligned} H_0 &= \langle w_0 \rangle \\ H_1 &= \langle w_0, w_1 \rangle \\ H_2 &= \langle w_0, w_2, w_2, w_1, w_2, w_2 \rangle. \end{aligned}$$

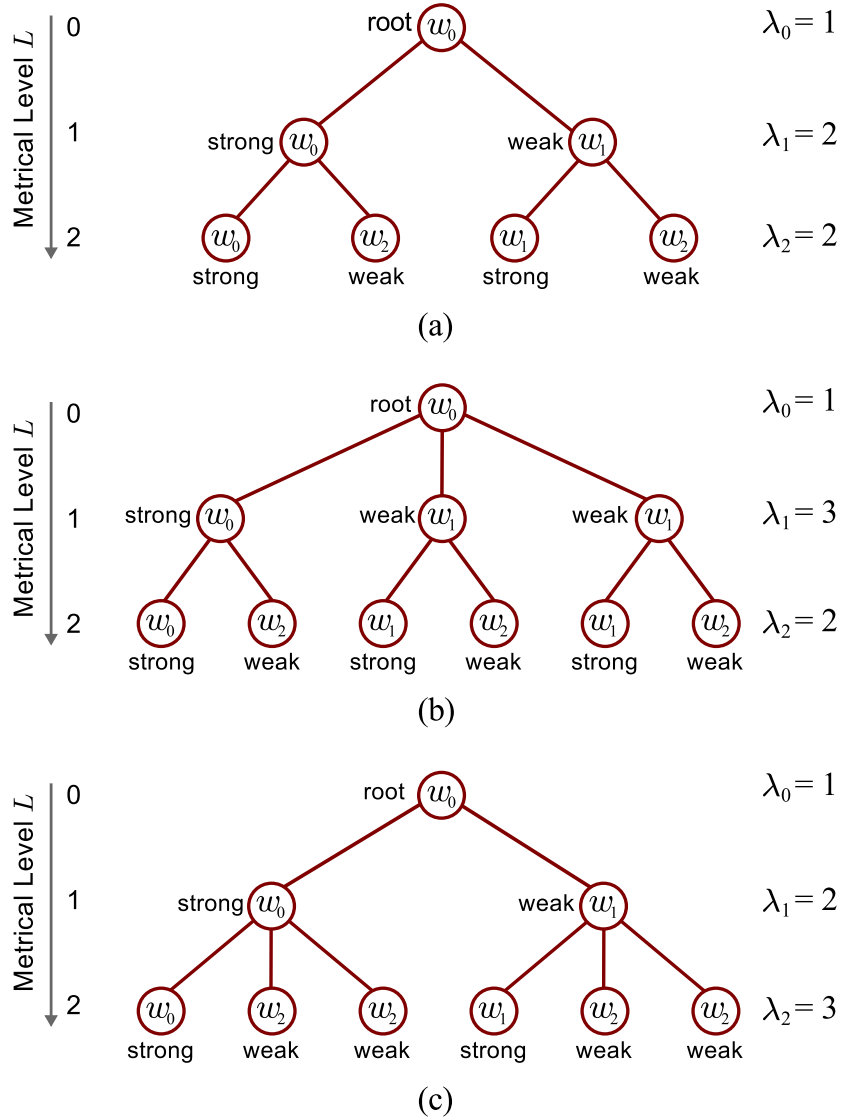


Figure 3.3: Metrical hierarchies for different time-signatures. (a) A simple-duple hierarchy dividing the bar into two groups of two (as with a 4/4 time-signature). (b) A simple-triple hierarchy dividing a bar into three beats, each of which is subdivided by two (e.g. 3/4 time-signature). (c) A compound-duple hierarchy dividing a bar into two beats, each of which is subdivided by three (e.g. 6/8 time-signature). Reading the weights from left to right in any level  $L$  gives the elements in sequence  $H_L$  (see Equations 3.16 and 3.17).

To keep the representation as general as possible, we allow  $\lambda_0 \geq 1$  (i.e. it is possible to have more than one top-level node). For  $L > 0$ , nodes must be subdivided so  $\lambda_L \geq 2$ .

## 3.2 Syncopation models

In Section 2.3.1, we categorised the models for syncopation into four broad groups: *hierarchical*, *off-beat*, *classification* and *autocorrelation*. Hierarchical models include Longuet-Higgins and Lee [LHL84], Pressing [Pre97], Toussaint’s metric complexity [Tou02] and Sioros and Guedes [SG11]. They all relate syncopation to the metrical hierarchy (Section 2.1.3).

Off-beat models mainly focus on capturing off-beat events. Two models in our study fall into this category: Gómez et al.’s Weighted Note-to-Beat Distance [GMRT05] and Toussaint’s off-beatness [Tou05].

Finally, Pressing’s and Keith’s model can be grouped as classification models, as they classify individual note or rhythmic sequence into predefined syncopation types. In the following sections, we review each of the models mentioned above<sup>3</sup>.

### 3.2.1 Longuet-Higgins and Lee 1984 (LHL)

The hypothesis of Longuet-Higgins and Lee’s [LHL84] model is that a syncopation occurs when a rest (R) in one metrical position follows a note (N) in a weaker position. Where such a note-rest pair occurs, the difference in their metrical weights is taken as a local syncopation score. Summing the local scores produces the syncopation prediction for the whole rhythm sequence.

Mathematically, the model decomposes the pattern into a tree structure using the metrical hierarchy from Section 3.1.4 with metrical weights  $w_L = -L$  for all  $w_L \in W$  i.e.  $W = \langle 0, -1, -2, \dots \rangle$  (Figure 3.4). In [LHL84], Longuet-Higgins and Lee describe a set of *realisation rules*, which are applied recursively to generate the tree structure for a rhythm-pattern before calculating syncopation values; we follow this approach to formulate our description of the process here. In contrast, implementations described elsewhere in [FR07, Thu08, SG11] have recast the LHL algorithm as an

---

<sup>3</sup>Another syncopation model, Keller and Schubert’s autocorrelation-based model, will be excluded in this review and the evaluation in Chapter 5, because it is designed to handle music sequences with melodic and durational variation. The evaluation process in this thesis uses un-pitched percussive stimuli so it is not appropriate to include their model here.



iterative process, starting by generating a complete metrical hierarchy down to  $L_{\max}$ , irrespective of the given rhythm-pattern. While this approach is equally valid, it introduces a problem of redundant rest nodes that must be dealt with before syncopation can be calculated; this caveat is dealt with in [Thu08] but omitted in [FR07] and [SG11].

Each terminal node  $\psi$  in the tree can be notated as a duple  $(\eta, w)$  where  $\eta \in \{\mathbf{N}, \mathbf{R}\}$  represents the node type (i.e. note  $\mathbf{N}$  or rest  $\mathbf{R}$ ) and  $w$  is its metrical weight. We define a function  $\kappa(B, w, L)$  that will recurse the tree for binary sequence  $B$  and return a sequence  $\Psi$  containing the terminal nodes in time order. For each node, if its individual binary sequence does not fall into one of the two terminal categories then it will be split into  $\lambda_{L+1}$  sub-sequences. These sub-sequences can be analysed in the same fashion recursively until all the terminal nodes are identified:

$$\kappa(B, w, L) = \begin{cases} \langle (\mathbf{N}, w) \rangle, & \text{if } B = \langle 1 \rangle * \langle 0 \rangle^{|B|-1}; \\ \langle (\mathbf{R}, w) \rangle, & \text{if } B = \langle 0 \rangle^{|B|}; \\ \bigodot_{a=0}^{\lambda_{L+1}-1} \kappa(\langle \cdot \rangle_a, \hat{w}_a, L+1), & \text{otherwise} \end{cases}$$

$$\text{for } \langle \cdot \rangle_a \in B|_{\lambda_{L+1}} \quad \text{and} \quad \hat{w}_a \in \langle w \rangle * \langle w_L \rangle^{\lambda_{L+1}-1}. \quad (3.18)$$

For a given sequence  $B$ , the sequence of terminal nodes  $\Psi$  is calculated starting with  $w_0$  and  $L = 0$ :

$$\Psi = \kappa(B, w_0, 0).$$

For a given node  $\psi_i \in \Psi$ , we will use the notation  $\psi_i^w$  denote its metrical weight and  $\psi_i^\eta$  its node type. Having calculated  $\Psi$ , we now find each rest-note pair for which  $\psi_j$  is the nearest note node preceding rest node  $\psi_i$ . If metrical weight  $\psi_i^w \geq \psi_j^w$  then we obtain a local syncopation value  $\psi_i^w - \psi_j^w$  for that pair. The total syncopation score for node sequence  $\Psi$  is the sum of all local scores given by the function

$$S_{\text{LHL}}(Y) = \sum_i (\psi_i^w - \psi_j^w) \quad (3.19)$$

for all  $\psi_i$  such that  $\psi_i, \psi_j \in \Psi : (\psi_i^\eta = \mathbf{R}, \psi_j^\eta = \mathbf{N})$  and  $(\psi_i^w \geq \psi_j^w)$  where  $j = \max(j < i)$ .

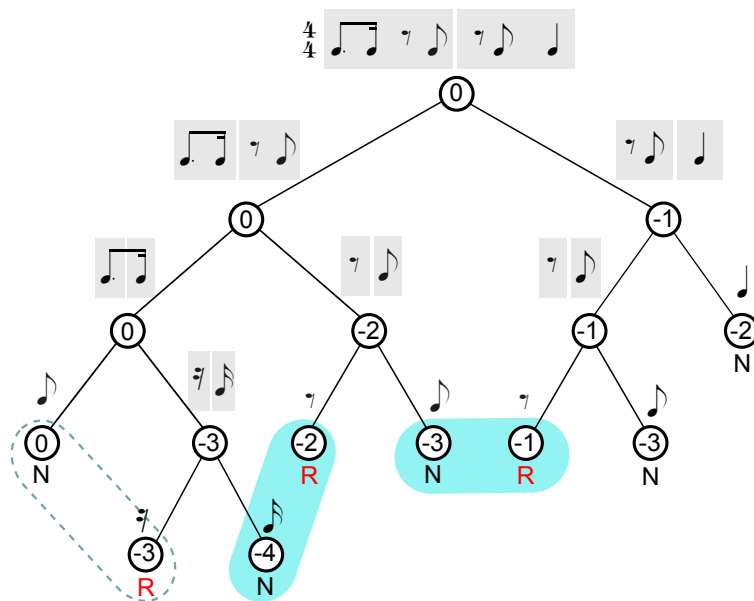


Figure 3.4: Tree decomposition of the Son clave rhythm for the LHL syncopation measure. For this rhythm-pattern from Figure 3.2c, the sequence of terminal nodes  $\Psi = \langle (N,0), (R,-3), (N,-4), (R,-2), (N,-3), (R,-1), (N,-3), (N,-2) \rangle$ . For each R (rest) node  $\psi_i$ , the preceding N (note) node  $\psi_j$  must be identified and where the metrical weight  $\psi_i^w \geq \psi_j^w$  a local syncopation of value  $\psi_i^w - \psi_j^w$  is said to have occurred (in this example there are two such cases, both of which score 2). The total syncopation score for a rhythm sequence  $Y$  is the sum of all local scores, in this case  $S_{\text{LHL}}(Y) = 2 + 2 = 4$ .

A practical point to consider for Equation 3.19 is that the absence of a syncopation score is not the same as a score of zero. A zero score will be produced where both nodes in a rest-note pair have the same weight<sup>4</sup>. In practice, when calculating the final sum, we check for the case where there are no rest-note pairs for which  $\psi_i^w \geq \psi_j^w$  and in that case return  $S_{\text{LHL}}(Y) = -1$ .

Each non-terminal node is split into the number of sub-sequences defined by  $\lambda_L$  so the LHL algorithm does not handle polyrhythmic sequences (such as in Figure 3.2b) because they contain nodes with rhythmic subdivisions outside that defined by the sequence  $\Lambda$ .

A special case that should be noted is a rhythm sequence that starts with a rest (e.g. of the form  $\langle 0 \rangle * \langle X \rangle^{|B|-1}$ ). The first R node will have no

<sup>4</sup>This can easily occur in a 6/8 meter for example where consecutive weak-beats have the same weight i.e.  $H_2 = \langle 0, -2, -2, -1, -2, -2 \rangle$

preceding N in this case, so calculating a local syncopation here requires an extra rule. One approach is to treat the sequence as a cycle so the local syncopation can be calculated by wrapping around and using the weight of the final N node. In the case of the rhythm-stimuli used to collect our human ratings however, a bar of metronome was presented before the rhythm-pattern under test (see Figure 5.1 in Section 5.1). For our purposes we will therefore use the final metronome beat as the preceding N node in this calculation instead.

### 3.2.2 Pressing 1997 (PRS)

Pressing’s cognitive complexity model [Pre97, PL93] specifies six prototype binary sequences and ranks them in terms of *cognitive cost*. The model analyses the cost for the whole rhythm-pattern and its sub-sequences at each metrical level determined by  $\lambda_L$ . The final output will be a weighted sum of the costs in each level.

Unfortunately the description of the prototype patterns is incomplete in the original papers. The *sub-beat* prototype (cost = 4) is not defined in [PL93] and has only the description “this type cannot occur in a cycle of length four” in [Pre97], so we omit it here. The descriptions and examples for the remaining prototypes are clear but do not cover all possible rhythm-patterns so we extend their definitions slightly in order to make a complete implementation possible.

The *null* prototype (cost = 0) has either a note or a rest in the first position of the sequence and rests thereafter (i.e. a pattern that would be considered a terminal node in the LHL algorithm.). The pattern is defined as follows

$$\langle null \rangle = \langle X \rangle * \langle 0 \rangle^{|B|-1} \quad (3.20)$$

e.g.  $\frac{4}{4} | \text{♩} \text{ } \text{ } \text{ } |$  and  $\frac{4}{4} | \text{ } \text{ } \text{ } \text{ } |$

The *filled* prototype (cost = 1) has a note in every position of the sequence:

$$\langle filled \rangle = \langle 1 \rangle^{|B|} \quad (3.21)$$

e.g.  $\frac{4}{4} | \text{♩} \text{♩} \text{♩} \text{♩} |$

The *run* prototype (cost = 2) has a note in the first position followed by a run of other notes (but not filled). We will define two prototype patterns that match this definition, first *run 1* ends with a 0 in the final position of the sequence (this is a generalisation of the pattern described in [PL93]):

$$\langle \text{run } 1 \rangle = \langle 1 \rangle * \langle X \rangle^{|B|-2} * \langle 0 \rangle \quad (3.22)$$

e.g.  $\frac{4}{4} | \text{♩} \text{♩} \text{♩} \text{♩} \text{♩} \text{♩} \text{♩} \text{♩} \text{♩} \text{♩} |$

Second, we define a pattern *run 2* that starts with a note in the first position, followed by a run of other notes but a 0 in the first position of the following sequence. It is necessary to define this second prototype in order that the set of all possible patterns can be matched.

$$\langle \text{run } 2 \rangle = \langle \langle 1 \rangle * \langle X \rangle^{|B|-1}, \langle 0 \rangle * \langle X \rangle^{|B|-1} \rangle \quad (3.23)$$

e.g.  $\frac{4}{4} | \text{♩} \text{♩} \text{♩} \text{♩} \text{♩} \text{♩} \text{♩} \text{♩} | \text{♩}$

The *upbeat* prototype (cost = 3) ends with a 1 in the final position of the sequence but also requires that the first position of the following sequence also be a 1.

$$\langle \text{upbeat} \rangle = \langle \langle 1 \rangle * \langle X \rangle^{|B|-2} * \langle 1 \rangle, \langle 1 \rangle * \langle X \rangle^{|B|-1} \rangle \quad (3.24)$$

e.g.  $\frac{4}{4} | \text{♩} \text{♩} \text{♩} \text{♩} \text{♩} \text{♩} \text{♩} \text{♩} | \text{♩}$

The *syncopated* prototype (cost = 5) has a 0 in the first position (i.e. the strongest metrical position):

$$\langle \text{syncopated} \rangle = \langle 0 \rangle * \langle X \rangle^{|B|-1} \quad (3.25)$$

e.g.  $\frac{4}{4} | \text{♩} \text{♩} \text{♩} \text{♩} \text{♩} \text{♩} \text{♩} \text{♩} |$

We may now define a function  $g(B, \hat{B})$  that will determine the cost for a given binary sequence  $B$  by comparing it to the above prototypes. However, to compare against these prototypes, we must first convert the

sequence  $B$  to its minimum-length representation  $B_{\min}$ . To illustrate,  $B = \langle 1, 0, 1, 0 \rangle$  matches Pressing's description of a *filled* pattern in [Pre97] but is not equivalent to the prototype as defined in Equation 3.21; reducing the sequence to  $B_{\min} = \langle 1, 1 \rangle$  allows the correct match to be made. Because prototypes *run 2* and *upbeat* require knowledge of the following sequence's first element, this function takes a second sequence  $\hat{B}$  as an argument as well.

$$g(B, \hat{B}) = \begin{cases} 0, & \text{if } B_{\min} = \langle \text{null} \rangle; \\ 1, & \text{if } B_{\min} = \langle \text{filled} \rangle; \\ 2, & \text{if } B_{\min} = \langle \text{run 1} \rangle; \\ 2, & \text{if } \langle B_{\min}, \hat{B} \rangle = \langle \text{run 2} \rangle; \\ 3, & \text{if } \langle B_{\min}, \hat{B} \rangle = \langle \text{upbeat} \rangle; \\ 5, & \text{if } B_{\min} = \langle \text{syncopated} \rangle \end{cases} \quad (3.26)$$

The prototype definitions are not mutually exclusive, so comparisons are evaluated in order of precedence from low cost to high.

At each metrical level, the binary sequence  $B$  of the input rhythm  $Y$  is divided into  $\mathcal{L}$  sub-sequences. Each sub-sequence is evaluated by function  $g(\langle \cdot \rangle_1, \langle \cdot \rangle_2)$ , the resulting costs summed and then the total normalised by  $\mathcal{L}$ :

$$q(B, \mathcal{L}) = \frac{\sum_{a=0}^{\mathcal{L}-1} g(\langle \cdot \rangle_a, \langle \cdot \rangle_{(a+1 \bmod \mathcal{L})})}{\mathcal{L}} \quad \text{for } \langle \cdot \rangle_a \in B \parallel_{\mathcal{L}} . \quad (3.27)$$

The calculation of the total score over all levels may be expressed recursively as follows:

$$f(B, L, \mathcal{L}) = \begin{cases} 0, & \text{if } |B| < 2; \\ q(B, \mathcal{L}) + f(B, L+1, \mathcal{L} \cdot \lambda_{L+1}) & \text{otherwise.} \end{cases} \quad (3.28)$$

where  $\lambda_L \in \Lambda$ . At each level, the value of  $q(B, \mathcal{L})$  is evaluated and then summed with  $f(B, L, \mathcal{L})$  for the next level until all levels in  $\Lambda$  have been evaluated. On each recursion, the current value of  $\mathcal{L}$  is multiplied by the current value of  $\lambda_L$  which means that in any given level  $L$ ,  $\mathcal{L} = \prod_{l=0}^L \lambda_l$ . The overall syncopation value for a given note sequence  $Y$  is therefore:

$$\mathcal{S}_{\text{PRS}}(Y) = f(B, 0, \lambda_0) \quad (3.29)$$

An example of how this algorithm is applied to the Son clave rhythm sequence is shown in Figure 3.5. The minimum-length time-span for the

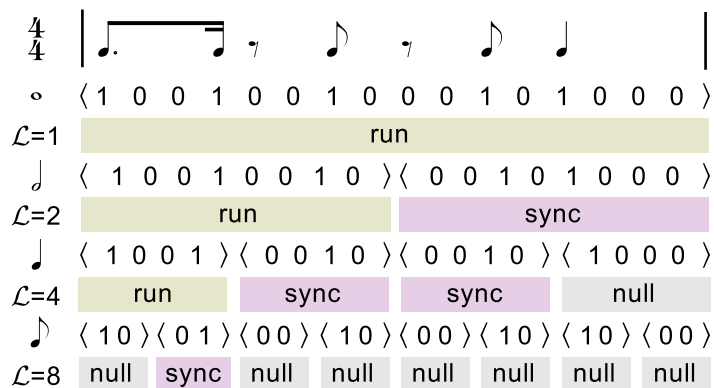


Figure 3.5: Example calculation of the Pressing syncopation measure for the Son clave rhythm-pattern. In each metrical level, the matching prototypes for each subdivision are shown.

sequence has  $|T| = 16$ . The results are summed in each level and normalised by  $\mathcal{L}$  giving  $\mathcal{S}_{\text{PRS}}(Y) = \frac{2}{1} + \frac{7}{2} + \frac{12}{4} + \frac{5}{8} = 9.125$ . Note that for this analysis  $\Lambda = \langle 1, 2, 2, 2 \rangle$ , we do not need to analyse at levels lower than eighth-notes because all spans would be nulls at lower levels for this rhythm-pattern.

### 3.2.3 Toussaint 2002 ‘Metric Complexity’ (TMC)

Toussaint’s *metric complexity* measure [Tou02] is another model that uses metrical hierarchy to calculate a syncopation prediction. In this model, the metrical weights are defined as  $w_L = L_{\text{max}} - L + 1$  so the highest weight will be  $w_0$  and the lowest will be  $w_{L_{\text{max}}} = 1$ .

The model first defines a measure of *metricity* (metrical simplicity)  $\varphi(B, H_{L_{\text{max}}})$  for binary sequence  $B$  which is the sum of the weights for each note; *simpler* rhythm sequences will have notes at stronger time positions in the hierarchy and hence a higher metricity score

$$\varphi(B, H_{L_{\text{max}}}) = \sum_{m=0}^{|B|-1} b_m h_m \quad (3.30)$$

where  $H_{L_{\text{max}}}$  is the sequence of metrical weights as defined in Equation 3.17 and  $L_{\text{max}}$  is chosen such that  $|H_{L_{\text{max}}}| = |B|$ . The hypothesis of the model is that the level of *metrical complexity* (i.e. syncopation) is the difference between the metricity for  $B$  and the maximum possible metricity for a

sequence containing the same number of notes

$$\begin{aligned} S_{\text{TMC}}(Y) &= \max(\varphi(\hat{B}, H_{L_{\max}})) - \varphi(B, H_{L_{\max}}) & (3.31) \\ \forall \hat{B} \in \{\hat{B} : \sum_m \hat{b}_m &= \sum_m b_m\} \text{ where } \hat{b}_m \in \hat{B}, b_m \in B \end{aligned}$$

For example, the Son clave rhythm from Figure 3.2c has 4/4 time-signature and  $|B_{\min}| = 16$  so we require  $L \in [0, 4]$  to represent its metrical hierarchy. The parameters for the calculation are therefore

$$\begin{aligned} W &= \langle 5, 4, 3, 2, 1 \rangle, & \Lambda &= \langle 1, 2, 2, 2, 2 \rangle, \\ H_4 &= \langle 5, 1, 2, 1, 3, 1, 2, 1, 4, 1, 2, 1, 3, 1, 2, 1 \rangle, \\ B_{\min} &= \langle 1, 0, 0, 1, 0, 0, 1, 0, 0, 0, 1, 0, 1, 0, 0, 0 \rangle. \end{aligned}$$

The metricity will therefore be  $5 + 1 + 2 + 2 + 3 = 13$  while the maximum metricity score for a five-note rhythm would be  $5 + 4 + 3 + 3 + 2 = 17$ . The syncopation prediction  $S_{\text{TMC}}$  for the Son clave rhythm would therefore be  $17 - 13 = 4$ .

### 3.2.4 Sioros and Guedes 2011 (SG)

The most recent model in our study, Sioros and Guedes [SG11, SHG12] also uses metrical hierarchy to determine syncopation. This model has three main hypotheses: First, accenting of notes affects perceived syncopation and should be included in the model (the only model in this study to do so, but it should be noted that the implementation of the SG model used in the evaluation in Chapter 5 does not include it because our chosen rhythm stimuli have equal velocity notes throughout). Second, humans try to minimise the syncopation of a particular note relative to its neighbours in each level of the metrical hierarchy. Third, syncopations at the beat level are more salient than those that occur in higher or lower metrical levels so the outcome should be scaled to reflect this [SMC<sup>+</sup>13].

The metrical weights for this model are  $w_L = L$  for all  $w_L \in W$ . To calculate the syncopation score<sup>5</sup>, we first define a function  $\vartheta(m, \hat{m})$  that

<sup>5</sup>The original description of the algorithm in [SG11, SHG12] is mostly given in prose but a Max/MSP patch and C++ source code for a Max/MSP external has been made available online at [Sio11] from which our mathematical formulation has been derived.

calculates a *difference level factor* between two notes in velocity sequence  $V$  with indices  $m$  and  $\hat{m}$ ,

$$\vartheta(m, \hat{m}) = (v_m - v_{\hat{m}}) \left( \frac{\beta |h_m - h_{\hat{m}}|}{4} + 1 - \beta \right) \quad (3.32)$$

where  $v \in V$ ,  $h \in H_{L_{\max}}$  and  $\beta$  is a weighting factor.

To obtain the syncopation score for a note at a given metrical level  $\ell$ , we define a function  $u(m, \ell)$  that calculates the average of the difference between the note at index  $m$  and its neighbours in the same metrical level:

$$u(m, \ell) = \frac{\gamma \cdot \vartheta(m, \varrho(m, \ell)) + \vartheta(m, \rho(m, \ell))}{\gamma + 1} \quad (3.33)$$

where a weighting factor  $\gamma$  is included to reduce the contribution of the previous note, a function  $\varrho(m, \ell)$  calculates the index of the previous note:

$$\varrho(m, \ell) = \arg \max_{\hat{m} \bmod |V|} (h_{(\hat{m} \bmod |V|)} \leq \ell, \hat{m} < m) \quad (3.34)$$

and a second function  $\rho(m, \ell)$  calculates the index of the next note:

$$\rho(m, \ell) = \arg \min_{\hat{m} \bmod |V|} (h_{(\hat{m} \bmod |V|)} \leq \ell, \hat{m} > m). \quad (3.35)$$

Values for the weighting factors are reported in [SG11] as  $\beta = 0.5$  and  $\gamma = 0.8$ .

A note may exist in multiple levels of the hierarchy and thus the syncopation score  $s_m$  is calculated by finding the minimum value of  $u(m, \ell)$  for each level of the hierarchy for which the note is a member:

$$s_m = \begin{cases} 0, & \text{if } v_m = 0; \\ \min (u(m, \ell)) \forall \{\ell : \ell \in [h_m, h_{\max}]\} & \text{otherwise.} \end{cases} \quad (3.36)$$

where

$$h_{\max} = \max(h_m \in H_{L_{\max}}) \quad (3.37)$$

Figure 3.6 demonstrates calculation of syncopation scores for the Son clave rhythm from Figure 3.2c. After personal communication with George Sioros [Sio14] we have used  $\Lambda = \langle 1, 2, 2, 2, 2 \rangle$  as our metrical hierarchy to implement the SG algorithm. It should be noted, however, that an alternative hierarchy  $\Lambda = \langle 2, 2, 2, 2 \rangle$  has been used in examples in [SG11]



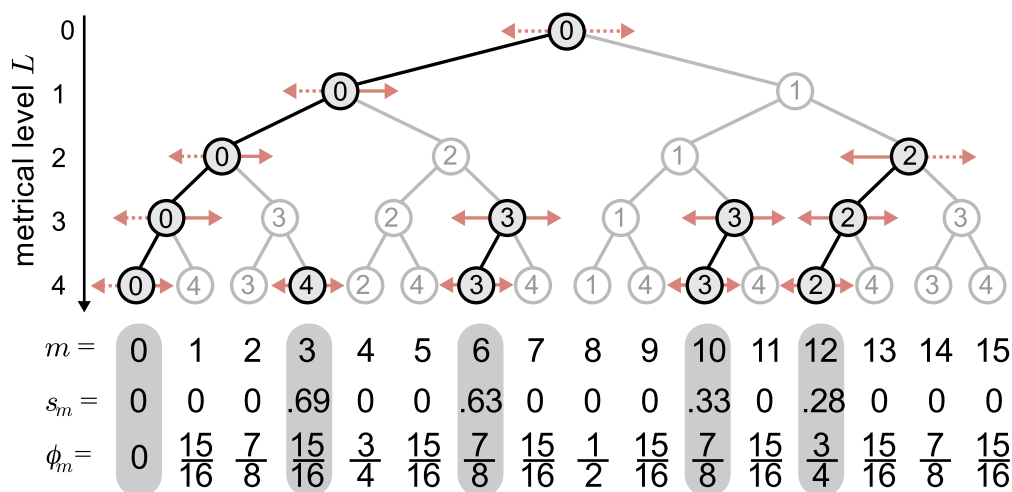


Figure 3.6: Sioros and Guedes syncopation scores and potentials for the Son clave rhythm. The metrical hierarchy is generated and the minimum syncopation score  $s_m$  for each note is calculated by comparing it against its neighbours in each of the metrical levels in which it resides (see Equation 3.36). Each score is then multiplied by the syncopation potential  $\phi_m$  and the results are summed to give the total syncopation value for the rhythm-pattern, in this case  $S_{SG} = 1.698$ .

and [SHG12] which produces a tree with two top-level nodes. This is explained in [SMC<sup>+</sup>13] as an attempt to correct for the effect of tempo on syncopation; an effect that has yet to be studied formally.

Once the syncopation scores have been calculated for each note in the sequence, they are weighted by a *syncopation potential*  $\phi_m$  according to their metrical level:

$$\phi_m = (1 - 0.5^{h_m}) \quad (3.38)$$

The total syncopation prediction from this model for a given sequence is the sum of all weighted scores for individual notes:

$$S_{SG}(Y) = \sum_{m=0}^{|V|-1} s_m \phi_m \quad (3.39)$$

Separate normalisation approaches for this model are reported in [SG11] and [SHG12] but, on the advice of [Sio14], we use the absolute value for our evaluation in Chapter 5.

### 3.2.5 Keith 1991 (KTH)

The hypothesis of Keith's model [Kei91] is that syncopations occur where notes start or end at *off-beat* positions. Two individual types of syncopated event are defined and given a weight  $k$ . These two types are *hesitation*, where a note ends off the beat ( $k = 1$ ) and *anticipation*, where a note begins off the beat ( $k = 2$ ). Where a note exhibits both a hesitation and an anticipation, a *syncopation* is said to occur and the weights are summed to give  $k = 3$ . (See Figure 2.12 for examples.) Keith constrains the model to time-signatures where the number of beats per bar is a power of two.

The first step in calculating this model is to find  $\Delta t$  for time-span  $T$  such that:

$$|T| = \arg \min_{2^\xi} (2^\xi \geq |T_{\min}|) \quad (3.40)$$

We may then calculate a value  $c_n$  for each note  $y_n$  which is the highest power of two less than or equal to its duration:

$$c_n = \arg \max_{2^\xi} (2^\xi \leq \frac{y_n^{t_d}}{\Delta t}) \quad (3.41)$$

In this model, the onset  $y_n^{t_s}$  or end time ( $y_n^{t_s} + y_n^{t_d}$ ) are considered *off beat* if they are not a multiple of  $c_n \Delta t$ . Note that Keith's model assumes note duration to be the inter-onset interval between consecutive notes i.e.  $y_n^{t_d} = y_{n+1}^{t_s} - y_n^{t_s}$ . Using this rule, we may define 'off-beat' functions  $\mathbf{o}_n$  and  $\mathbf{e}_n$  that determine whether the onset or end of note  $y_n$  are off the beat respectively:

$$\mathbf{o}_n = \begin{cases} 0, & \text{if } \frac{y_n^{t_s}}{\Delta t} \bmod c_n = 0; \\ 2, & \text{otherwise (anticipation)} \end{cases} \quad (3.42)$$

and

$$\mathbf{e}_n = \begin{cases} 0, & \text{if } \frac{(y_n^{t_s} + y_n^{t_d})}{\Delta t} \bmod c_n = 0; \\ 1, & \text{otherwise (hesitation)} \end{cases} \quad (3.43)$$

The Keith syncopation weight for note  $y_n$  is therefore

$$k_n = \mathbf{o}_n + \mathbf{e}_n. \quad (3.44)$$

For a sequence  $Y$  comprising  $|Y|$  notes, the Keith syncopation score  $\mathcal{S}_{\text{KTH}}(Y)$

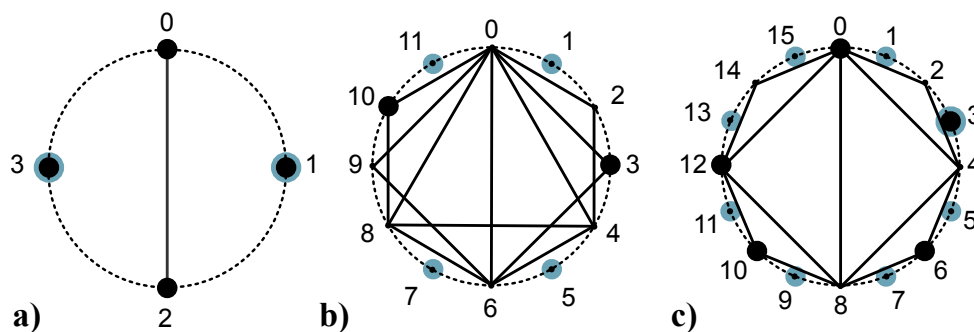


Figure 3.7: Geometric representation of  $B$  for the three rhythm patterns in Figure 3.2. The solid lines inside each cycle show the regular subdivisions for each time-span. Positions in a time-span that contain note events are shown filled in black on the circumference of each circle. The *off-beat* positions are shown in light blue on the circumference of each cycle. The four consecutive quarter-notes ( $|V| = 4$ ) in sequence (a) can only be divided evenly by 2 so the first and third positions will be considered off-beat, giving  $S_{\text{TOB}} = 2$  for this rhythm. The binary sequence for sequence (b) has  $|T| = 12$  so positions 1, 5, 7 and 11 are off-beat; as a result  $S_{\text{TOB}} = 0$ . The Son clave rhythm-pattern in (c) has  $|T| = 16$  and can therefore be subdivided by factors 2, 4 and 8 thus all the odd indices are considered ‘off-beat’. There is only one event on an odd index ( $m = 3$ ) so  $S_{\text{TOB}} = 1$  for this rhythm.

is the sum of all  $k$  values for the notes in the sequence:

$$S_{\text{KTH}}(Y) = \sum_{n=0}^{|Y|-1} k_n \quad (3.45)$$

For example, the  $k$  values for the notes of the polyrhythm pattern Figure 3.2b are 3 and 2 respectively, therefore the total syncopation value is 5.

### 3.2.6 Toussaint 2005 ‘Off-Beatness’ (TOB)

The off-beatness measure [Tou05] is a geometric model that treats the time-span of a rhythm sequence as a  $|T|$ -unit cycle. The hypothesis, as applied to syncopation, is that syncopated events are those that occur in ‘off-beat’ positions in the cycle; the definition of *off-beatness* in this case being any position that does not fall on a regular subdivision of the cycle

length  $|T|$ . The off-beatness  $\varsigma_m$  of a position can be calculated as follows:

$$\varsigma_m = \begin{cases} 0, & \text{if } m \bmod z = 0 \\ \forall \{z : |T| \bmod z = 0 : 1 < z < |T|\} \\ 1, & \text{otherwise} \end{cases} \quad (3.46)$$

For example, a time-span sequence of  $|T| = 12$  can be evenly subdivided by the values two, three, four and six. Therefore the dimensions of the sequence for which  $\varsigma_m \neq 0$  are those that are not divisible by these factors (i.e. dimensions 1, 5, 7 and 11) and so these are considered to be off-beat positions. Using this model, the total syncopation score for a sequence  $Y$  may be calculated by summing the number of syncopated events it contains:

$$S_{\text{TOB}}(Y) = \sum_{m=0}^{|B|-1} b_m \varsigma_m \quad (3.47)$$

Figure 3.7 shows a visual representation of the off-beatness measure applied to the three rhythm-pattern examples introduced in Figure 3.2.

### 3.2.7 Gómez 2005 ‘Weighted Note-to-Beat Distance’ (WNBD)

The WNBD model of Gómez et al. [GMRT05] defines note events that start in between beats in the notated meter to be ‘off-beat’ thus leading to syncopation. The syncopation value for a note is determined by its distance from the nearest beat<sup>6</sup>, notes being assumed to be contiguous in time with one ending as the next begins.

The position of a note  $y_n$  may be defined in terms of a distance measure  $d$  relative to its nearest beats  $\mu_i$  and  $\mu_{i+1}$  (i.e. the onset of  $y_n$  falls between  $\mu_i$  and  $\mu_{i+1}$ , see Figure 3.8).

$$\mu_i \leq y_n^{ts} \leq \mu_{i+1} \quad (3.48)$$

$$d(y_n, \mu_i) = \frac{y_n^{ts} - \mu_i}{\mu_{i+1} - \mu_i} \quad (3.49)$$

---

<sup>6</sup>Gómez et al. use the term ‘strong-beat’ in their paper but clarify that they mean the metric pulse, rather than strong-beats as defined with respect to metrical hierarchy as discussed in Section 3.1.4

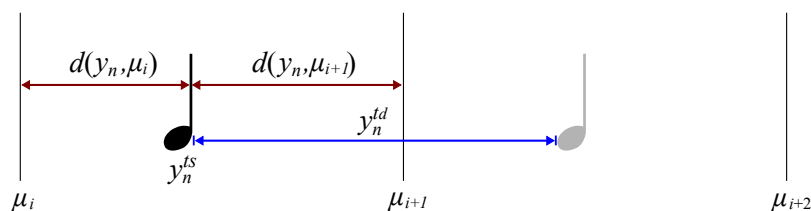


Figure 3.8: Illustration of the relationship between note  $y_n$  and the beats from  $\mu_i$  to  $\mu_i + 2$ .

To calculate the WNBD measure  $\mathcal{W}(y_n)$  for note  $y_n$ , we first find  $\mathcal{T}(y_n)$ , the distance from  $y_n$  to its closest beat.

$$\mathcal{T}(y_n) = \min(d(y_n, \mu_i), d(y_n, \mu_{i+1})) \quad (3.50)$$

The value of  $\mathcal{W}(y_n)$  can then be found by

$$\mathcal{W}(y_n) = \begin{cases} 0, & \text{if } d(y_n, \mu_i) = 0 \\ \frac{2}{\mathcal{T}(y_n)}, & \text{if } \mu_{i+1} < y_n^{ts} + y_n^{td} \leq \mu_{i+2} \\ \frac{1}{\mathcal{T}(y_n)}, & \text{otherwise} \end{cases} \quad (3.51)$$

For a note that starts on the beat (i.e.  $d(y_n, \mu_i) = 0$ ),  $\mathcal{W}(y)$  will be 0. For a note that starts off the beat (i.e.  $d(y_n, \mu_i) \neq 0$ ) and ends on or before the next beat  $\mu_{i+1}$ ,  $\mathcal{W}(y_n)$  will be  $\frac{1}{\mathcal{T}(y_n)}$ . Where a note is held on past  $\mu_{i+1}$  but ends on or before  $\mu_{i+2}$ ,  $\mathcal{W}(y_n)$  is  $\frac{2}{\mathcal{T}(y_n)}$ , weighting tied notes more highly than others. For notes that end after  $\mu_{i+2}$ ,  $\mathcal{W}(y_n)$  is set to  $\frac{1}{\mathcal{T}(y_n)}$ . If  $Y$  is a sequence of  $|Y|$  notes, the WNBD score for  $Y$  is the normalised sum of the  $\mathcal{W}$  values for each note in the sequence:

$$S_{\text{WNBD}}(Y) = \frac{1}{|Y|} \sum_{n=0}^{|Y|-1} \mathcal{W}(y_n) \quad (3.52)$$

To illustrate, the  $\mathcal{W}$  values for the notes of the Son clave example in Figure 3.2c are 0, 8, 4, 2 and 0 respectively, so the WNBD predicted syncopation is  $\frac{0+8+4+2+0}{5} = 2.8$ .

### 3.3 Summary

This chapter developed a consolidated mathematical representation for rhythm, metrical hierarchy and seven syncopation models. The main

purpose of this is to provide an in-depth review and to clarify ambiguities of the syncopation models that are frequently used in other studies. The secondary purpose is to implement these syncopation models into programming codes by transferring the corresponding mathematical equations. The implementation of the models facilitates the evaluation of these models in the later chapters. In the next chapter, we will switch to the investigation of syncopation in the area of perception, which enables a direct and formal evaluation of the syncopation models reviewed in this chapter.

# Chapter 4

## Syncopation and the score

In this chapter, we begin to explore syncopation perception: we manipulate the rhythmic score as an objective correlate of perceived syncopation. The main method in our experiment was to ask listeners to rate the degree of syncopation they perceived in response to a rendering of each score. Section 4.1 specifies the materials and the procedure in the experiment. We test the hypothesis that the following will have a degree of influence on perceived syncopation: i) time-signature, ii) whether the down-beat is present or missing, iii) presence of polyrhythms or monorhythms (which we will define here as any rhythm-pattern which is not polyrhythmic) and finally iv) within-bar location of rhythm-components. Results are discussed in Sections 4.2 and 4.3.

### 4.1 Experiment 1: Score

We asked musicians to give informed ratings of perceived syncopation for renderings of various three-bar scores. The ratings were taken over a fixed, five-point rating scale. In this experiment we required the listeners to judge a large number of rhythms, with a potentially large range of syncopation ratings. The fixed rating scale was intended to provide the minimum complexity in the experimental interface and the maximum efficiency during the procedure; the aim being that listeners would not be hampered by unnecessary precision in the interface and would be able to focus on their immediate perceptual response. We acknowledge that such methods may be prone to minor biases (e.g. range bias, end-point bias [Pou89]) but we argue that such biases are offset by the overall scale

of the syncopation continuum and stimuli. In other words, the stimuli we employed ranged between *not syncopated* and *highly syncopated*, so we trade finer detail in the data for an efficient method. All listeners used the whole range of the scale (i.e. each listener gave at least one minimum and one maximum rating).

#### 4.1.1 Participants

We recruited ten participants, nine male and one female, with an average age of 30 years (standard deviation 5.8 years). All participation was voluntary (unpaid). In order to maximize the degree of homogeneity of the group, all participants are trained musicians. Their musical training included formal performance and theory over a range of instruments, music production and engineering. All participants had trained for an average of 15 years (standard deviation 5 years). Six of them reported proficiency in multiple instruments. All participants confirmed that they were confident in their understanding and rating of syncopation. All participants reported normal hearing.

#### 4.1.2 Stimuli

Each score, rendered to produce a single stimulus, was constructed of three bars. The first bar was always metronome alone (either 4/4 or 6/8). The second and third bars were repetitions of a one-bar rhythm-pattern constructed from concatenation of two basic, half-bar rhythm-components. Figure 4.1 provides a schematic diagram which illustrates the steps taken when generating the stimuli. First, various half-bar rhythm-components (Figure 4.1a) were paired to produce one-bar rhythm-patterns (Figure 4.1b). The rhythm-components were categorised as either binary (two notes) or ternary (three notes). Next, the rhythm-patterns were concatenated and a metronome was added to produce the final score (Figure 4.1c). Finally, the stimulus was rendered to produce the acoustic waveform (Figure 4.1d) which was ultimately heard by the listener. Rhythms were played concurrently with the metronome (following the single bar of introductory metronome) (Figure 4.1c).



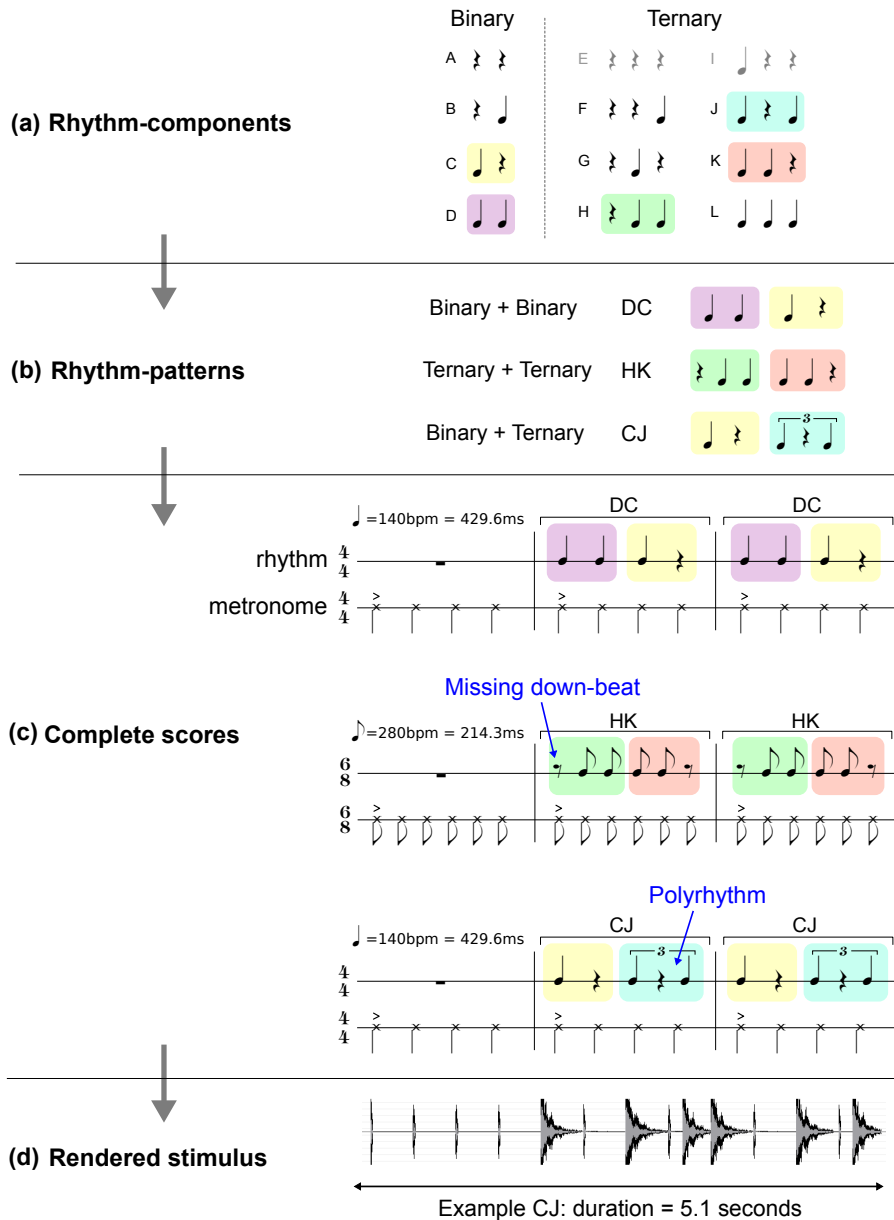


Figure 4.1: Construction of stimuli. A schematic diagram illustrating the process of generating the stimuli. (a) Rhythm-components. Ten basic rhythm-components are created, categorised into binary or ternary depending on the number of events. (b) Rhythm-patterns. Half-bar rhythm-components are paired to create one-bar rhythm-patterns. (c) Complete scores. Rhythm-patterns (and metronome) are used to produce a three-bar score, including rhythm-patterns featuring missing down-beats and polyrhythms. The combinations of two binary or one binary and one ternary rhythm-components are notated with a time-signature of 4/4; two ternary rhythm-components fit into 6/8. The tempo for both signatures is 140 quarter-note per minute (QPM). (d) Rendered stimulus. The score is rendered as a waveform.

Figure 4.1a shows the ten half-bar rhythm-component notations (A-L) from which concatenated whole-bar pairs were produced in all possible combinations. These base rhythm-components include notations featuring rhythmic structures that are anticipated to result in syncopation: missing down-beats, off-beat notes and polyrhythms when presented in relation to a metronome. Example rhythm-pattern pairings are given in Figure 4.1b. Rhythm-patterns composed of a given pair of rhythm-components were presented separately in both forward and reverse order (e.g. CJ and JC). By comparing such pairs, we are able to investigate the effect of location (e.g. of missing strong-beats) within the bar.

Scores for example stimuli, including metronome, are given in Figure 4.1c. There were 99 unique pairs, after excluding redundant patterns E and I, which were replaced with A and C respectively (which are equivalent in 4/4). The time-signature was set to 6/8 for all combinations of two ternary rhythm-components and 4/4 for the rest. As a result, the overall stimuli comprises three rhythm-categories: 4/4 monorhythms, 6/8 monorhythms and (3:2) 4/4 polyrhythms. The potential combinations that result in (2:3) 6/8 polyrhythms are excluded in order to limit the length of the required listening test. While this combination of stimuli provides a representative range of rhythm-patterns in two time-signatures, it should be noted the proportions of examples between 4/4 and 6/8 time-signatures, and between monorhythms and polyrhythms differ.

The stimuli were rendered (synthesised) at a sampling rate of 44.1 kHz 16-bit using MIDI sequencing (see Figure 4.1d for an example waveform). A percussive snare drum sample was used for the musical rhythm and a ‘cow-bell’ sample was used for the metronome. We chose a uni-tone percussive drum sound for rhythm-patterns in order to avoid the interaction between pitch and rhythm, and to remove confounding factors such as note duration [Lon04, p.28].

The snare drum sample was approximately 700 milliseconds (ms) in duration, with approximately 7 ms attack, 130 ms sustain and 450 ms decay. The metronome sample was relatively impulsive and of approximately 20 ms duration. The metronome was dynamically accented on the

first beat of the bar and was also accented in pitch; the fundamental frequency of the accented note was 940 Hz and the remaining notes were of 680 Hz. Thus, our metrical cue (metronome) was clearly differentiable (by timbre and pitch) from the overlaid drum rhythm. By accenting the first beat of metronome in 6/8, we do not explicitly rule out a 3/4 grouping of beats.

The tempo of the metronome was set to 140 BPM for all rhythm-patterns in a time-signature of 4/4 and 280 BPM for those in 6/8. This corresponds to an interval of 428.6 ms per quarter-note in both time signatures. In 4/4 the metronome beat quarter-notes at this interval and in 6/8 it beat eighth-notes (i.e. an interval of 214.3 ms per beat). Hence, in 4/4 stimuli that contained polyrhythmic components, the interval between triplet quarter-notes was 285.7 ms. The resulting stimuli durations (per trial) were 5.1 seconds in 4/4 (i.e. three bars of four quarter-note beats) and 3.9 seconds in 6/8 (i.e. three bars of six eighth-note beats).

### 4.1.3 Procedure

Stimuli were presented individually and at the instigation of the listener. All stimuli were presented within a single block. For each trial, the listener gave a rating between zero and four, where zero indicated no syncopation and four indicated maximum syncopation. The listener was free to listen to each pattern repeatedly before giving their rating. The stimuli were presented in randomised order (i.e. a different order for each listener). Before the experimental session, the listeners heard a broad range of example stimuli and were given a practice run (the resulting data was discarded). Each participant was free to adjust the sound level at any time so as to be comfortable. Headphones were used to present the stimuli. All presentation was dichotic (the same in both ears). Tests were completed in approximately 30-50 minutes. Listeners were encouraged to take breaks during the session.

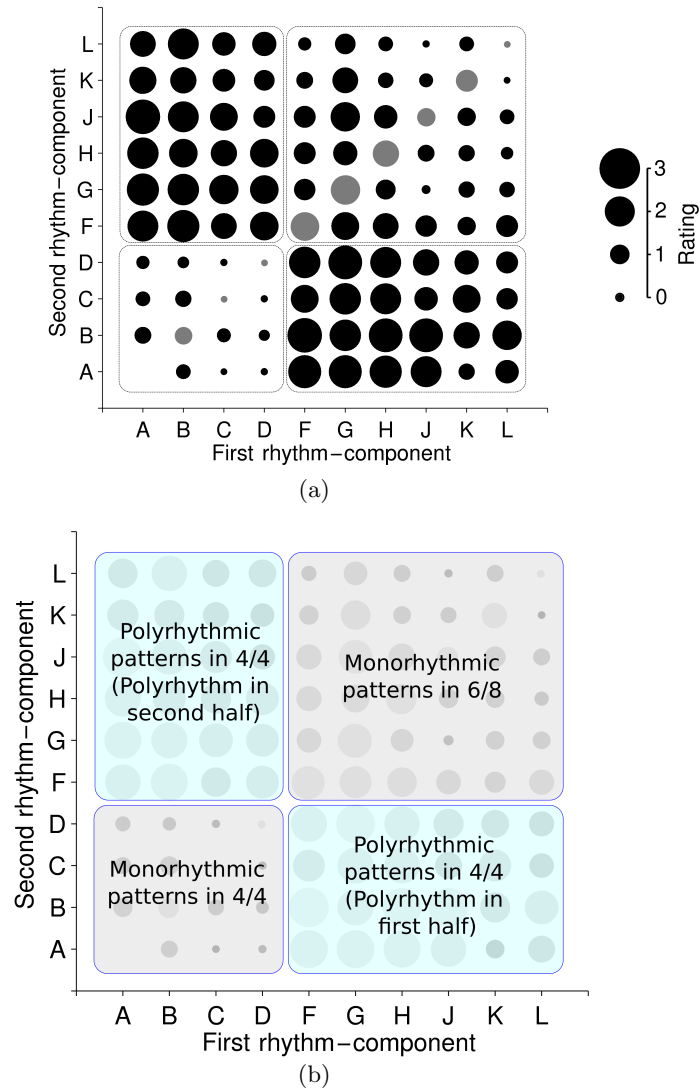


Figure 4.2: Group mean syncopation ratings for rhythm-patterns. (a) A matrix showing group mean syncopation ratings for rhythm-patterns. The upper triangle of the matrix refers to rhythm-patterns where the horizontal axis denotes the first rhythm-component of the rhythm-pattern, and where the vertical axis denotes the second rhythm-component. For the lower triangle of the matrix the reverse is true. This provides a general way to compare the mean ratings between the two orders of presentation for any given pair of rhythm-components. Same rhythm-component pairs (e.g. BB) are shown in grey. Note that the pair AA is excluded because it represents a full bar of rests. (b) A map of the matrix shown in (a), broken down into regions corresponding to score features: polyrhythmic and monorhythmic patterns in both 4/4 and 6/8. This map illustrates how the data is categorised in the subsequent analyses.

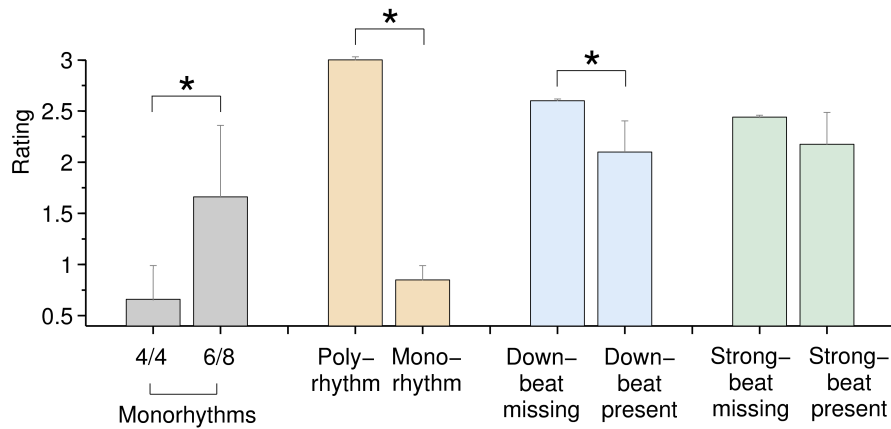


Figure 4.3: Categorical analysis. Group mean and 95% confidence intervals for pooled ratings, averaged for each listener, composed (selectively) for comparison of ratings for all stimuli categorised within the following paired conditions: monorhythms in 4/4 versus those in 6/8 (see Figure 4.2b), polyrhythms versus monorhythms, down-beat missing versus down-beat present, strong-beat missing versus strong-beat present. \* denotes significance ( $p < 0.05$ , *Wilcoxon Signed-Rank Test*, uncorrected).

## 4.2 Results

Figure 4.2a broadly summarises the syncopation ratings in a matrix representation of the group mean ratings for each rhythm-pattern. The horizontal axis shows the first rhythm-component of the respective rhythm-pattern, and the vertical axis shows the second rhythm-component. Therefore, the upper-left triangular area of the matrix corresponds to the opposite pair-wise ordering of rhythm-components within the same rhythm-pattern to those in the lower-right triangular area of the matrix. Figure 4.2b provides a ‘map’ corresponding to Figure 4.2a, which illustrates grouping of the ratings for subsequent analyses. The average correlation coefficient (*Spearman*) between each pair of listeners in the group is 0.47, suggesting that the ratings are reasonably consistent between listeners. Figures 4.3 and 4.4 show various selective groupings of the ratings data (across all listeners), where the data ( $N = 10$  listeners) were selected to test the following hypotheses: 1) 6/8 is more syncopated than 4/4; 2) polyrhythms are more syncopated; 3) missing down-beats result in syncopation; and 4) switching component order affects syncopation.

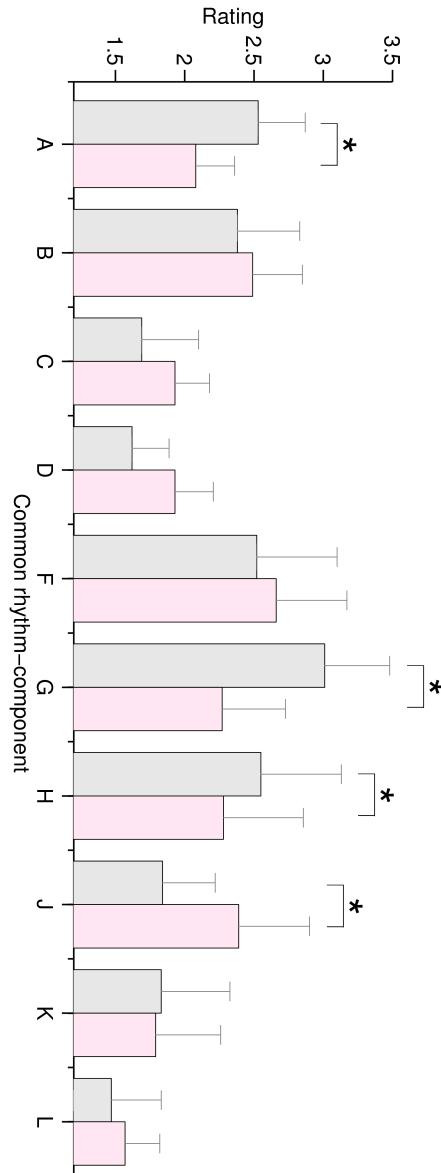


Figure 4.4: Syncopation by rhythm-component. Mean and 95% confidence intervals for ratings pooled by rhythm-component. For each distribution, all ratings for rhythm-patterns featuring each respective rhythm-component were selected and separated into groups by location of the rhythm-component within the rhythm-pattern (e.g. AB + AC + AD versus BA + CA + DA.). Grey indicates the location of the rhythm-component is on the first half of the bar, and pink indicates that on the second half. \* denotes significance ( $p < 0.05$ , Wilcoxon Signed-Rank Test, uncorrected).

#### 4.2.1 6/8 is more syncopated than 4/4

For each listener, all ratings were separately pooled and averaged for all stimuli featuring time-signatures of 4/4 and 6/8. This gives a pair of

ratings distributions which may be compared to see whether either time-signature was more or less highly rated (for syncopation). Figure 4.3 shows that 6/8 is more highly rated than 4/4 ( $W = 1, Z = -2.55, p < 0.01, r = 0.81$ , *Wilcoxon Signed-Rank Test*).

#### 4.2.2 Polyrhythms are more syncopated

Next, for each listener, all ratings were separately pooled and averaged for all stimuli that constituted a polyrhythm (i.e. in 4/4 see Figure 4.2b and all stimuli that did not. The resulting ratings distributions are likewise compared to establish the existence of significant differences that may indicate a pre-disposition of polyrhythms to result in the perception of syncopation. Figure 4.3 shows that polyrhythms are much more highly rated than monorhythms ( $W = 55, Z = 2.8, p < 0.01, r = 0.89$ , *Wilcoxon Signed-Rank Test*).

#### 4.2.3 Missing down-beats result in syncopation

For each listener, ratings for all rhythm-patterns featuring ‘missing down-beats’ were pooled and averaged. The same pooled averages were calculated for rhythm-patterns not containing missing down-beats. The resulting group ratings distributions are compared in Figure 4.3 and show that rhythm-patterns featuring missing down-beats are more highly syncopated than those not featuring missing down-beats ( $W = 54, Z = 2.7, p < 0.01, r = 0.85$ , *Wilcoxon Signed-Rank Test*). A similar analysis was performed for all pairs featuring missing strong-beats, with a similar (albeit not significant) outcome ( $p > 0.05$ , *Wilcoxon Signed-Rank Test*).

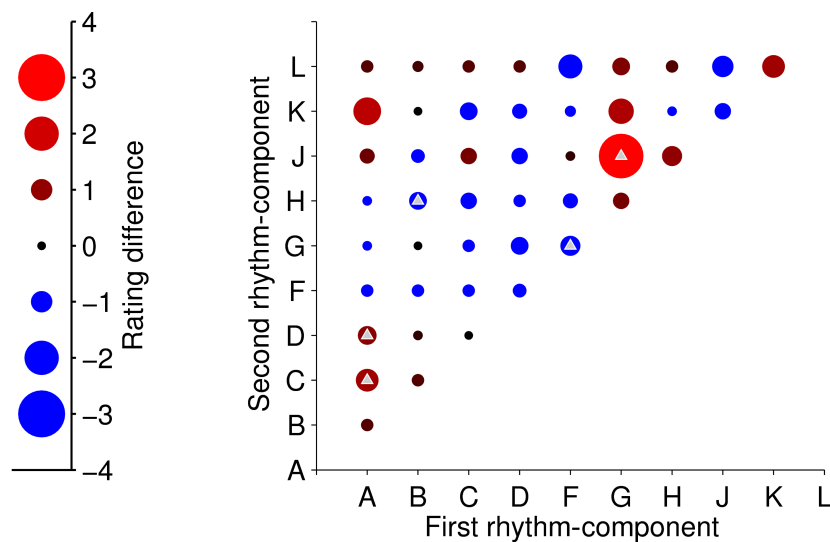
#### 4.2.4 Switching component order affects syncopation

In order to investigate the effect of location of each rhythm-component within the rhythm-pattern, the ratings resulting from each of the two possible orders were compared. Where certain rhythm-components are associated with high degrees of syncopation (e.g. rhythm-components which feature a missing down-beat), we can observe the effect of location within the rhythm-pattern (bar). For each listener, ratings for all

rhythm-patterns featuring a given rhythm-component were pooled and averaged for both possible locations of a given rhythm-component (within the rhythm-pattern). The group mean and 95% confidence intervals for the resulting distributions are plotted in Figure 4.4. Only rhythm-patterns featuring rhythm-components A ( $W = 34.5, Z = 2.31, p < 0.05, r = 0.73$ ), G ( $W = 44, Z = 2.57, p < 0.05, r = 0.81$ ), H ( $W = 41, Z = 2.15, p < 0.05, r = 0.68$ ) and J ( $W = 0, Z = -2.67, p < 0.05, r = 0.85$ ) showed significant differences (*Wilcoxon Signed-Rank Test*, uncorrected) which held regardless of the other rhythm-components within the various rhythm-patterns. The average ratings were larger when A, G and H were in the first half of the bar, but the opposite was true for J. The overall shape of the graph is consistent with the comparison of missing down-beats shown in Figure 4.3, in that rhythm-patterns featuring rhythm-components A, B, F, G and H show higher mean syncopation ratings.

In order to find out exactly which rhythm-patterns were sensitive to location of the rhythm-components, the analysis was refined to focus on the pair-wise comparison of ratings for each rhythm-pattern between the two possible orders of the rhythm-components. Figure 4.5 shows a matrix plot of the difference in group mean rating for each rhythm-pattern, caused by change in the rhythm-component order (i.e. within the bar). Significant changes in rating are indicated with overlaid triangles ( $p < 0.05$ , *Wilcoxon Signed-Rank Test*, uncorrected). Rhythm-components which significantly changed when the rhythm-component order was switched were: AC ( $W = 28, Z = 2.56, p < 0.05, r = 0.81$ ), AD ( $W = 15, Z = 2.21, p < 0.05, r = 0.7$ ), BH ( $W = 0, Z = -2.21, p < 0.05, r = 0.69$ ), FG ( $W = 0, Z = -2.22, p < 0.05, r = 0.7$ ), GJ ( $W = 34, Z = 2.28, p < 0.05, r = 0.72$ ) (see Figure 4.5b). Again, significant changes occur for rhythm-patterns featuring rhythm-components A, B, F, G, H, all of which feature missing down-beats. In other words, rhythm-components resulting in missing down-beats contribute significantly more to the perception of syncopation than the same rhythm-components in the second half of the bar (rhythm-pattern).





(a)



(b)

Figure 4.5: Pair-wise changes in ratings when rhythm-component order was switched. (a) The change in group mean rating (for each rhythm-pattern) caused by switching the rhythm-component order (i.e. this is equivalent to a subtraction of the lower-triangle ratings of Figure 4.2a from the upper-triangle ratings of Figure 4.2a). Triangles denote significance ( $p < 0.05$ , *Wilcoxon Signed-Rank Test, uncorrected*). Interestingly, the significant changes (when order was switched) correspond to missing down-beat rhythm-patterns. (b) The notations for each pair of rhythm-patterns that reached significance.

### 4.3 Discussion

In this chapter, we have shown that there is more potential for syncopation in 6/8 in polyrhythms and in rhythms featuring a missing down-beat. We have also shown that the location of rhythm-components that give rise to

syncopation is critical to its perceived degree. These results demonstrate that syncopation cannot simply be predicted (i.e. in a model) by summation of ‘syncopation values’ calculated for individual notes according to the relationship between each note and the assumed metrical structure. We also identify three questions for further investigation: i) Is syncopation tempo-dependent? ii) Why do the 4/4 monorhythm patterns exhibit lower syncopation levels than monorhythms in 6/8? iii) Do listeners reinterpret the meter of a given rhythm-pattern in order to reduce the level of perceived syncopation?

### 4.3.1 4/4 versus 6/8

We employ the standard terminology for meters (i.e. time-signatures) in Western music [Lon04]; the terms duple and triple to refer to two- and three-beat bars respectively, and the terms simple and compound to refer to the binary and ternary subdivision of beats in a bar. Here, we investigated the signatures 4/4, which is simple-duple meter (i.e. two groups of two quarter-notes), and 6/8 which is compound-duple meter (two groups of three eighth-notes).

6/8 monorhythmic patterns were rated as more syncopated than those in 4/4 (Figure 4.3). There are several potential explanations for this observation. First, given that a time-signature must be rendered (or performed) according to a specified tempo, a major difference between the stimuli in these two time-signatures is their speed. The beat rate in the 6/8 stimuli was twice as fast as those in 4/4 because eighth-notes are half as long as quarter-notes and the tempi were chosen to maintain the same duration for quarter-notes in both.

It has been shown that tempo influences various aspects of music perception, such as rhythm recognition [Han93], pitch perception [DGM88], music preference [LeB81] and perception of emotion in music [vZWvdB11]. In particular, the ability to discriminate differences between rhythms [Han93], perception of meter from polyrhythms [HO81, HL83] and production of rhythmic timing [RWD02, DH94] all appear to be influenced by tempo. Therefore, we expect that tempo may affect the perceived syncopation

and this may explain the higher ratings in 6/8 than in 4/4.

Another possible reason for higher ratings in 6/8 than 4/4 may be that the rhythmic structure of 4/4 is inherently less ambiguous – 4/4 is simple-duple meter (duple subdivision of duple) and 6/8 is compound-duple meter (triple subdivision of duple). Several studies have shown that listeners of all ages naturally show bias towards processing (and preference for) rhythms that incorporate binary rather than ternary metrical subdivisions [LJ83, PE85, Dra93, BT06]. Indeed, it has been shown that the accuracy of rhythm reproduction in binary subdivisions of beat is higher than ternary subdivisions [Dra93]; people are inclined to tap on the binary subdivisions to isochronous auditory sequences when they are asked to tap at a fast rate [Dra97]; also, both adults and infants react more quickly and accurately to the alterations in pitch, melody and harmony in binary meter than in triple meter [BT06, SC89].

Syncopation has been associated with human metrical processing [FR07, SP00, SK01, TS03], and metrical processing has also been related to time-signature [LJ83, PE85, Dra93, BT06, SC89]. Our finding, that 6/8 monorhythms are perceived as more syncopated than those in 4/4, suggests that time-signature and perceived syncopation are inherently related and hence may explain the previously reported relationship between metrical processing and time-signature.

### 4.3.2 Missing down-beats

Syncopation models predict that missing strong-beats (the absence of events at strong metrical positions) result in syncopation [LHL84]. The models also predict that a missing down-beat (the first beat of the bar) generates a higher degree of syncopation than a missing strong-beat in a lower metrical level (e.g. the third quarter-note in 4/4 or the fourth eighth-note in 6/8) result in syncopation.

In general, our results agree with the modelling predictions; the patterns with missing down-beats tend to have higher average ratings (Figure 4.3). This is also clear in Figure 4.4, which shows that rhythms starting with a rest (components A, B, F, G and H) contribute to higher average

ratings, while patterns including components C, D, K or L have relatively low average ratings (these do not start with a rest). However, we did not find strong evidence suggesting that rhythms that feature missing strong-beats have an effect on syncopation. This may be due to the small number of participants in the study.

The latter modelling prediction, that missing down-beats will have a higher degree of syncopation than equivalent missing strong-beats, is partially supported in Figure 4.4: Rhythm-patterns beginning with rhythm-components A, G and H (which contain missing down-beats) have higher average ratings than those with A, G or H respectively in the second half (Figure 4.4). The pair-wise comparisons (in Figure 4.5) for pairs AC/CA, AD/DA and GJ/JG also support this.

### 4.3.3 Possible interpretation of 6/8 as 3/4

In Figure 4.5, we can observe a significant difference in syncopation ratings for the 6/8 patterns FG/GF and GJ/JG depending on component order. We might expect to see this for GJ/JG because GJ has a missing down-beat whereas JG does not. Note, however, that this does not explain why other similar 6/8 patterns do not show an equivalent significant difference. In contrast, FG and GF both exhibit a missing down-beat so it is interesting that there should be a significant difference (due to switching order) in this case and prompts further explanation. In listening tests, Povel and Essens [PE85] found that, given a choice, listeners select the meter which minimises metrical contradiction (i.e. syncopation). Looking at the rhythm-patterns in question (notated in Figure 4.5), we can see that for FG and JG, all the notes fall on strong-beats in 3/4 (i.e. eighth-note positions 1, 3 and 5 in 6/8) whereas in GF and GJ, this is not the case. Indeed, using the clock model of Povel and Essens [PE85], patterns FG and JG are strongly predicted to be interpreted as 3/4 time whereas GF and GJ would be predicted as 6/8. It is possible therefore that the listeners are interpreting some 6/8 patterns as 3/4, which would thus reduce the anticipated level of syncopation. The clock model also makes similar predictions with regards to the results shown in Figure 4.4d. The

ternary components G, H and J show significant differences according to their location in the bar where other ternary components do not. The component order corresponding to low syncopation ratings in these cases may be explained as being a result of listeners interpreting the meter as 3/4. Such metrical interpretation is broadly consistent with the findings of Hannon et al. [HSEK04], who showed that when judging meter, listeners were more likely to choose 6/8 when the tempo was fast but more likely to choose 3/4 when the tempo was slow.

#### 4.3.4 Polyrhythms

Polyrhythms were rated as more syncopated than monorhythms (Figure 4.3). In music psychology, polyrhythms are usually dealt with as a separate concept to syncopation [Lon04, LHL84]. However, if we accept the definition of syncopation as being a contradiction to the prevailing meter, then the introduction of a competing meter (i.e. within a polyrhythm) would clearly also give rise to this phenomenon. The fact that we found polyrhythms to be more syncopated than monorhythms suggests that the challenge to the prevailing meter, from a counter meter, is more substantial than that caused by emphasising weak-beats over strong-beats in monorhythms.

In Figure 4.5, one pattern containing a polyrhythm, BH/HB, shows significant difference when the order of rhythm-components is switched. Both components of BH/HB are missing the strong-beat yet HB was rated as significantly more syncopated than BH. This may be explained by the fact that component B is a monorhythm in 4/4 but H is a polyrhythm in that meter. When H is placed in the first half of the pattern it is a polyrhythm that has a missing down-beat, which implies that the syncopation is compounded in this case.

## 4.4 Summary

In this chapter, we evaluated the relationship between notated rhythm and perceived syncopation. We used a metronome to provide explicit cues

to the prevailing rhythmic structure (as defined in the time-signature). Three-bar scores with time-signatures of 4/4 and 6/8 were constructed using repeated one-bar rhythm-patterns, with each pattern built from basic half-bar rhythm-components. Our manipulations gave rise to various rhythmic structures, including polyrhythms and rhythms with missing strong- and/or down-beats. Listeners were asked to rate the degree of syncopation they perceived in response to a rendering of each score. We observed higher degrees of syncopation in time-signatures of 6/8 for polyrhythms and for rhythms featuring a missing down-beat. We also found that the location of a rhythm-component within the bar has a significant effect on perceived syncopation.

This experiment also forms a dataset that consists of 99 rhythm-patterns and the corresponding humans perceptual ratings on syncopation. In the following chapter, we will give in-depth reviews of several well-known syncopation models and evaluate them against this dataset.

# Chapter 5

## Evaluation of the models

The studies in which the syncopation models have previously been evaluated [GTT07, Thu08, SH07] have been tested against measures presumed to be indirectly related to syncopation; these include rhythmic complexity and difficulty in rhythm reproduction or rhythm recognition [PE85, Ess95, SP00, FR07]. In this chapter, we introduce a complete dataset for syncopation perception and test the models directly on it. The dataset, detailed in Section 5.1, is an extension of the work from Chapter 4 where the perception of syncopation was investigated explicitly by asking musicians to rate the degree of perceived syncopation in response to rhythm-patterns in time-signatures of 4/4 and 6/8.

Our evaluations in Section 5.2 follow Chapter 4 by splitting the data into three rhythm-pattern categories: 4/4 monorhythm, 6/8 monorhythm and 4/4 polyrhythms. Some models are not designed to handle all three categories, so we present individual results for each model as appropriate. Finally, we analyse the respective strengths and weaknesses of each model.

### 5.1 Dataset 1

In Chapter 4, we introduced Experiment 1, in which we asked ten experienced musicians to give informed ratings over a five-point rating scale, of perceived syncopation for renderings of 99 three-bar scores. We then extended this experiment to include 12 more rhythm-patterns at the eighth-note level for a total of 111 rhythms by replicating the methodology in Section 4.1.

We recruited a further ten trained musicians, eight male and two female, with an average age of 32 years (standard deviation 5.2 years). All participants had trained for an average of 18.5 years (standard deviation 7.9). All of them reported proficiency in multiple instruments. All participants confirmed that they were confident in their understanding and rating of syncopation. Four of them had participated in the previous experiment. All participants reported normal hearing.

As in the part of Experiment 1 that we explored in Chapter 4, each score, rendered to produce a single stimulus, was constructed of three bars. The first bar was always metronome alone. The second and third bars were repetitions of a one-bar rhythm-pattern constructed from concatenation of two basic, half-bar rhythm-components out of ten (see Figure 4.1 for an illustration of the steps taken when generating the stimuli). The combination of a binary and a ternary rhythm-component in 4/4 meter creates a polyrhythm. In contrast, a monorhythm is any rhythm-pattern which is not polyrhythmic, which means that it is constructed from either two binary rhythm-components in 4/4 meter or two ternary in 6/8. The extended 12 rhythm-patterns (4/4 monorhythms) were constructed from binary rhythm-components A-D (after removing the duplications of rhythm-patterns formed in the experiment described in Chapter 4), and each of which was scaled down to a quarter-note-duration in a time signature of 4/4 to generate eighth-notes (example in Figure 5.1).

The stimuli were rendered (synthesised) at a sampling rate of 44.1 kHz 16-bit using MIDI sequencing. As described in Chapter 4, a percussive snare drum sample was used for the musical rhythm and a ‘cow-bell’ sample was used for the metronome. The tempo of the metronome was set to 140 BPM.

The procedure exactly followed that set out in Section 4.1.3; Participants were unpaid volunteers and gave informed verbal consent before the experiment. Participants were free to withdraw at any point. Tests were arranged informally and conducted at the convenience of the participants. Written consent was not deemed necessary due to the low (safe) sound pressure levels employed in the test. The experimental protocol (including consent) was approved by the ethics committee of Queen Mary



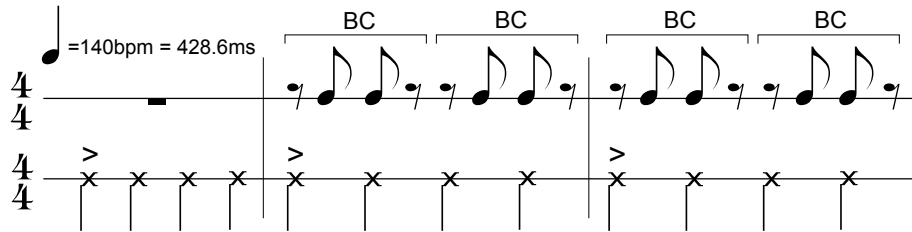


Figure 5.1: The example score of rhythm-pattern BCBC. Rhythm-components B and C are paired to create a half-bar rhythm-pattern BC; BC is then repeated once to produce a one-bar rhythm-pattern BCBC. The three-bar score is generated from one bar of metronome alone, and two bars of repetitions of the one-bar rhythm-pattern BCBC.

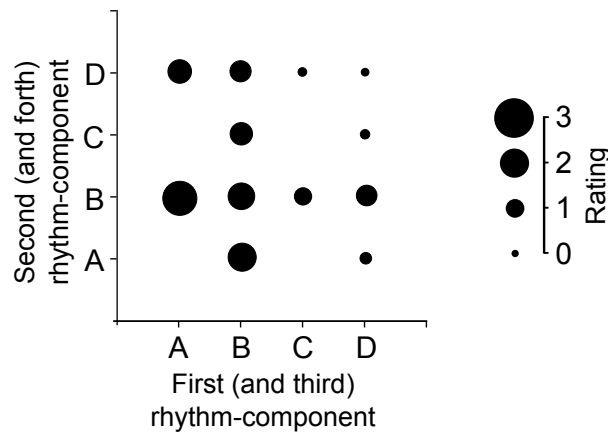


Figure 5.2: Group mean syncopation ratings for the extended stimuli. This matrix shows the group mean syncopation ratings for the 12 extended 4/4 monorhythms. The horizontal axis denotes the first and third rhythm-components of the rhythm-pattern, and where the vertical axis denotes the second and forth rhythm-components. The empty elements in the matrix are either full-rest rhythm (e.g. AAAA) which is excluded or duplicated rhythm-patterns as in the existed stimuli (e.g. ACAC is identical with BB).

University of London.

The group mean ratings for the extended rhythm-stimuli are shown Figure 5.2. Overall, Dataset 1 includes 27 4/4 monorhythms, 36 6/8 monorhythms and 48 polyrhythms, altogether 111 rhythm-stimuli. Looking at Figures 5.2 and 4.2 together, we can form an idea of the averaged ratings for Dataset 1. The complete dataset is plotted in ranked order of

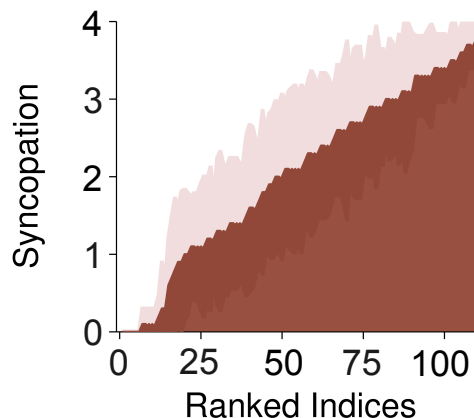


Figure 5.3: The ranked mean ratings of entire dataset. The dark-red shows the increasing degree of perceived syncopation across stimuli that contains 111 rhythms patterns. The light-colour represents the 95% confidence intervals.

mean syncopation rating in Figure 5.3, including 95% confidence intervals. The overall distribution is relatively linear between zero syncopation and maximum syncopation and hence provides a good means to evaluate the predictions of the models.

## 5.2 Evaluation results

The human ratings are not normally distributed, therefore we have calculated the Spearman's rank correlation coefficient between each model and the perceptual data. The predictions of each model were tested against the human ratings data; each prediction of the model for a given stimulus was compared to the mean of the human ratings for that stimulus. Correlation coefficients (*Spearman*) were used to quantify the quality of the predictions for each model and were performed for subsets of the human data as appropriate to the scope of each model.

Figure 5.4 plots the predictions of the models as a function of the mean human ratings for 4/4 monorhythms, including the regression line ( $\pm 95\%$  confidence intervals). The PRS model performed best ( $r = 0.95$ ,  $p < 0.01$ ) and the TMC model also performed well ( $r = 0.92$ ,  $p < 0.01$ ). In contrast,

the TOB model performed poorly ( $r = 0.36$ ,  $p > 0.05$ ).

Figure 5.5 shows the same plots for 6/8 monorhythms. Again, the best predictions were made by the PRS model ( $r = 0.95$ ,  $p < 0.01$ ). The LHL, SG and TMC models performed similarly while the TOB model again performed poorly ( $r = 0.17$ ,  $p > 0.1$ ).

Figure 5.6 shows that polyrhythms have generally been overlooked in design of the models: only three are applicable and only the WNBD model performed modestly well ( $r = 0.41$ ,  $p < 0.01$ ).

### 5.3 Discussion: strengths and weaknesses of models

In order to compare the syncopation models, evaluation results in terms of the correlations between model predictions and human ratings have been presented within each subset of our data (Figures 5.4 - 5.6). In this section, we will discuss the strength and weaknesses of the models with reference to the categories we introduced in Section 2.3.1.

#### 5.3.1 Hierarchical models

The hierarchical models include LHL (Equation 3.19), TMC (Equation 3.31), PRS (Equation 3.29) and SG (Equation 3.39). They generally work better for monorhythms than the other classes of model, suggesting that metrical hierarchy is critical in explaining the perception of syncopation. They can detect a missing down-beat, which is known to give rise to syncopation (Section 4.2.3). The PRS model stands out in this group. Its main advantage may be the result of the model integrating rhythm over a larger window (rather than considering momentary events) and classifying rhythmic structure at different levels of hierarchy as defined syncopation types.

The inherent limitation of these models is that they are only applicable to monorhythms. In polyrhythms, competing groupings of events give rise to more than one metrical hierarchy, but only one of them can be presented in the hierarchical models. Therefore, there will be some notes that fall outside the metrical positions defined in the presented metrical

hierarchy, and hence these cannot be captured. Take Figure 2.14b for example, hierarchical models will form the metrical hierarchy of the time-signature of 2/4 (the tree structure of the top line), but the second and third triplet quarter-notes do not fall on the metrical positions on this metrical hierarchy (see Figure 2.14).

Another potential limitation is their application of theoretical metrical hierarchy (Figure 3.3, Equations 3.16 and 3.17) instead of a perceptual hierarchy<sup>1</sup>. The hierarchy weights may be considered as free parameters, and reflect hypotheses about the perceptual importance of note positions [PK90]. Therefore, in principle, the modelling fits of the hierarchical models could be optimised by adjusting these weights. This optimisation process would then yield predictions of the perceptual importance of note positions which could be compared to measures of perceptual hierarchies [PK90]. Smith and Honing have implemented a version of the LHL model that incorporates perceptual hierarchies and compares these against the theoretical hierarchy [SH07]. Their results show that perceptual hierarchy did not help LHL's syncopation prediction get closer to Shmulevich and Povel's dataset of rhythm complexity [SP00]. However, this set of rhythm-stimuli lacks metrical context which controls perceived meter to be the same as the defined metrical structure when modelling, which may introduce errors in the model's prediction.

The LHL model adopts a unique modelling approach, which is to search N-R pairs and take the difference in weights within the N-R pair as the syncopation measurement (Equation 3.19). Regardless of the rationale behind it (Section 2.2.2), this method can sometimes result in a type II error, i.e. a false negative. For example, the rhythm presented in Figure 5.7a starts with a missing down-beat that is supposed to be syncopated, but no note is preceded by this rest, therefore no N-R pair can be formed. The rationale behind this design of LHL model may be that it assumes human listeners naturally interpret rhythm in a way to avoid syncopation,

---

<sup>1</sup>Palmer and Krumhansl reported listeners' mean ratings of perceptual importance of each metrical position in different metrical contexts (e.g. 4/4, 3/4, 6/8), which reflect the perceptual metrical hierarchy of different meters [PK90]. Perceptual hierarchy strongly correlates with the theoretical hierarchy ([PK90], Table 2), but the weights of each metrical position differ.

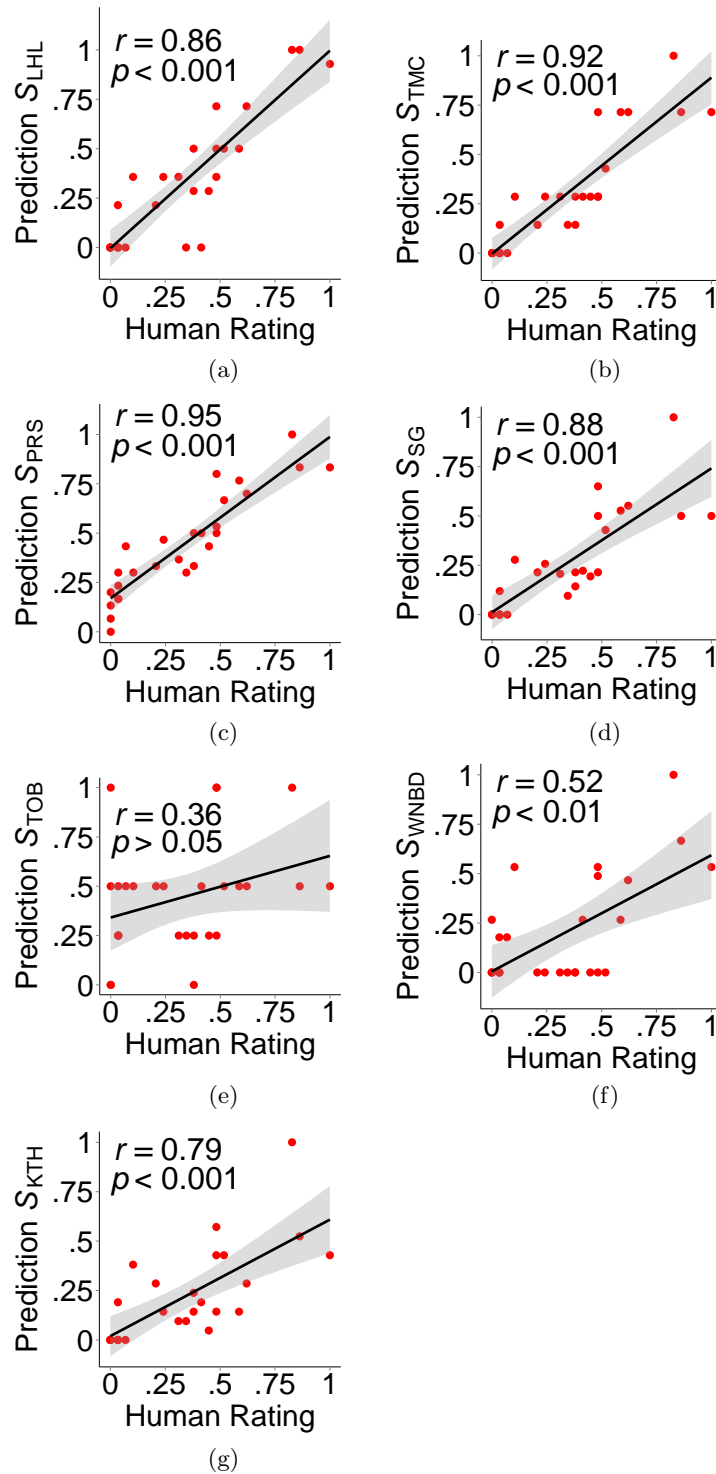


Figure 5.4: Comparisons of model predictions for 4/4 monorhythms. The normalised predictions are plotted against the normalised mean human ratings. Spearman-rank correlation coefficients ( $r$ ,  $p$ ) are given for each model. Linear regression lines (and 95% confidence interval) are plotted for illustration.

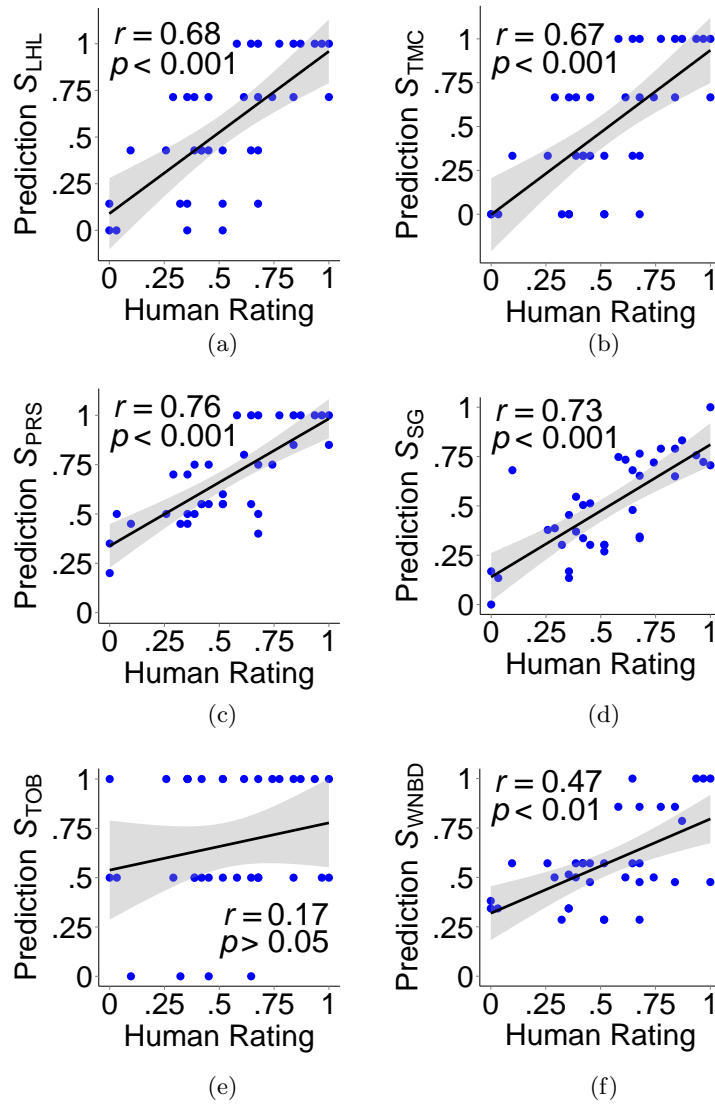


Figure 5.5: Comparisons of model predictions for 6/8 monorhythms. The normalised predictions are plotted against the normalised mean human ratings. Spearman-rank correlation coefficients ( $r$ ,  $p$ ) are given for each model. Linear regression lines (and 95% confidence interval) are plotted for illustration.

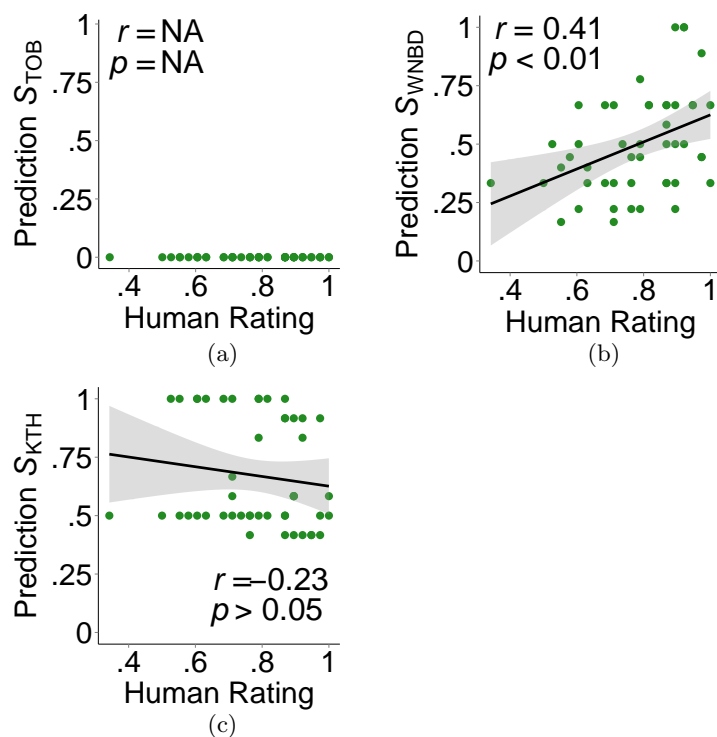


Figure 5.6: Comparisons of model predictions for polyrhythms. The normalised predictions are plotted against the normalised mean human ratings. Spearman-rank correlation coefficients ( $r$ ,  $p$ ) are given for each model. Linear regression lines (and 95% confidence interval) are plotted for illustration.

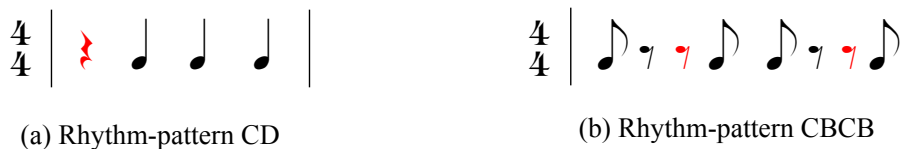


Figure 5.7: Examples of rhythms with syncopation that cannot be captured by the LHL model. Both (a) and (b), assuming they are the start of a musical piece, contain rests on strong metrical positions (indicated in red), but are not preceded by notes and therefore cannot form an N-R pair.



Figure 5.8: Examples of non-syncopated rhythms that are measured as syncopated by off-beat models. Rhythms in (a) and (b) both have all beat positions filled with notes, and some off-beat notes (indicated in red). They are perceived as non-syncopated but the off-beat notes are counted as syncopation by the off-beat models.

therefore rhythm does not generally start with a rest. However, it neglects the known fact that the representations of metrical hierarchy are formed preattentively in the human auditory system [LH09, PK90], hence starting with a missing down-beat needs to be detected. Figure 5.7b also shows a rhythm that contains rests on strong metrical positions and is perceived as syncopated, but cannot be captured by the LHL model.

### 5.3.2 Off-beat models

The off-beat models, including TOB (Equation 3.47) and WNBD (Equation 3.52), start with locating beat (or strong-beat) positions, then search for notes that fall in between beats. The key strength of these models is that they are capable of capturing polyrhythms because any note outside the metrical positions is treated as ‘off-beat’ and hence contributes to syncopation.

However, the hypothesis that any off-beat note leads to syncopation is not consistent with the observation of syncopation resulting from the accenting of weak-beats and diminishing of strong-beats [Ran86, Hur06]. As in the examples shown in Figure 5.8, there are several cases of rhythms containing both off-beat notes and filled strong-beats that are not syncopated. The off-beat models also cannot detect a missing down-beat because only *sounded notes* are captured, not rests.

It has been demonstrated that switching the order of rhythm-components within the bar can affect syncopation (Section 4.2.4). The WNBD model cannot capture such details, because it focuses only on the distance of





Figure 5.9: A specific limitation of the WNBD model. The rhythm-components in (a) are switched to generate the rhythm-pattern in (b). The short black lines indicate the metrical positions on tatum level, and the grey dots indicate the strong-beats as defined by the time-signature of 6/8. After switching the order of the rhythm-components, the distance of the off-beat note to its nearest strong-beat remains unchanged. Therefore, these rhythms are predicted by the WNBD model to be equally syncopated, whereas their perceptual ratings are not the same.

an off-beat note to its nearest strong-beat without consideration of its metrical position within the bar (Figure 5.9).

Specific limitations of the TOB model are presented under two conditions. The first is whether the divisors of the dimension of time-span ( $|V|$ ) include more than one prime numbers (e.g.  $|V| = 12$  or  $24$ ). Take Figure 3.7b for example, a 12-unit time-span ( $|V| = 12$ ) can represent both a 4/4 and a 6/8 meter. Music theory defines on-beat positions in 4/4 meter as the set  $\{0,3,6,9\}$  on the circle (quarter-notes); and on-beat positions are the set  $\{0,6\}$  (dotted quarter-notes) in 6/8 meter. However, the TOB model defines on-beat positions as all positions that can evenly divide the circle (the divisor is greater than one),  $\{0,2,3,4,6,8,9,10\}$ , which is the *union*<sup>2</sup> of the on-beat positions of two meters. This is problematic because on-beat positions  $\{3,9\}$  in 4/4 are known to be off-beat in 6/8, but are still treated as on-beat when modelling 6/8 rhythms. As a result, this model confuses time-signatures and ignores metrical structure in the calculation. This problem directly leads to the incorrect prediction that polyrhythms are not syncopated (Figure 5.6). The second limitation is when  $|V|$  is 1 or any prime number, the circle cannot be divided by any divisor that is greater than one. Therefore, the TOB model cannot define

<sup>2</sup>In set theory, the union of a collection of sets is the set of distinct elements in the collection [HJ99].

on-beat and off-beat positions.

### 5.3.3 Classification models

The classification models, PRS (Equation 3.29) and KTH (Equation 3.45), generally perform well in predicting the data for 4/4 monorhythms. This may be because they are able to capture missing down-beats. The PRS model performs evidently better than the KTH model (Figure 5.4). This may be because the PRS model takes account of hierarchical metrical structure more than the KTH model, and it has a finer categorisation of syncopation types to capture certain features of a rhythm-pattern, whereas KTH only differentiates two categories (on-beat and off-beat) to classify the metrical position of start/end for an event.

In the KTH model, off-beat is defined as instances when the rounded duration of the note (Equation 3.41) is divisible by the start or end position of this note (Equations 3.42 and 3.43) and this definition<sup>3</sup> does not seem complete. For example, any note with duration 1 in time-span representation will be measured as starting and ending on-beat because both starting and ending locations of the note are divisible by 1 (which is also 1's nearest power of two), even if it is not actually on the beat.

The KTH model performs poorly in predicting the data for polyrhythms, but it was probably not originally designed to do so. Also, the KTH model and the off-beat models merely focus on detecting whether a certain event is on-beat or off-beat. However, the contradiction to the established meter that polyrhythms elicit is due to incompatible periodicities of rhythm and meter, not simply due to off-beat events. Because of this, this method is not suitable for measuring polyrhythms. Another limitation of KTH model is that it is only designed to capture binary-divisible meters where the number of beats in a bar is a power of two, therefore the range of its applicability is restricted.

---

<sup>3</sup>It should be noted that the *off-beat* KTH specifies is in relation to the note duration and is therefore variable. This is opposed to the *off-beat* defined in WNBD and TOB, which is determined by metrical structure and is therefore fixed in a given time-signature.

### 5.3.4 General discussion

Overall, all the models predict better at 4/4 monorhythms than 6/8 monorhythms. This can be partially explained by the fact that most of the models were designed to account for 4/4 monorhythms (in [Pre97, Kei91], only 4/4 monorhythms examples are given). Secondly, the poor performance of 6/8 monorhythms may be due to the adoption of an implicit 6/8 metronome (i.e. only accenting the first beat in a bar), instead of an explicit one (i.e. accenting the first and the fourth beats in a bar). The implicit metronome allows listeners to interpret a bar of 6 eighth-notes as three groups of two (3/4) or two groups of three (6/8). Listeners are naturally inclined to choose the meter which minimises syncopation [PE85], therefore their perceived metrical structure may not necessarily be the same as the fixed time-signature the model uses to predict.

In conclusion, a comprehensive syncopation model should emphasise metrical hierarchy so that factors that contribute to syncopation (e.g. a missing down-beat, the location of rhythm-components within a bar) will be considered. The model should also be capable of capturing polyrhythms. The PRS model has shown a better performance in general. This may be due to its unique mechanism where a rhythm is analysed over several larger windows (e.g. bar- or half-bar long window), rather than merely momentary events, hence syncopation is calculated on a continuous time-scale, which may be closer to how humans process rhythm information in a continuous, context-dependent manner.

## 5.4 Summary

In this chapter, we evaluated the models against Dataset 1, which includes mean perceptual ratings of 111 rhythm-patterns. We followed Chapter 4 by splitting the data into three rhythm-categories, resulting in 27 4/4 monorhythms, 36 6/8 monorhythms and 48 polyrhythms, each of which was tested by all the applicable models. Our results suggest that there is much room for improvement, particularly in polyrhythms. We have identified the strengths and weaknesses of the various modelling architectures,

based on which we conclude that a unified mathematical model of synco-  
pation will need to retain both the hierarchical meter structure and the  
flexibility of off-beat models.

## Chapter 6

# Tempo affects syncopation

Tempo describes the speed of a piece of music and typically indicates the rate of the perceived beats (Section 2.1.4). As a fundamental ingredient of music, tempo does not only function as a framework for timing to enable the prediction of future events, but also plays a role in rhythm perception in general [McA10]. In this chapter, we investigate the effects of tempo on the perception of syncopation. Particularly, we investigate how the strength of syncopation perception varies with the change in tempo.

Based on Experiment 1 (Section 4.1), we conducted a second experiment in which we asked musicians to rate the perceived syncopation of eight rhythm-patterns, each of which played at eight different tempi from 30 to 480 QPM. The eight rhythm-patterns chosen were all rated as syncopated at 140 QPM in Experiment 1, comprising a mixture of three rhythm-categories: 4/4 monorhythms, 6/8 monorhythms and 4/4 polyrhythms.

Our main hypothesis is that tempo will influence the perceived syncopation. In addition, we tested whether tempo effects on syncopation are different for: i) polyrhythms and monorhythms, ii) time-signatures of 4/4 and 6/8 and iii) individual rhythm-patterns.

This chapter starts with a literature review on the known effects of tempo on some aspects of rhythm perception in Section 6.1. In Section 6.2, the materials and procedure of Experiment 2 are explained, followed by the results and discussion in Sections 6.3 and 6.4.

## 6.1 Background

The manipulation of tempo causes musical events to be transposed in time. Although this seems to not affect the inner-relationships among the events, it strongly influences the perception of music in various ways. Putting aside the numerous reported tempo effects on pitch perception [DGM88], on physiological responses and emotional state [CH01, vZWvdB11], on music preference [LeB81] and on biophysical behaviours such as dining and driving [CH99, Bro02], here we only focus on studies addressing the relationship between tempo and rhythm perception.

### 6.1.1 Tactus perception and tempo

Tactus is the beat level that is most naturally tapped or danced to (see Section 2.1.2). Various studies, reviewed below, have demonstrated that the perception of tactus (i.e. the perception of the beat level to be selected as tactus) is tempo-dependent and is bounded within ranges of tempi.

Duke asked musicians to tap with perceived beats in response to isochronous (i.e. equal time-interval) tones presented at different rates [Duk89]. The tapping rates range mostly from 60 to 120 BPM regardless of the speed of the stimulus, and 80 BPM was the most frequently occurring tapping rate.

Parncutt conducted a beat-tapping experiment using several rhythmic patterns (of tones) at six different tempi [Par94]. He found the histogram of tapping periods roughly yielded a log-normal distribution with a mean around 710 ms (about 85 BPM) and a standard deviation corresponding to 400 - 1190 ms (about 50 - 150 BPM). Combined with Duke's finding, the region from 50 to 150 BPM may be where tactus is mostly likely to be perceived, and the beat rates from 80 to 100 BPM are preferred for tactus perception.

The beat-tapping paradigm was further investigated in the broader context of a large corpus of musical pieces heard on the radio and in recordings of several styles [vNM99]. Unlike the experimental studies introduced above that involve controlling tempo, this study was observational because it aimed to measure the beat-tapping rates from listeners

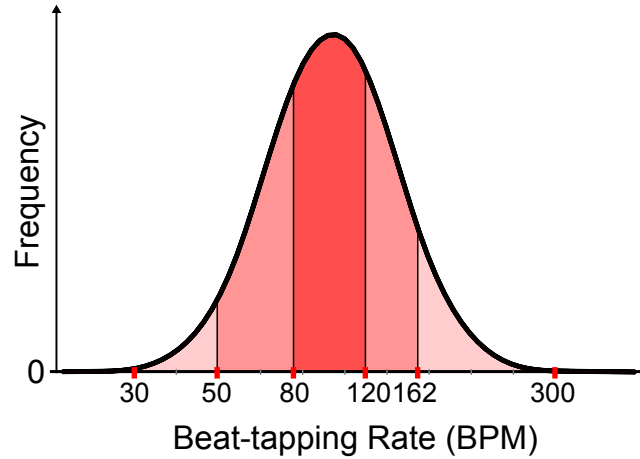


Figure 6.1: Histogram of beat-tapping rates. A schematic histogram of beat-tapping rates, combining the findings from a number of studies [Fra63, Duk89, Par94, vNM99]. The preferred tapping rates of listeners are in the range of 80 - 120 BPM (indicated with the darkest shading). Listeners tend to retain the tapping rate between 50 and 162 BPM (medium shading). The extremes between 30 to 50 and between 160 to 300 BPM (lightest shading) can afford tactus perception, but are much less likely to be tapped.

to existing music without manipulating the tempo of the music. The distribution of tapping rates also roughly yielded a log-normal distribution that was consistent with Parncutt's findings (see [vNM99] for comparisons of distributions of tempi from several sets of experimental data). The peak of the distribution is located around 120 BPM (500 ms) and the 'octave' 81-162 BPM (370 - 740 ms) generally covers the region of commonly perceived tactus rates.

We have reviewed several studies that investigated the relationship between tempo and tactus perception by tapping experiments. Figure 6.1 illustrates the range of beat-tapping rates from converging evidence [Fra63, Duk89, Par94, vNM99]. Overall, the histogram of tapping rates (on a logarithmic scale of BPM) approximately yields a normal distribution. Listeners prefer to tap in a region from 80 to 120 BPM (500 - 750 ms), and generally retain the tapping rate within 50 to 162 BPM (370 - 1190 ms).

### 6.1.2 Tempo limits of tactus and meter perception

Intuitively, the perception of beat or meter must be bounded in time: we cannot separate two sounds if the inter-onset interval is too short [HM90], and we cannot subjectively group events separated by long intervals and form an anticipation of between the future events [Hur06].

The range of 200 - 2000 ms is generally accepted to cover the existence region of tempo for tactus perception [Lon04]. This is estimated by combining observations from several tapping experiments (Section 6.1.1) [Par94, vNM99, HO81]. However, the tempo range that enables the perception of meter is far wider than for tactus. Forming a sense of meter requires listeners to organise beats into groups and to synchronise with the beats [Lon04]. Several studies have investigated the limits of tempi for *subjective rhythmisation*, i.e. perceived groupings of identical and isochronous events. Repp found a lower limit for tapping in phase with every fourth tone by musicians at 100 ms [Rep03]. Fraisse found that 1800 ms is the upper limit for subjective rhythmisation [Fra82]. Mates et al. found that above 2400 ms listeners can no longer synchronise and anticipate accurately [MMPR93]. London suggested an even higher upper boundary for meter perception, which may extend to 5 or 6 seconds. As noted in [Lon04, p. 30]:

... if 2 seconds is the limit for hearing successive events as temporally connected outside of a metric hierarchy, then it makes sense that the absolute value for a measure might be from about 4 to 6 seconds (that is, twice or three times the length of the slowest possible beat).

To summarise, evidence from several experiments has indicated that the range 200 to 2000 ms (30 - 300 BPM) may cover the boundaries of tempi that afford a tactus perception. The perception of meter may be bounded within a wider range of tempo, roughly from 100 ms to 5 or 6 seconds (10 - 600 BPM). Therefore, tactus perception appears to be consistently inside the range of meter perception.



### 6.1.3 Dynamic meter perception influenced by tempo

Multiple studies suggest that the relationship between meter perception and tempo is two-way. On one hand, the perception of tempo is affected by the construction of metrical structure, for example subdivided inter-beat intervals are perceived as longer (i.e. having a slower tempo) than unfilled intervals [Rep08, WK00], and performers exhibit systematic variation in tempo when they shift attention to different metrical levels [MP01]. On the other hand, change of tempo affects the perception of metrical structure and directs the ‘selection’ of *primary rhythmic level* [CM60] (i.e. tactus) from a multi-level metrical structure.

Figure 6.2 illustrates the process of shifting tactus between metrical levels in response to the variation of tempo. The selection of tactus level is biased towards the preferred tempi where listeners tend to tap (Section 6.1.1). When the tempo of the beat level (defined by time-signature) is outside of the suitable tempo range for tactus, any other beat level with a periodicity that is closer to the preferred region of tempo will be perceived as the tactus. It is also possible that more than one beat level may be located in the tempo region that allows a tactus perception, resulting in multiple acceptable tapping rates that are related by simple integer ratios [MM04].

This phenomenon has been demonstrated in a number of studies [Fra63, Par94, Duk89, LCH06, MS99]. Duke found subjects perceived a subdivision of the stimulus tones as a beat when they were presented slower than 60 tones-per-minute (TPM), and perceived alternative tones as the beats at presentation rates faster than 120 TPM [Duk89]. London’s study on the perception of anacruses (i.e. up-beats, one or more notes prior to the first down-beat) also suggested a tendency to shift the perceived tactus to higher metrical levels at faster tempo [LCH06]. He found that listeners were significantly more inclined to perceive anacruses in the short-short-long (SSL) rhythm-pattern as tempo increases. This is a result of perceiving the higher metrical levels as the tactus level at faster tempo, which caused the longer note in SSL rhythm-pattern to be perceived as the down-beat.

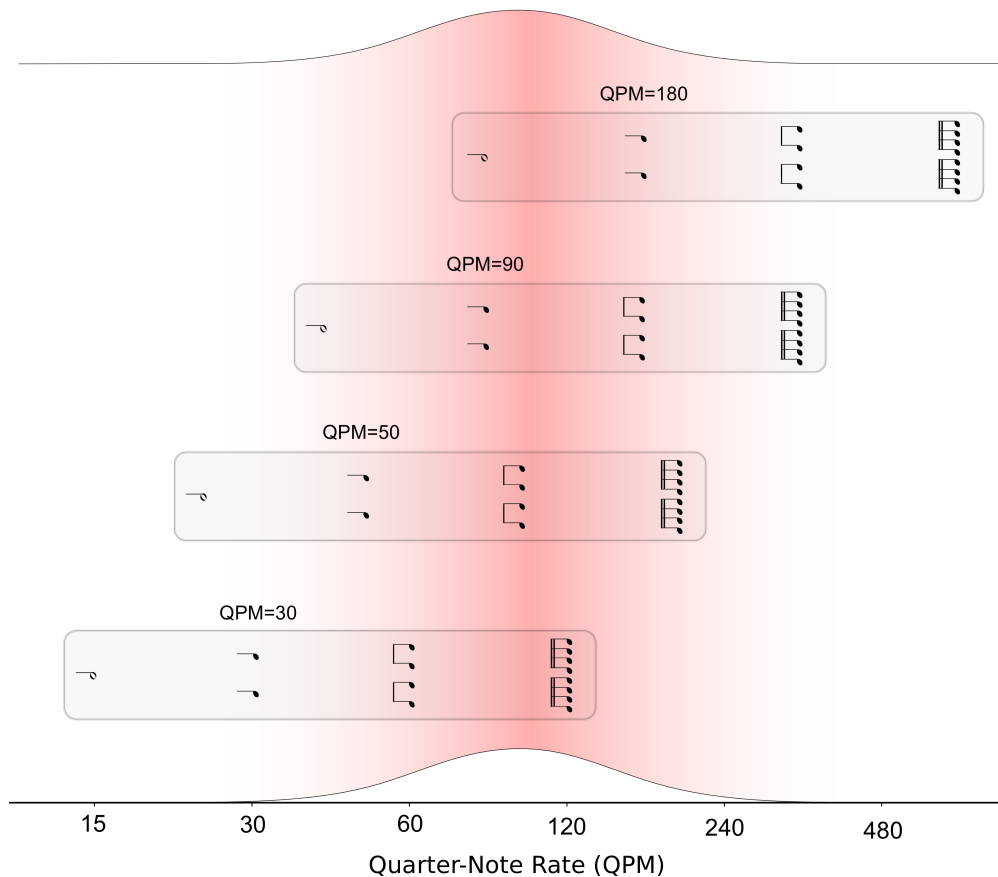


Figure 6.2: Dynamic adjustment of tactus level with change in tempo. A schematic diagram illustrating how change in tempo (QPM) affects the selection of tactus level within the metrical hierarchy. The shaded area indicates the perceptual strength of tactus as in Figure 6.1. The beat level that falls in the range of 50-150 BPM is likely to be selected as tactus; the closer to the ‘hottest’ area from 80-120 BPM, the more likely to be selected. Therefore at 30 QPM, both the eighth-note and sixteenth-note levels fall in the suitable range for tactus, but the sixteenth-note level (120 BPM) is more likely to be tapped at. At 50 QPM, the eighth-note level (100 BPM) is most likely to be selected as tactus. At 90 QPM, the quarter-note level is most likely to be selected; but at 180 QPM, only the half-note level falls in the range suitable for tapping.

In addition to the rhythms that project an unambiguous metrical structure, tempo also plays a role in rhythms that elicit an ambiguous metrical interpretation. For example, in the experiment of Honnon et. al, listeners heard short metrically ambiguous melodies, and were asked to choose

whichever meter they perceive between 3/4 and 6/8 meter, and to rate how firm their perception was [HSEK04]. The melodies were played at two tempi, either 200 ms per note (fast) or 300 ms per note. The results suggest that listeners tend to perceive the meter which has an inter-beat interval<sup>1</sup> of 600 ms. This is consistent with Fraisse's findings [Fra63, Fra82].

Similarly, for highly conflicting rhythm constructions, Handel and Os-hinsky tested several two-train polyrhythms at a broad range of tempi, e.g.  $3 \times 4$  polyrhythm,  $2 \times 5$  polyrhythm [OH78, HO81]. In this paradigm, global tempo determines the inter-onset intervals within each train of rhythms. At slow tempi, the onsets of a pulse train with intervals above 600 - 800 ms are perceived unconnected. At fast tempi, the onsets with intervals below 200 - 300 ms are perceived as grouped because they are too fast to be heard separately, therefore are unsuitable to serve as meter in either case. In general, these findings suggest that listeners tend to choose the train of pulses as tactus whose inter-onset intervals fit within the window of 200 - 800 ms; but, if neither train of pulses satisfies these time constraints, the listeners would use other cues to assist in meter perception (such as pitch).

In summary, how human listeners perceive the primary rhythmic level and the entire metrical structure dynamically adapts to the variation of tempo. This closely relates to the natural preference for a certain range of beat rates (Section 6.1.1). The mental representation of meter influences various aspects of rhythm perception, because it is the fundamental step in the processing of temporal patterns. Thus the investigation of tempo and meter may help us understand the relationship between tempo and the broader rhythmic perceptions.

#### 6.1.4 Hypotheses for tempo effects on syncopation

Previous studies have examined the tempo effects on tactus perception (Section 6.1.1) and meter perception (Section 6.1.3). What has not been systematically tested is the relationship between tempo and syncopation.

---

<sup>1</sup>This inter-beat interval indicates the time-span of three eighth-notes that is consistent with how 'beat' is defined in the time-signature of 6/8.

From a music-theory perspective, Cooper and Meyer predicted the tempo-dependent feature of syncopation:

... whether there is syncopation or not depends upon how the beat or pulse continuum is felt and hence upon the tempo of the piece as well as the performer's articulation of the meter. If the tempo is too slow or if the performer overarticulates lower metric levels, the effect of syncopated notes may be weakened. Or if the tempo is too fast, what should be a higher metric level is felt to be primary metric level, and notes not intended to be syncopated become so. ([CM60, p. 100])

Here Cooper and Meyer were approaching syncopation and tempo from the perspective of the effects of tempo on perception of metrical structure. Listeners naturally adapt the primary rhythmic level to fit in a certain range of tempi (Section 6.1.3). As a result, increase in tempo induces a shift of tactus to a higher metrical level and leads to more off-beat events, resulting in more syncopation; conversely the decrease in tempo shifts the tactus to lower metrical level and merges the notes that were intended to be off-beat into the beat level, resulting in less syncopation.

To our knowledge, Sioros et. al made the first attempt to incorporate the tempo effect in syncopation modelling [SMC<sup>+</sup>13]. They assumed that syncopation exists within a range of beat rates, and arbitrarily set the lower and higher bounds at 500 and 1000 ms. However, this was entirely drawn on their intuitions, and this has not yet been scientifically verified.

Relevant behavioural experiments have been conducted by Handel and colleagues (Section 6.1.3). They correlated syncopated polyrhythms and tempo, and found that the patterns of metrical interpretation depend on tempo and the rhythmic construction of polyrhythms. However, the intensity of syncopation perception of polyrhythms in relation to the change of tempo was not addressed in their experiments.

In the following sections, we aim to investigate the following questions. Is syncopation perception a function of the global tempo? How is the relationship between syncopation and tempo characterised if there is one? Are the temporal limits on meter perception applicable to syncopation,

such that the perception of syncopation will disappear beyond the limits of meter?

In order to address these questions, we tested the degree of perceived syncopation of several syncopated rhythm-patterns being presented at different tempi. Our hypothesis is that a similar relationship between tempo and beat perception would be reflected in syncopation, where maximum syncopation is perceived at the moderate range of tempi, but less or none is perceived at slow and fast tempi.

## 6.2 Experiment 2: Tempo

We replicated the method of Experiment 1, as described in Section 4.1, by asking musicians to give subjective ratings of syncopation for renderings of syncopated rhythm-patterns at a wide range of tempi. This method addresses our objective to investigate whether and how syncopation perception varies with tempo. All the selected rhythm-patterns were (on average) rated as syncopated at a fixed tempo (140 QPM) in Experiment 1. In Experiment 2, we changed the same rhythm-patterns to different global tempi and observed the elicited syncopation perception. Our hypothesis will be corroborated by evidence that the relationship between syncopation and tempo forms an inverted-U-shaped curve, i.e. the average syncopation ratings appear high within the middle range of tempi and decrease for very slow or very fast tempi.

### 6.2.1 Participants

We recruited fifteen trained musicians, eleven male and four female, with an average age of 32 years (standard deviation 6 years). Their musical training included formal performance and theory over a range of instruments, music production and engineering. All participants had trained for an average of 19.5 years (standard deviation 8.5 years). Six of them reported proficiency in multiple instruments. All listeners reported normal hearing and the procedure was approved by the ethics committee of Queen Mary University of London. All listeners reported that they were

comfortable with the ratings scales, confident about what was meant by the terms and in their ability to estimate and rate the intensity of their perception.

### 6.2.2 Stimuli

Figure 6.3 shows the musical scores for eight perceptually syncopated rhythm-patterns selected from Experiment 1 (Sections 4.1 and 5.1). This set of rhythms represents a wide range of perceived intensity of syncopation (mean ratings range from 1.4 to 3.8 at 140 QPM on the 0 - 4 rating scale); and covers three categories of rhythms: monorhythms in a time-signature of 4/4, 3:2 polyrhythms in 4/4 and monorhythms in 6/8.

In order to provide listeners with a stronger meter cue especially at fast tempi, the introductory metronome of the stimuli was extended to two bars (in contrast to only one bar in Experiment 1, Section 4.1), followed by the concurrent two-time-repetitions of a one-bar rhythm-pattern.

Each rhythm-score was rendered at each of eight tempi: 30, 60, 90, 120, 180, 240, 360 and 480 QPM. These chosen tempi cover a broad range of rates, past the temporal limits of tactus and meter perception. In this range, they are roughly logarithmically spaced. It should be noted that QPM is different from how tempo is commonly described, in BPM. However, the metronome beat quarter-notes in 4/4 meter and in 6/8 it beat eighth-notes. Because of the difference of beat level in the hierarchical metrical levels, using BPM would have made it more difficult to compare the rhythms in these two time-signatures. Another common practice is to describe tempo is *inter-beat intervals* in time domain [Fra63, Par94, HSEK04]. Table 6.1 lists the corresponding time intervals between quarter-notes of each tempo in QPM.

We adopted the same synthesising method as in Section 4.1.2. The same snare drum sound sample and the pitched ‘cow-bell’ sound samples were used here again for rhythm and metronome respectively. The durations of stimuli varied depending on the time-signature and the tempo. The shortest trials were 1.5 seconds (i.e. four bars of three quarter-notes at 480 QPM) and the longest trials were 32 seconds (i.e. four bars of four

**4/4 Monorhythms**

---

**4/4 Polyrhythms**

---

**6/8 Monorhythms**

Figure 6.3: Rhythmic scores for Experiment 2. Eight rhythm-patterns taken from the established rhythm set (Experiment 1), including monorhythms and polyrhythms in a time-signature of 4/4, and monorhythms in 6/8. Each stimulus always starts with two bars of metronome introduction and followed by two-time-repetitions of a one-bar rhythm-pattern with concurrent metronome.

Table 6.1: Tempo (QPM) in relation to quarter-note time interval (ms).

Tempo (QPM)	Quarter-note time interval (ms)
30	2000
60	1000
90	667
120	500
180	333
240	250
360	167
480	125

quarter-notes at 30 QPM).

### 6.2.3 Procedure

Blocks of 64 stimuli (8 rhythm-patterns  $\times$  8 tempi) were presented in random order. The procedure remained the same as in Experiment 1 (Section 4.1.3). In brief, listeners were initially asked to complete a practice session to familiarise themselves with the computer interface and listening materials. Then in the experimental session, listeners gave a rating between zero and four to indicate the intensity of their sense of syncopation for each stimulus, where zero indicated no syncopation and four indicated maximum syncopation.

## 6.3 Results

We adopted a top-down approach for data analysis, by starting with an overview of the relationship between tempo and ratings averaged across all rhythm-stimuli, then moving to group comparisons categorised by either time-signature or rhythm-category, and finally examining the tempo effects on individual rhythm-patterns. The following sections are structured in the same order. It should be noted that the focus of all analysis is on the relative ratings, i.e. how the ratings of syncopation perception may vary with tempo, instead of absolute ratings, i.e. how strong the syncopation perception is for certain rhythms at a particular tempo.



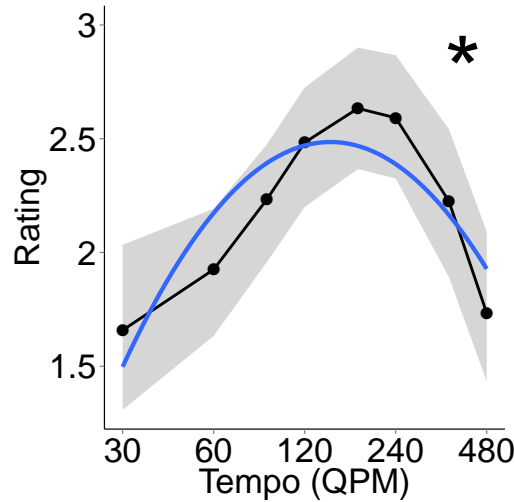


Figure 6.4: Grand mean syncopation ratings as a function of tempo. The group mean syncopation ratings at different tempi (on a logarithmic scale) are represented by the dots. The shaded area represents 95% confidence intervals. The blue curve indicates the regression line that fits a log-quadratic relationship between the mean ratings and tempi. \* denotes significant ( $p < 0.05$ , *Friedman Rank Sum Test*).

### 6.3.1 Syncopation is a function of tempo

Syncopation ratings were collapsed across all rhythm-stimuli at each tempo and averaged for each listener. These grand mean ratings with 95% confidence intervals are plotted in Figure 6.4. As the ratings are not normally distributed, a Friedman Rank Sum Test was performed with the mean ratings as the dependent variable and the tempo conditions as the independent variable. The result suggests that there is an effect of tempo on syncopation ratings ( $\chi^2(7) = 48.03, p < 0.001$ , *Friedman Rank Sum Test*). As Figure 6.4 shows, the relationship between syncopation and tempo seems to yield an inverted-U-shape but not entirely symmetrical relationship with tempo.

In order to characterise the relationship between syncopation and tempo (i.e. how the syncopation rating varies with tempo) and compare this tempo effect between rhythms, we applied log-quadratic fits to the grand mean ratings as shown in Figure 6.4. This function provides a good fit to the data ( $r = 0.86, p < 0.01$ , *Spearman's Rank Correlation*). The use of

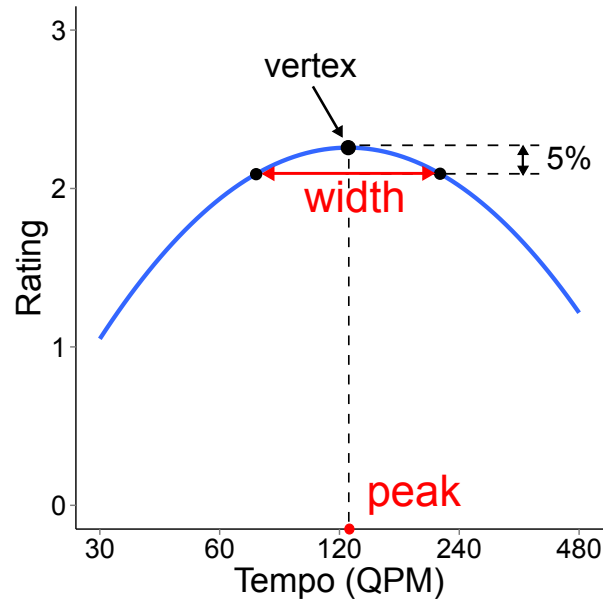


Figure 6.5: Peak and width of a quadratic curve. The peak is the x-coordinate of vertex, referring to the tempo value in QPM where it arouses the maximum syncopation perception. The width refers to the range of tempi that corresponds to top range of syncopation perception. The threshold is arbitrarily set to 5% below the vertex.

quadratic fits to characterise the shape of the data allows the comparisons of merely two parameters, the peak and the width. It is much simpler to compare these than histograms of ratings. Compared to an alternative procedure, the log-normal distribution fit, the log-quadratic fit is more robust as it can be applied to non-normally distributed data, hence it is a better choice for characterising the shape of the data.

In the next section, we give a brief review of quadratic functions to serve a better understanding of the further analysis.

### 6.3.2 Quadratic function

If the *general form* of the equation for a quadratic function is:

$$f(x) = ax^2 + bx + c, \text{ with } a \neq 0 \quad (6.1)$$

The turning point on a quadratic curve is referred to as the *vertex*, which has an x-coordinate that is also the axis of symmetry of the curve.

The location of the vertex is:

$$\left(-\frac{b}{2a}, -\frac{b^2 - 4ac}{4a}\right) \quad (6.2)$$

This is derived by converting the quadratic function into *vertex form*:

$$f(x) = a\left(x + \frac{b}{2a}\right)^2 - \frac{b^2 - 4ac}{4a} \quad (6.3)$$

The *roots* of a quadratic function are known as the two values of  $x$  for which  $f(x) = 0$ . The distance between roots reflects the width of the curve, i.e. with a fixed vertex, the further apart the roots are, the wider the curve is. The equation for calculating roots is:

$$f^{-1}(0) = \frac{-b \pm \sqrt{b^2 - 4ac}}{2a} \quad (6.4)$$

Similarly, given any number  $y$  with  $y \in f(x)$ , we can calculate the two values of  $f^{-1}(y)$  notated as  $x_1$  and  $x_2$ :

$$\begin{aligned} x_1 &= \frac{-b + \sqrt{b^2 + 4a(y - c)}}{2a} \\ x_2 &= \frac{-b - \sqrt{b^2 + 4a(y - c)}}{2a} \end{aligned} \quad (6.5)$$

Based on Equations 6.3 and 6.5, we define two variables summarising a quadratic curve: the *peak* and the *width*. The peak is the corresponding tempo value of the vertex (Equation 6.2). It estimates the ‘sweet spot’ of tempo that maximises syncopation perception; in this study, it is constrained to vary within the tested range of tempi from 30 to 480 QPM:

$$peak = e^{-\frac{b}{2a}}, \text{ with } peak \in [30, 480] \quad (6.6)$$

The width refers to the absolute difference between the two tempo values of  $f^{-1}(y)$  where  $y$  is set to the 5% lower than the vertex (Equation 6.2), which constrains the curve itself to open downwards. The upper bound of width is set to the maximum tested tempo 480 QPM.

$$y = 0.95 * \left(-\frac{b^2 - 4ac}{4a}\right),$$

$$width = |x_1 - x_2|, \text{ with } width \in [0, 480] \quad (6.7)$$

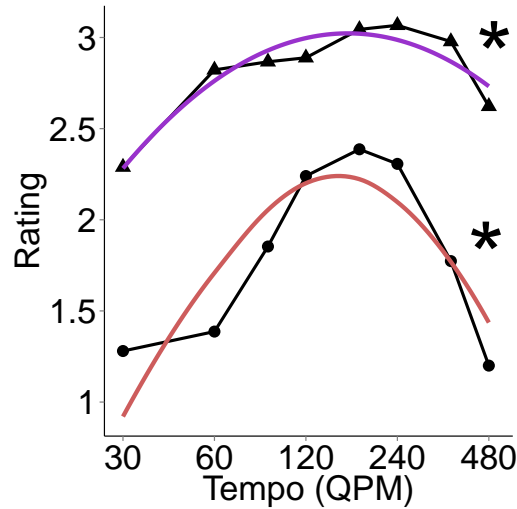


Figure 6.6: Tempo effects between rhythm-categories. The group mean syncopation ratings in two rhythm-categories are plotted: circles mark the monorhythms, triangles mark the polyrhythms. \* denotes significant ( $p < 0.05$ , *Friedman Rank Sum Test*). The red curve indicates the regression line that fits a log-quadratic relationship between the mean ratings of monorhythms and tempi. The purple curve indicates the same for the polyrhythms group.

### 6.3.3 Polyrhythms are more resistant to tempo changes

All ratings of monorhythms were separately pooled from those of polyrhythms, then averaged for each listener at each tempo. Figure 6.6 presents the mean ratings in both rhythm-categories, and the corresponding fitted log-quadratic curves. Again, the mean ratings in both rhythm-categories vary significantly across eight tempi conditions, and the effect of tempo (i.e. the effect size  $\chi^2$ ) appears to be stronger for monorhythms ( $\chi^2(7) = 47.92, p < 0.001$ , *Friedman Rank Sum Test*) than polyrhythms ( $\chi^2(7) = 16.84, p < 0.05$ , *Friedman Rank Sum Test*).

Then, for each listener ( $N = 15$ ), ratings of all monorhythms and polyrhythms were separately pooled, and within each group of rhythm-categories ratings were averaged across rhythm-patterns. The same log-quadratic fitting procedure (see Sections 6.3.1 and 6.3.2) was applied to each listener's data in each group. This resulted in 15 fitted curves for mean ratings of all monorhythms and 15 fitted curves for mean ratings of all polyrhythms.

Some *outliers* emerged during this procedure, where the fitted curves for some listeners' data failed to meet the constraints defined in Equations 6.6 and 6.7. This reflects the imperfect nature of the data where it shows more variance at the level of the individual listener, and that the quadratic modelling is not ideal when being applied to specific sub-groups of data. In this circumstance, outlier exclusion is a way to remove noise in the data when it gets down to specific categorical comparisons.

Two strategies were adopted to remove outliers, leading to two ways of implementing group comparison. The first is referred to as *unpaired-subject group comparison*. Outliers within each group were removed separately, resulting in different remaining subjects (unpaired) between monorhythms group ( $N = 13$ ) and polyrhythms group ( $N = 8$ ). Following this procedure, the mean tempi (and 95% confidence intervals) of peaks and widths for both groups were plotted in Figure 6.7. It shows that no significant difference in peaks between two groups is evident ( $p > 0.05$ , *Mann-Whitney U Test*). The average peak of fitted curves for both monorhythms and polyrhythms is around 133 QPM. Yet, the fitted curves for polyrhythms are generally wider than monorhythms ( $U = 24$ ,  $Z = -2.03$ ,  $p < 0.05$ ,  $r = 0.44$ , *Mann-Whitney U Test*) by about 30 QPM on average.

The alternative is *paired-subject group comparison*, which requires removing outliers across groups, i.e. the listener who constituted an outlier in either monorhythms or polyrhythms group will be removed from both groups. This results in paired subjects ( $N = 8$ ) in both groups. Figure 6.8 presents the comparison of peaks and widths between groups. We observed the same results as the unpaired-subject procedure: the peaks of the tempo effects between two groups appear not significantly different ( $p > 0.05$ , *Wilcoxon Signed-Rank Test*), but the tempo effect for monorhythms is again significantly stronger than polyrhythms ( $W = 0$ ,  $Z = -2.52$ ,  $p < 0.01$ ,  $r = 0.89$ , *Wilcoxon Signed-Rank Test*).

#### 6.3.4 No evidence of an effect of time-signature

All ratings were categorised by time-signatures at each tempo then averaged for each listener. Figure 6.9 shows the group mean ratings in both

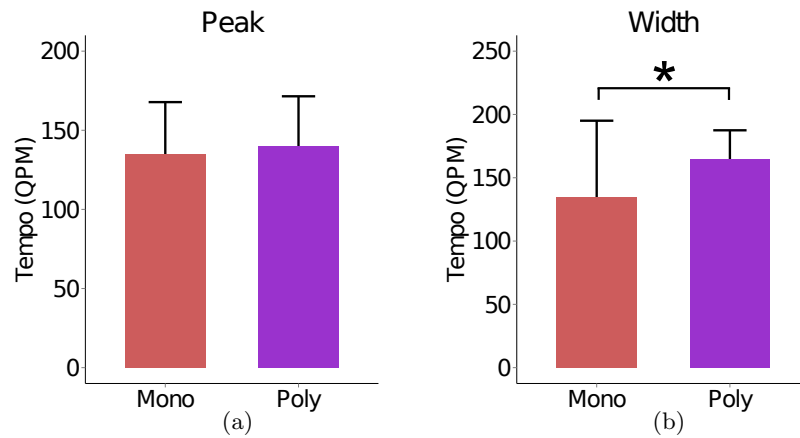


Figure 6.7: Unpaired-subject comparisons of peaks and widths between rhythm-categories. Red and purple indicate monorhythms and polyrhythms respectively. (a) The group means and 95% confidence intervals of the peaks of the fitted log-quadratic curves averaged for each listener. (b) The group means and 95% confidence intervals of the widths of the fitted log-quadratic curves averaged for each listener. \* denotes significance in difference for pair-wise comparison ( $p < 0.05$ , *Wilcoxon Signed-Rank Test*).

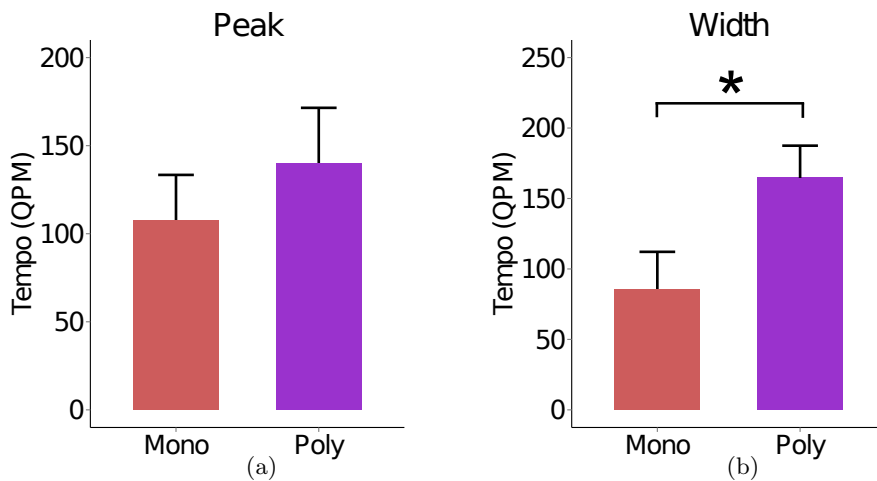


Figure 6.8: Paired-subject comparisons of peaks and widths between rhythm-categories. Red and purple indicate monorhythms and polyrhythms respectively. (a) The group means and 95% confidence intervals of the peaks of the fitted log-quadratic curves averaged for each listener. (b) The group means and 95% confidence intervals of the widths of the fitted log-quadratic curves averaged for each listener. \* denotes significance in difference for pair-wise comparison ( $p < 0.05$ , *Wilcoxon Signed-Rank Test*).

groups of time-signature, and the fitted log-quadratic curves. The effects of tempo on the mean ratings in both groups are significant, and the effect

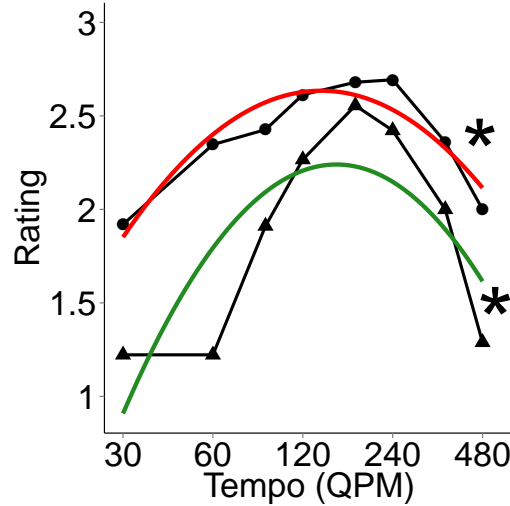


Figure 6.9: Tempo effects between time-signatures. The group mean syncopation ratings under two conditions of time-signature are plotted: circles mark the 4/4 group, triangles mark the 6/8 group. The red curve indicates the regression line that fits a log-quadratic relationship between the mean ratings in the 4/4 group and tempi. The green curve indicates the same for the 6/8 group. \* denotes significance ( $p < 0.05$ , *Friedman Rank Sum Test*).

in 6/8 group ( $\chi^2(7) = 39.47, p < 0.001$ , *Friedman Rank Sum Test*) seems to be stronger than 4/4 group ( $\chi^2(7) = 25.11, p < 0.001$ , *Friedman Rank Sum Test*).

Next, for each listener ( $N = 15$ ) ratings were separately pooled and averaged for all stimuli in 4/4 and those in 6/8. The same log-quadratic fitting procedure was applied to each listener's data in each group. Then the unpaired-subject comparison between two groups was repeated (see Section 6.3.3). First, the outliers within each group were removed, leading to unpaired subjects between the 4/4 group ( $N = 8$ ) and the 6/8 group ( $N = 11$ ). Figure 6.10 plots the mean tempi (with 95% confidence intervals) of the peaks and widths in both groups. We found no evidence to suggest that the peaks or the widths are significantly different between two time-signatures ( $p > 0.05$ , *Mann-Whitney U Test*). The mean peaks are roughly 132 QPM and 147 QPM in 4/4 and 6/8 group respectively.

We then conducted the paired-subject group comparison between the 4/4 and the 6/8 group ( $N = 7$ ) by removing outliers across groups (see

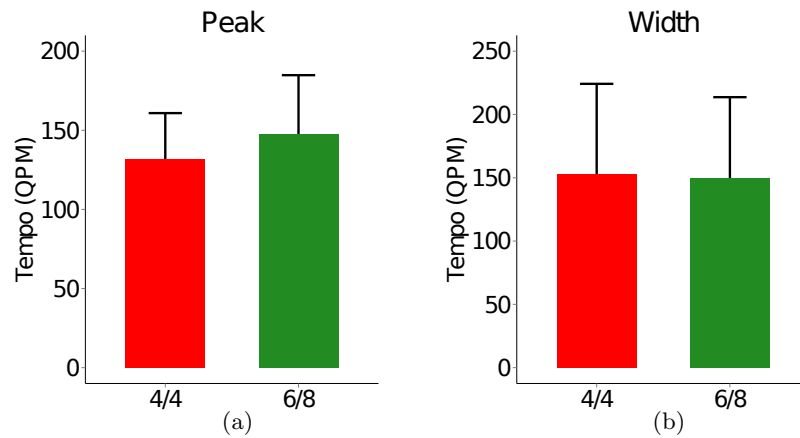


Figure 6.10: Unpaired-subject comparisons of peaks and widths between time-signatures. Red indicates the 4/4 group and green indicates the 6/8 group. (a) The group mean and 95% confidence intervals of the peaks of the fitted log-quadratic curves averaged for each listener. (b) The group mean and 95% confidence intervals of the widths of the fitted log-quadratic curves averaged for each listener.

Section 6.3.3). Figure 6.11 shows the mean tempi (with 95% confidence intervals) of peaks and widths of fitted curves in both groups. The difference in peaks between the two groups remains insignificant ( $p > 0.05$ , *Wilcoxon Signed-Rank Test*). However, in contrast to Figure 6.10, the widths of the fitted curves for 4/4 group appear to be significantly wider than for 6/8. The difference in widths between these two groups is on average about 23 QPM ( $W = 27, Z = 2.20, p < 0.05, r = 0.83$ , *Wilcoxon Signed-Rank Test*).

Only the 4/4 group, not the 6/8 group, includes polyrhythms, therefore the effect of polyrhythms may be a confounding factor. In order to rule out the influence of polyrhythms, we replicate the above procedure but only pooling ratings for monorhythms in 4/4 and monorhythms in 6/8. Two lines of evidence suggest that the effects of tempo are similar for monorhythms in 4/4 and monorhythms in 6/8. First of all, tempo strongly affects monorhythms in both signatures as shown in Figure 6.12 (in 4/4,  $\chi^2(7) = 23.96, p < 0.001$ , *Friedman Rank Sum Test*; in 6/8,  $\chi^2(7) = 39.47, p < 0.001$ , *Friedman Rank Sum Test*). Additionally, Figure 6.13 plots the comparison of peaks and widths generated by unpaired-subject group comparison, and 6.14 shows the same by paired-subject



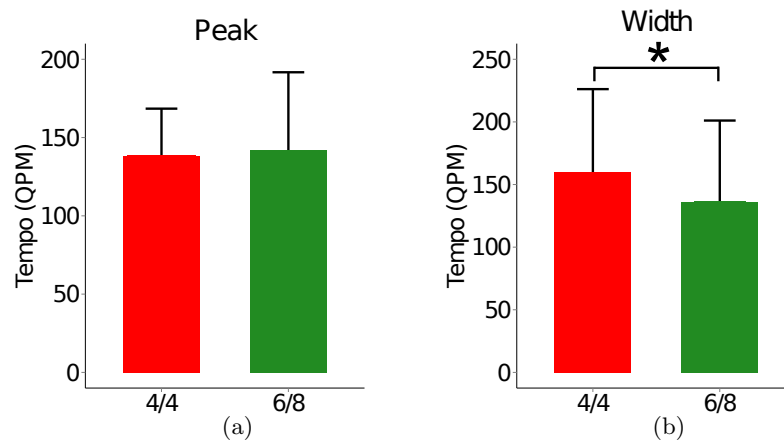


Figure 6.11: Paired-subject comparisons of peaks and widths between time-signatures. Red indicates the 4/4 group and green indicates the 6/8 group. (a) The group mean and 95% confidence intervals of the peaks of the fitted log-quadratic curves averaged for each listener. (b) The group mean and 95% confidence intervals of the widths of the fitted log-quadratic curves averaged for each listener. \* denotes significance ( $p < 0.05$ , *Wilcoxon Signed-Rank Test*).

group comparison. Both suggest there is no significant difference in either peaks or widths of the fitted curves for monorhythms between the two time-signatures ( $p > 0.05$  for both *Mann-Whitney U Test* and *Wilcoxon Signed-Rank Test*). Thus, we can conclude that there is no strong evidence to suggest that tempo affects rhythms in 4/4 differently from those in 6/8.

### 6.3.5 Individual rhythms show different sensitivity to tempo

In order to investigate whether the tempo effect is rhythm-pattern dependent, we compared the relationships between tempo and individual rhythm-patterns. Ratings of each rhythm-pattern were separately pooled and averaged for each listener. Figure 6.15 plots the mean ratings and 95% confidence interval of each of the eight rhythm-patterns against tempi. The results of *Friedman Rank Sum Tests* showed in total five rhythm-patterns have significant differences in ratings at different conditions of tempo. These rhythms are GD ( $\chi^2(7) = 14.98, p < 0.05$ ), FF ( $\chi^2(7) = 28.52, p < 0.001$ ), BBBB ( $\chi^2(7) = 24.13, p < 0.001$ ), GJ ( $\chi^2(7) = 35.29, p < 0.001$ ) and HF ( $\chi^2(7) = 18.73, p < 0.01$ ) (Figure 6.15b, 6.15d - 6.15g).

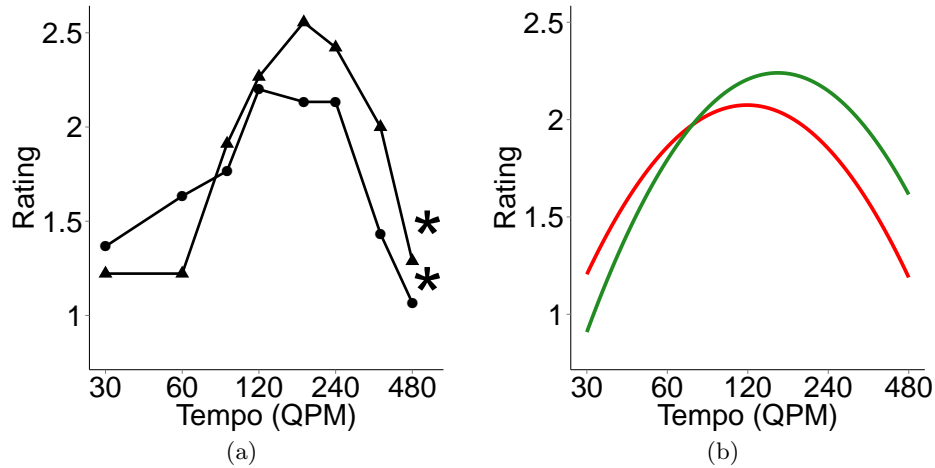


Figure 6.12: Tempo effects on monorhythms between time-signatures. (a) The group mean syncopation ratings of monorhythms in two time-signatures: circles mark the 4/4-mono group, triangles mark the 6/8-mono group. \* denotes significance ( $p < 0.05$ , *Friedman Rank Sum Test*). (b) The regression line that fits a log-quadratic relationship between the mean ratings in either group and tempi. The red curve indicates the 4/4-mono group and the green curve indicates the 6/8-mono group.

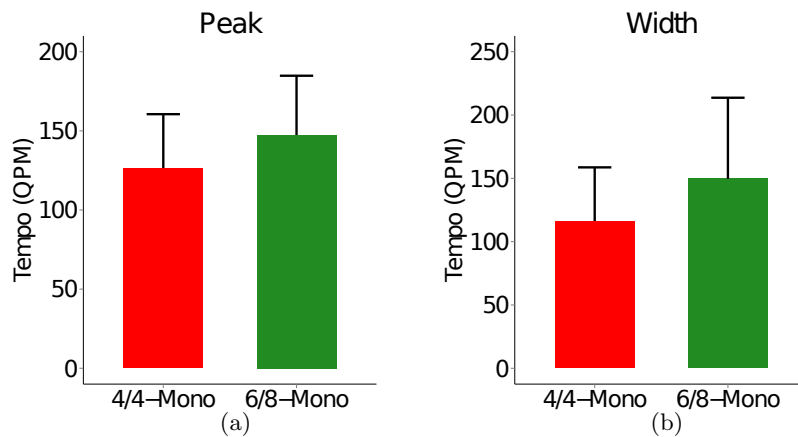


Figure 6.13: Unpaired-subject comparisons of peaks and widths between time-signatures for monorhythms. Red indicates monorhythms in 4/4 and green indicates monorhythms in 6/8. (a) The group mean and 95% confidence intervals of the peaks of the fitted log-quadratic curves averaged for each listener. (b) The group mean and 95% confidence intervals of the widths of the fitted log-quadratic curves averaged for each listener.

We then narrowed the comparisons down to these five rhythm-patterns that presented a strong tempo effect. For each listener, the same quadratic

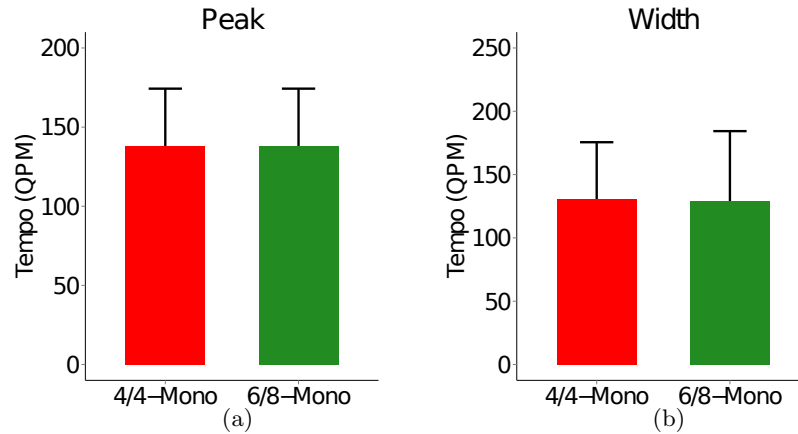


Figure 6.14: Paired-subject comparisons of peaks and widths between time-signatures for monorhythms. Red indicates monorhythms in 4/4 and green indicates monorhythms in 6/8. **(a)** The group mean and 95% confidence intervals of the peaks of the fitted log-quadratic curves averaged for each listener. **(b)** The group mean and 95% confidence intervals of the widths of the fitted log-quadratic curves averaged for each listener.

fitting procedure was replicated to the ratings separately pooled for each of the five rhythm-patterns. In parallel to the analyses discussed in Section 6.3.3 and 6.3.4, we first implemented the unpaired-subjects comparisons. The outliers within each rhythm-pattern were removed, and the resulting distributions of peaks and widths of fitted curves for GD ( $N = 8$ ), FF ( $N = 10$ ), BBBB ( $N = 12$ ), GJ ( $N = 13$ ) and HF ( $N = 10$ ) were compared pair-wise as shown in Figure 6.16. No significant difference were observed between the peaks for any pair of rhythm-patterns ( $p > 0.05$ , *Mann-Whitney U Test*). However, the curve generated from GD is significantly wider than BBBB by about 30 QPM ( $U = 22$ ,  $Z = -2.01$ ,  $p < 0.05$ ,  $r = 0.45$ ) and wider than FF by about 24 QPM ( $U = 17$ ,  $Z = -2.04$ ,  $p < 0.05$ ,  $r = 0.48$ , *Mann-Whitney U Test*, uncorrected), though this significance is only marginal. This result is consistent with the observation in Section 6.3.3 that the tempo effect on polyrhythms (GD) may be generally weaker than monorhythms (BBBB and FF).

Then for the paired-subject comparison between pairs of rhythm-patterns, outliers were removed across each pair of rhythm-patterns. For example, the group of rhythm BBBB and the group of rhythm FF contain three

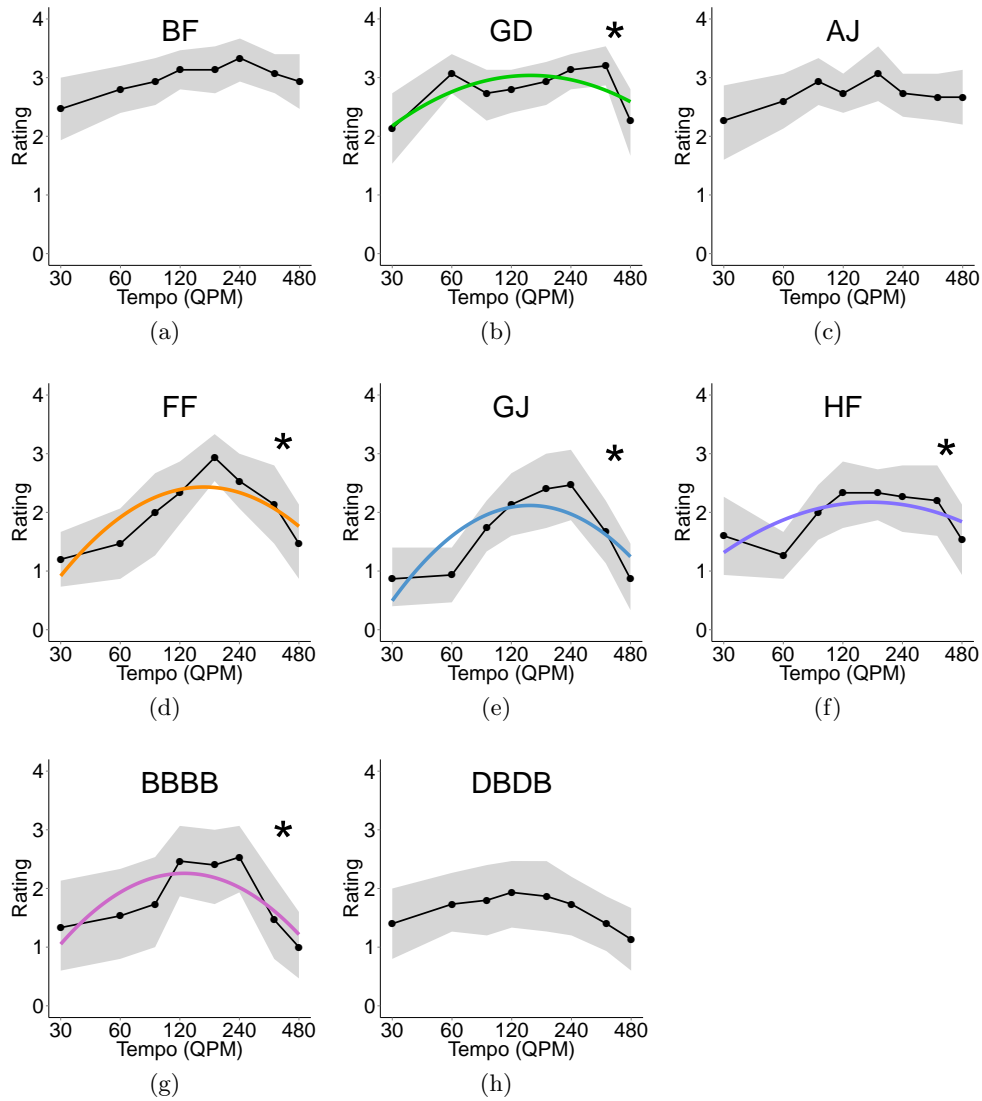


Figure 6.15: Tempo effects between rhythm-patterns. The group means syncopation ratings of each rhythm-pattern against tempi are plotted. The shaded areas indicate 95% confidence intervals. \* denotes significance ( $p < 0.05$ , *Friedman Rank Sum Test*). The rhythms in the first row, (a)-(c), are 4/4 polyrhythms; those in the second row, (d)-(f), are 6/8 monorhythms; and those in the third row, (g) and (h), are 4/4 monorhythms. The coloured fitted log-quadratic curves were fitted and plotted for the rhythm-patterns that have shown a significant tempo effect.

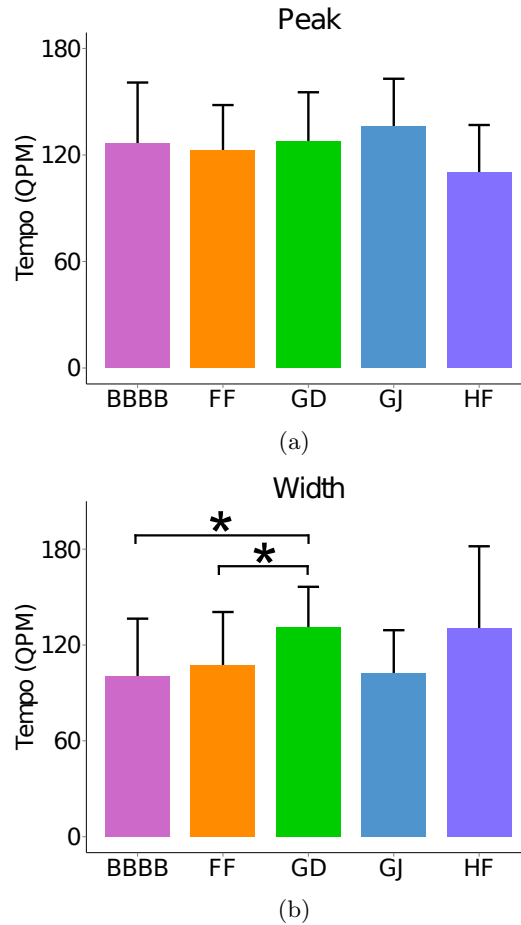


Figure 6.16: Unpaired-subject comparisons of peaks and widths between rhythm-stimuli. The colours used represent different the rhythm-stimuli, as in Figure 6.15. **(a)** The group means and 95% confidence intervals of the peaks of the fitted log-quadratic curves averaged for each listener. **(b)** The group means and 95% confidence intervals of the widths of the fitted log-quadratic curves averaged for each listener. \* denotes significance in difference for pairwise comparison ( $p < 0.05$ , *Mann-Whitney U Test*, uncorrected).

and five outliers respectively, two in common; therefore, six subjects were removed across two groups in total. Figure 6.17 shows the comparisons of peaks and widths between each pair of rhythm-patterns. Again, no single pair presents a significant difference in peak of the fitted curves ( $p > 0.05$ , *Wilcoxon Signed-Rank Test*). Only one pair shows a significant difference in width: the fitted curves of rhythm GD is on average wider than GJ by about 35 QPM ( $W = 2, Z = -2.03, p < 0.05, r = 0.76$ , *Wilcoxon*

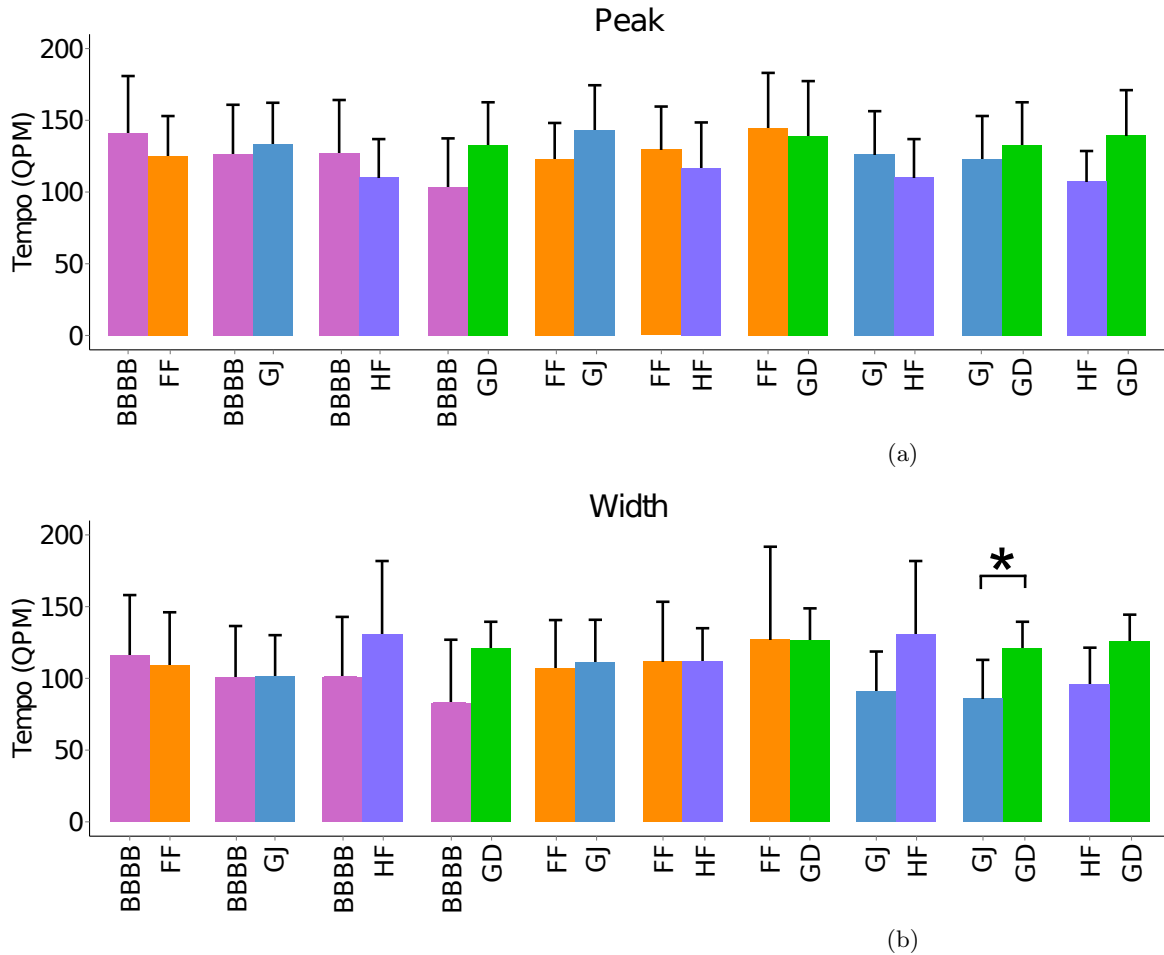


Figure 6.17: Paired-subject comparisons of peaks and widths between pairs of rhythm-stimuli. The colours used represent different the rhythm-stimuli, as in Figure 6.15. **(a)** The group means and 95% confidence intervals of the peaks of the fitted log-quadratic curves averaged for each listener. **(b)** The group means and 95% confidence intervals of the widths of the fitted log-quadratic curves averaged for each listener. \* denotes significance in difference for pair-wise comparison ( $p < 0.05$ , *Wilcoxon Signed-Rank Test*, uncorrected).

*Signed-Rank Test*, uncorrected).

An alternative paired-subject comparison requires removing outliers across all five rhythm-patterns. Yet, this method suffers from too few common subjects ( $N = 5$ ) throughout entire rhythm-patterns, resulting in too weak a power of the analysis. Therefore we choose not to implement

it.

In summary, we observed a diversity of tempo effects on individual rhythm-patterns. Syncopation elicited by rhythm-patterns BBBB, FF, GD, GJ and HF is strongly affected by tempo, whereas the tempo effect on other rhythms was not significantly affected by tempo. The five rhythm-patterns have similar estimated tempi that correspond to maximum syncopation, i.e. the peaks of fitted quadratic curves. However, the tempo effect on GD seems to be significantly wider than BBBB, FF, and GJ. This can be interpreted as further evidence supporting the theory that syncopation aroused by polyrhythms is less sensitive to tempo changes.

## 6.4 Discussion

We collected ratings of syncopation perception for several syncopated rhythm-patterns being transposed over a wide range of tempi. Overall, the results confirm our hypothesis that the strength of syncopation perception is maximised at middle range tempi and weakened towards the extreme tempi (Figure 6.4). We have also found that monorhythms are more strongly affected by tempo than polyrhythms (Figures 6.6 - 6.8).

The causes of these phenomena may be two-fold: tempo influences the perception of tactus and tempo prompts the adjustment of tactus between metrical levels. Our data show a weaker tempo effect on rhythms in 4/4 meter than 6/8 (Figures 6.9 - 6.11), but this may be mostly due to the difference in tempo effects between polyrhythms and monorhythms, as the 4/4 group is a mixture of monorhythms and polyrhythms but the 6/8 group only includes monorhythms. Indeed, after excluding polyrhythms from the comparison there is no longer any evidence to suggest a significant difference (Figures 6.12 - 6.14). Therefore, we can conclude that tempo effect does not appear to differentiate between the time-signatures of 4/4 and 6/8.

Additionally, we found no substantial difference in the tempo effects among individual rhythm-patterns (Figures 6.15 - 6.17). The marginally significant difference in widths of fitted curves between GD and FF, between GD and BBBB (Figure 6.16), or between GD and GJ (Figure 6.17)

can be interpreted as the difference in tempo effects between monorhythms and polyrhythms. In Section 6.4.6, we provide possible explanations for the observations that time-signature and rhythm-patterns do not have an effect.

#### **6.4.1 The tempo effect on syncopation parallels the tempo effect on tactus**

Based on the evidence reviewed in Section 6.1.1 and 6.1.2, the range of beat rates known to afford a perception of tactus is approximately from 200 ms to 2000 ms (30 - 300 BPM) [Lon04]. The overall probability function of beat-tapping rates roughly yields a normal distribution on a logarithmic-scale of tempo [Par94, Moe02]. The preference of tapping rates may reflect the perceptual strengths of beat salience [Fra82, Moe02]. In this case, the perception of beat should be maximised at a moderate range of tempi (500 - 750 ms, 80 - 120 BPM), and decay towards the boundaries of tactus perception.

Syncopation is the product of rhythm foreground contradicting the metrical background. When the beat is weakly perceived (or even not perceivable), then it cannot serve as the background for the contradiction that arouses the perception of syncopation. This could help with explaining the observed log-quadratic relationship between syncopation and tempo, which appears similar to the relationship between tactus perception and tempo.

To be more specific, when the metronome is presented at 30 BPM, which is the lower limit of tactus perception (2000 ms), listeners will have difficulty in hearing successive beats as a continuous stream [Fra82]. Instead, the beats are perceived as unconnected events, imposed onto the rhythmic events. In this case, it is possible that listeners no longer hear the rhythm and metronome as two streams that interact with each other, but rather one sequence of unrelated events.

As the metronome speeds up, the perceptual strength of beat salience increases, hence the perception of metrical background is better formed. As a result, the contradiction between rhythm and meter becomes more



evident, leading to a stronger perception of syncopation.

At very fast tempi (e.g. 360 and 480 BPM in Figure 6.4), the rates of metronome ticks are beyond the upper limit of tactus perception (about 200 ms, 300 BPM), and are getting close to the limits of meter perception (about 100 ms, 600 BPM). Then, the metronome is too fast to be perceivable as a tactus, whereas rhythm-patterns that possess longer inter-onset intervals than the metronome can still be perceived. Two streams of events, metronome and rhythm, are rendered as different sounds. This allows listeners to segregate the metronome events from the rhythm events. However, when the metronome becomes too fast to be perceived, it effectively turns into noise, being superimposed onto the perceivable rhythm. Then, it is possible that listeners are inclined to only process the information in the rhythms and ignore this noise. As a result, the perception of syncopation will be weakened because listeners are no longer hearing the contradiction between rhythms and meter, but may either interpret different meter induced by the rhythm [Lon04] or may process rhythms in a nonmetric way, i.e. the rhythm interpretation strategy that does not involve extracting periodic pulses from the rhythms [HL83].

In short, the effect of tempo on the perception of syncopation can be explained by the known effects of tempo on tactus perception. The extreme slow or fast tempi undermine the perception of tactus, on which the perception of syncopation depends. While this explains the general shape of tempo effect on syncopation, it cannot explain why the curve of the tempo effect on tactus perception does not fully coincide with that of syncopation. In the following sections, we attempt to provide an explanation for this based on the findings of other studies that show that tempo influences the adjustment of tactus in between metrical levels.

#### **6.4.2 Adjustable tactus level and syncopation**

In Section 6.1.3, we introduced the phenomenon of shifting tactus between metrical levels to adapt to the change in tempo. To maintain the beat-intervals of tactus in a preferred range, listeners tend to move it to lower metrical levels when the tempo (of the defined beat level) is too slow, or

move it to higher metrical levels if the tempo is too fast. Some evidence suggests that the selection of tactus level is centred around a beat interval of 100 BPM (600 ms) [HSEK04, Fra82]; others suggest a range of 60 - 120 BPM (500 - 1000 ms) [Duk89] or 75 - 300 BPM (200 - 800 ms) [HO81].

As Cooper and Meyer hypothesised (Section 6.1.4), the adjustment of tactus level may directly affect the perception of syncopation. For monorhythmic patterns (e.g. BBBB, FF) at 30 QPM, listeners may perceive tactus at a lower rhythmic level than the beat level of metronome by interpolating beats. In consequence, some notes that were supposed to be off-beat become on-beat, hence the syncopation is diminished. At the other end of the tempo scale, when beat rates exceed 120 QPM, listeners may shift tactus to a higher metrical level by effectively ‘under-sampling’ the metronome ticks. Therefore some notes that were originally on-beat become off-beat, resulting in syncopation.

### 6.4.3 Peak tempo of syncopation is lagged to that of tactus

The theory of adjusting tactus level with change in tempo may further explain why the tempo that corresponds to the maximal syncopation (180 - 240 QPM, Figure 6.4) is faster than the peak tempo for tactus perception (varying from 80 to 120 BPM, Section 6.1.1), and the slightly asymmetrical shape of the log-tempo curve. When tempo exceeds the upper limit of preferred tactus rates, the tactus rate moves back to the preferred range by adjusting the tactus level. This causes the perceptual strength of tactus to *decrease* with the increasing tempo, but meanwhile syncopation *increases* due to the adjustment of tactus level. This tendency may continue until tempo becomes too fast to allow the adjustment of tactus level.

### 6.4.4 Polyrythms versus monorhythms

Syncopation elicited by polyrythms is less affected by tempo than monorhythms (Section 6.3.3, Figure 6.6). For polyrythms, but not monorhythms, shifting tactus to a lower metrical level at slow tempi could not reduce the contradiction between the polyrythm and meter. This is because the nature of polyrythms is to produce a constant mismatch between rhythm

and meter at any tempo because polyrhythms contain dissonant periodicities [HO81, Yes76]. Therefore in polyrhythms, some notes can never coincide with the metrical positions at any beat level and hence there will always be a contradiction to the meter.

Nevertheless, polyrhythms still exhibit a mild tendency of diminished syncopation towards extreme tempi, which may be due to the decreasing strength of meter perception in general (Section 6.4.1). Handel tested the relationship between rhythm discrimination and tempo, and found that the same patterns played at different tempi were perceived as different rhythms [Han93]. Perhaps at extreme tempi, listeners have more difficulty in precisely judging the inter-relationships between notes in polyrhythms compared to patterns played at moderate tempi. It is possible that the affected timing structure between notes also changes the relationship between rhythm and meter, making it less contradictory.

#### 6.4.5 Possible meter induction at extremely fast tempi

In Section 6.4.1, we suggested that at extremely fast tempi, rhythm-patterns may be separately processed from the noise-like metronome. These rhythm-patterns may induce a different metrical interpretation for the judgement of syncopation. Interestingly, we found that the syncopation of rhythms BBBB, GJ and FF decrease more steeply than HF after peak tempi (roughly 180 - 240 QPM, Figure 6.15). These three rhythms all contain evenly spaced notes (Figure 6.3), which are more likely to induce periodic beats that align with the notes [PE85]. In contrast, the notes in rhythm HF are not evenly distributed. Therefore, it is plausible that the syncopation perception of rhythms BBBB, GJ and FF decreases more quickly at fast tempi because they naturally induce a meter that fits well with the rhythm-patterns, and hence are perceived as less syncopated.

#### 6.4.6 Time-signature

For monorhythms, the peak tempi and the widths for the fitted curves are more or less the same for different time-signatures and individual rhythm-patterns (Figure 6.12b and 6.15). Although these monorhythms may elicit

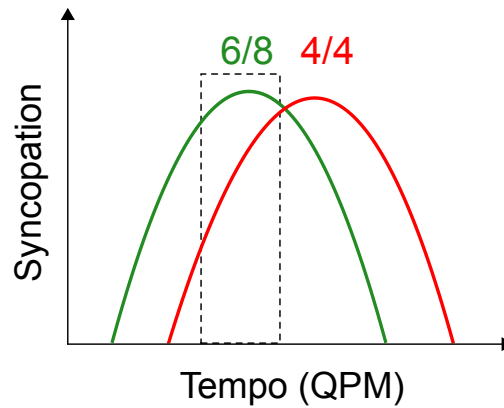


Figure 6.18: Hypothetical explanation for the effect of time-signature in Experiment 1. A schematic diagram showing the fitted curves of tempo effect for the 4/4 and 6/8 rhythms in Experiment 1, and explaining why 6/8 rhythms were more syncopated in the experiment. Assuming the rhythms with same tatum rate have the same peak on the curve of tempo effect, then the peak tempo for 4/4 rhythms will be faster than 6/8 because the tatum rate of 4/4 was half slower than that of 6/8. As a result, the dashed area shows that at 140 BPM (in Experiment 1), which is near the peak tempo for 6/8 rhythms (Figure 6.13), the syncopation of 6/8 rhythms will be higher than the 4/4 rhythms.

different perceptions of beat groupings (that is affected by time-signature) and note-distribution (affected by the construction of rhythm-patterns), their lowest metrical levels all happen to be the eighth-note level, therefore they all have the same tatum rate (Section 2.1.3). Perhaps the identical tatum rate caused similar tempo effects (in terms of peak and width) for different time-signatures and rhythm-patterns.

In Experiment 1, we observed an effect of time-signature on syncopation, where rhythm-patterns in 6/8 are perceived significantly more syncopated than those in 4/4 (Figure 4.3). We attempted to explain this phenomenon by their difference in beat rates, i.e. tatum rates in this case (Section 4.3.1). If the hypothesis that tatum rate determines the shape of tempo effect on syncopation is corroborated, it is conceivable that the fitted curve of tempo effect for 4/4 rhythms (in Experiment 1) would reside at a higher range on tempo scale than that of 6/8 rhythms (see Figure 6.18). This is because the tatum rate of these 4/4 rhythms was half of that of the 6/8 rhythms in the experiment (thus they would have to be played twice as fast to be the same tatum rate). In this case, the

syncopation of 6/8 rhythms would therefore be higher than 4/4 because the former has reached maxima at peak tempo but the latter has not (e.g. the dashed area shown in Figure 6.18). However, this speculation requires further investigation into how the syncopation perception of 4/4 rhythms in Experiment 1 varies with change in tempo.

## 6.5 Summary

In this chapter, we have evaluated the relationship between tempo and perceived syncopation by manipulating the tempo of rhythm-patterns that were known to give rise to syncopation in Experiment 1. Listeners were asked to rate the degree of syncopation they perceived in response to a rendering of each of 64 rhythm-stimuli (e.g. eight rhythm-patterns  $\times$  eight tempi). Our main hypothesis that the perception of syncopation is a function of tempo is confirmed, and such relationship can be well-captured by a log-quadratic function. We also found that the tempo effect on monorhythms is significantly stronger than that on polyrhythms. Yet, no clear evidence was found to suggest a difference in tempo effects between time-signatures and between rhythm-patterns.

Our observations appear to be related to the known effects of tempo on tactus perception and meter perception. A weakened sense of beat and meter at very slow and very fast tempi may simultaneously reduce the contradiction between rhythm and meter, and hence lead to less syncopation. The theory that listeners naturally adjust tactus level to retain a ‘comfort’ tactus rate could explain why the peak tempo for syncopation is higher than that of tactus, and why polyrhythms are more resistant to tempo than monorhythms. We also suggest a possible meter induction from rhythm-patterns over the non-processable metronome, which could explain some rhythms that are more likely to induce a meter are perceived as less syncopated at fast tempi than those are not. Finally, the similar tempo effects between time-signatures and rhythm-patterns might be the result of the identical tatum rate of all the monorhythms.

The study in this chapter not only presents evidence for some theoretical speculations of the relationship between tempo and syncopation [CM60],

but also provides new insight into syncopation modelling that is tempo-dependent. In the next chapter, to suggest the ways in which the models may be improved, we combine the findings from evaluation results of existing syncopation models (Chapter 5) to select the best model(s), and the curves characterising the tempo effects on syncopation that we found in this chapter.

# Chapter 7

## Improving syncopation modelling

The evaluation results of existing syncopation models against Dataset 1 presented in Chapter 5 suggest that no single model can predict this entire dataset well, and there is still much room for improvement for 6/8 monorhythms and polyrhythms. In this chapter, we explore ways to improve current syncopation modelling. Having highlighted the strengths and weaknesses of the various modelling architectures in Section 5.3, and considering the limited scope of each model, it would appear that the most immediate solution to predicting the data as a whole is a combination of the models.

In Sections 7.1 and 7.2, we introduce three combined models, all of which adopt techniques of linear regression to seek better fits to Dataset 1. These combined models requires identification of time-signature and discrimination of rhythm-categories. We then validate them with Dataset 1, compare them with the individual existing syncopation models and with each other in Section 7.3. Based on that, we attempt to incorporate the tempo-dependent nature of syncopation found in Experiment 2 to syncopation modelling, and extend the three combined models to capture Dataset 2. Finally, we validate these three tempo-dependent models against Dataset 2 and the combination of two datasets in Section 7.5.

### 7.1 Best-Single Combined models (BSC)

The simplest implementation of a combined model is to select the (single) model best suited to predicting the particular subset of rhythms that lies within their scope, then conditionally combine them.

	PRS	WNBD	Intercept
4/4 Mono	0.07*		
6/8 Mono	0.14*		-0.30
4/4 Poly		0.24*	2.42*

Table 7.1: Linear regression coefficients for the BSC model.

\* denotes significance ( $p < 0.05$ ).

### 7.1.1 The three-way BSC model ( $BSC_3$ )

The predictions of individual syncopation models against human ratings from Dataset 1 were plotted in Figures 5.4 - 5.6. Pressing's model (PRS) is the optimal candidate for both 4/4 monorhythms ( $r = 0.95, p < 0.001$ ) and 6/8 monorhythms ( $r = 0.76, p < 0.001$ ), and the WNBD model is optimal for polyrhythms ( $r = 0.41, p < 0.001$ ).

Table 7.1 shows all the coefficients estimated by least-square regression to get the best fit to each subset. The equation for the combination of this three-way BSC models is as follows:

$$S_{BSC_3}(Y) = \begin{cases} 0.07S_{PRS}(Y), & \text{if 4/4 monorhythms;} \\ 0.14S_{PRS}(Y) - 0.3, & \text{if 6/8 monorhythms;} \\ 0.24S_{WNBD}(Y) + 2.42, & \text{if polyrhythms.} \end{cases} \quad (7.1)$$

where  $S_{PRS}$  and  $S_{WNBD}$  were defined in Equations 3.29 and 3.52 respectively.

### 7.1.2 The two-way BSC model ( $BSC_2$ )

Alternatively, since the PRS model showed the best performance for monorhythms in both time-signatures, we can divide the entire dataset into two sub-categories: monorhythms and polyrhythms, then combine the predictions of PRS model for monorhythms and predictions of WNBD model for polyrhythms to capture all.

Table 7.2 shows the coefficients estimated by least-square regression to get the best fit to each of the two subsets of the data. The equation for the two-way BSC model is as follows:



	PRS	WNBD	Intercept
Mono	0.10*		
Poly		0.24*	2.42*

Table 7.2: Linear regression coefficients for the BSC<sub>2</sub> model.\* denotes significance ( $p < 0.05$ ).

	LHL	PRS	TMC	SG	TOB	WNBD	KTH	Intercept
4/4 Mono	0.02	0.08*	0.07	-0.29	-0.08	0.003	0.04	-0.10
6/8 Mono	0.47	0.20*	-0.81*	0.55*	0.13*	0.11	-	-1.92*
4/4 Poly	-	-	-	-	-	0.31*	-0.07*	2.81*

Table 7.3: Coefficients of the full models of multiple linear regression.

- indicates that such model cannot serve as a predictor. \* denotes significance ( $p < 0.05$ ).

$$S_{\text{BSC}_2}(Y) = \begin{cases} 0.1S_{\text{PRS}}(Y), & \text{if monorhythms;} \\ 0.24S_{\text{WNBD}}(Y) + 2.42, & \text{if polyrhythms.} \end{cases} \quad (7.2)$$

## 7.2 Weighted-Multiple Combined model (WMC)

The weighted-multiple combined model (WMC) utilises two layers of combining. In the inner layer, we employ multiple linear regression to combine multiple syncopation models that are weighted to get the best fit to each of the three subsets of the data: 4/4 monorhythms, 6/8 monorhythms and 4/4 polyrhythms). In the outer layer, the three models best-fitted for individual subsets of the data are combined into the final model.

### Full models

For each subset (i.e. inner layer), a multiple linear regression model is fitted where all the applicable syncopation models are considered as predictors. In multiple linear regression, a *full model* refers to a model that includes all the possible predictors. Table 7.3 shows the regression coefficients of each full model for its corresponding subset.

### Reduced models

A full model may contain a large amount of predictors and some of them may be redundant (i.e. the predictors that are not significant or are given with small coefficients so that they effectively did not add much to the model). We then adopt *stepwise regression* procedure [Mil90] to select the best set of predictors while retaining a good predictive ability. The resulting model that contains a subset of predictors in a full model is referred as a *reduced model*.

For each subset, we tested two common approaches for stepwise regression, *forward selection* and *backward elimination* [Mil90], to select the most suitable method. The forward selection procedure starts with no predictor in the model and incrementally adds predictors until there are no further improvement of the model. In contrast, backward elimination starts with a full model and gradually removes predictors while keeping the same level of performance. The criterion for predictor selection we used is the *bayesian information criterion* [Aka77], which is designed to balance the performance and the complexity of the model. To be more specific, this criterion tries to optimise goodness of fit of the model while retaining the minimum number of free parameters to avoid over-fitting.

Forward selection and backward elimination produce identical results for 6/8 monorhythms ( $R^2 = 68.0\%$ ,  $F(4, 31) = 19.58$ ,  $p < 0.001$ ), and for 4/4 polyrhythms ( $R^2 = 22.2\%$ ,  $F(2, 45) = 7.69$ ,  $p < 0.01$ ). However, forward selection shows a slight advantage over backward elimination for 4/4 monorhythms (forward selection,  $R^2 = 87.7\%$ ,  $F(3, 23) = 62.87$ ,  $p < 0.001$ ; backward elimination,  $R^2 = 86.6\%$ ,  $F(2, 24) = 85.16$ ,  $p < 0.001$ ). We therefore adopt the set of predictors optimised by forward stepwise regression for each subsets. The updated coefficients of the reduced models for each subset are shown in Table 7.4.

In the outer layer, the combination of the full models and the combination of the reduced models have shown basically equal-well performance, (full model,  $r = 0.90$ ,  $R^2 = 85.1\%$ ,  $F(1, 109) = 627.8$ ,  $p < 0.001$ ; reduced model,  $r = 0.89$ ,  $R^2 = 84.6\%$ ,  $F(1, 109) = 603.2$ ,  $p < 0.001$ ), but the reduced models for subsets of 4/4 monorhythms and 6/8 monorhythms are

	LHL	PRS	TMC	SG	TOB	WNBD	KTH	Intercept
4/4 Mono	0.05*	0.09*			-0.08*			-0.11
6/8 Mono		0.17*	-0.22*	0.67*	0.11*		-	-1.19*
4/4 Poly	-	-	-	-	-	0.31*	-0.07*	2.81*

Table 7.4: Coefficients of the reduced models of multiple linear regression.

- indicates that such model cannot serve as a predictor. \* denotes significance ( $p < 0.05$ ).

much simplified than the corresponding full models. We therefore choose the combination of the reduced models to be the final WMC model, resulting in the following equation:

$$S_{\text{WMC}}(Y) = \begin{cases} 0.05S_{\text{LHL}}(Y) + 0.09S_{\text{PRS}}(Y) - 0.08S_{\text{TOB}}(Y) - 0.11, \\ \text{if 4/4 monorhythms;} \\ 0.17S_{\text{PRS}}(Y) - 0.22S_{\text{TMC}}(Y) + 0.67S_{\text{SG}}(Y) + 0.11S_{\text{TOB}}(Y) - 1.19, \\ \text{if 6/8 monorhythms;} \\ 0.31S_{\text{WNBD}}(Y) - 0.07S_{\text{KTH}}(Y) + 2.81, \\ \text{if polyrhythms.} \end{cases} \quad (7.3)$$

where the equations of individual syncopation models refer back to Section 3.2

### 7.3 Validation of combined models for Dataset 1

Among individual syncopation models, only the WNBD (Equation 3.52) and TOB models (Equation 3.47) are able to predict the entire Dataset 1. Figure 7.1 plots the predictions of these two models and the three new combined models, BSC<sub>2</sub> (Equation 7.2), BSC<sub>3</sub> (Equation 7.1) and the WMC model (Equation 7.3) against Dataset 1 for comparison.

All three combined models showed a marked improvement over the WNBD and TOB models (BSC<sub>2</sub>,  $r = 0.85$ ,  $p < 0.001$ ; BSC<sub>3</sub>,  $r = 0.87$ ,  $p < 0.001$ ; WMC,  $r = 0.89$ ,  $p < 0.001$ ; WNBD,  $r = 0.44$ ,  $p < 0.001$ ; TOB,  $r = -0.54$ ,  $p < 0.001$ , *Spearman's Rank Correlation*). This suggests that the combined modelling architecture is effective.

The two-way BSC model (BSC<sub>2</sub>,  $r = 0.85$ ,  $R^2 = 74.9\%$ ,  $F(1, 109) =$

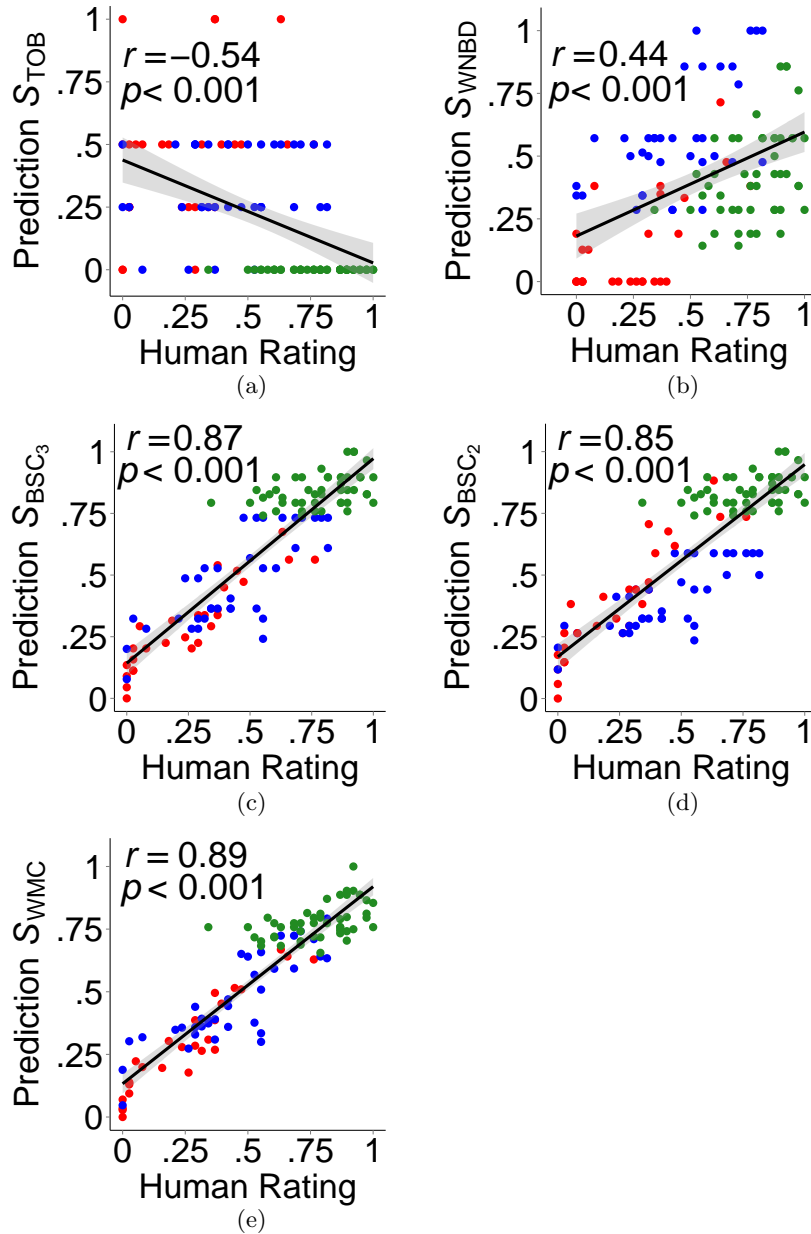


Figure 7.1: Predictions of combined models for Dataset 1. The normalised predictions are plotted against the normalised mean human ratings. Red data points indicate 4/4 monorhythms, blue indicates 6/8 monorhythms and green indicates 4/4 polyrhythms. Spearman-rank correlation coefficients ( $r, p$ ) are given for each model. Linear regression lines (and 95% confidence interval) are plotted for illustration.

327.4,  $p < 0.001$ ) does not perform as well as the three-way BSC model (BSC<sub>3</sub>,  $r = 0.87$ ,  $R^2 = 80.0\%$ ,  $F(1, 109) = 443.5$ ,  $p < 0.001$ ). This is probably because the BSC<sub>2</sub> model is under-fitted by a singular linear regression model when trying to accommodate two subsets at the same time. In contrast, the BSC<sub>3</sub> model generates fewer errors because it uses two separate models to capture subset.

The WMC model (WMC,  $r = 0.89$ ,  $R^2 = 84.6\%$ ,  $F(1, 109) = 603.2$ ,  $p < 0.001$ ) performs better than any of the BSC models. This is not surprising because multiple regression features a greater number of free parameters, which on the other hand is likely to cause overfitting.

## 7.4 Tempo-dependent models

One of the major findings in Experiment 2 is that tempo has a strong effect on syncopation, and the relationship between syncopation and tempo can be characterised by a log-quadratic function (Figure 6.4). However, this has not been considered by any of the existing syncopation models. In this section, we propose an extension to any syncopation model to allow it to be tempo-dependent.

### 7.4.1 General design

Figure 7.2 gives a schematic showing the addition of tempo-dependence to an existing syncopation model  $M$ , forming the tempo-dependent model  $M \sim T$ . Crucially, we assume the prediction given by this syncopation model corresponds to the maximum syncopation value at peak tempo. Also, we restrict the tempo to be within the range from 30 to 480 QPM.

### 7.4.2 Tempo-dependent combined models

In Experiment 2, we found that the fitted curves for mean ratings of polyrhythms are significantly wider than those for mean ratings of monorhythms (Figures 6.6 - 6.8, Section 6.3.3). This suggests that when applying tempo-dependent scaling to syncopation models, monorhythms and polyrhythms

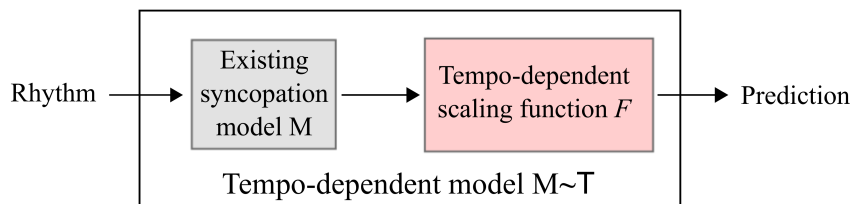


Figure 7.2: A tempo-dependent model. A schematic diagram showing that a tempo-dependent model  $M \sim T$  is generated by applying a tempo-dependent scaling function  $F$  to an existing syncopation model  $M$ , providing the final prediction of syncopation for a rhythm.

need separate scaling functions. Here, we use  $F_m$  and  $F_p$  to represent the scaling function for monorhythms and polyrhythms respectively.

The flow chart in Figure 7.3 shows the overall algorithm for tempo-dependent combined models. For example, the syncopation value of a monorhythm in 4/4 is calculated by the first sub-equation in Equation 7.1, and then scaled by scaling function of monorhythms  $F_m$  to generate the final syncopation prediction of  $BSC_3 \sim T$  model.

The tempo-dependent scaling functions serve the purpose of moderating syncopation at any tempo in relation to the maximum syncopation at peak tempo, consistent with the observed tempo effect on syncopation in Experiment 2. They are therefore generated by normalising the log-quadratic functions fitted to the mean ratings of monorhythms and polyrhythms (Figure 7.4), resulting in the following equations, where tempo  $\Upsilon \in [30, 480]$ :

$$F_m(\Upsilon) = -0.22 \ln^2(\Upsilon) + 2.18 \ln(\Upsilon) - 4.39 \quad (7.4)$$

$$F_p(\Upsilon) = -0.08 \ln^2(\Upsilon) + 0.86 \ln \Upsilon - 1.20 \quad (7.5)$$

Based on the above scaling functions, we can define the equation for  $M \sim T$  model by multiplying the equation for  $M$  model with tempo-dependent scaling functions. For example, the equation for  $WMC \sim T$  model is as follows:

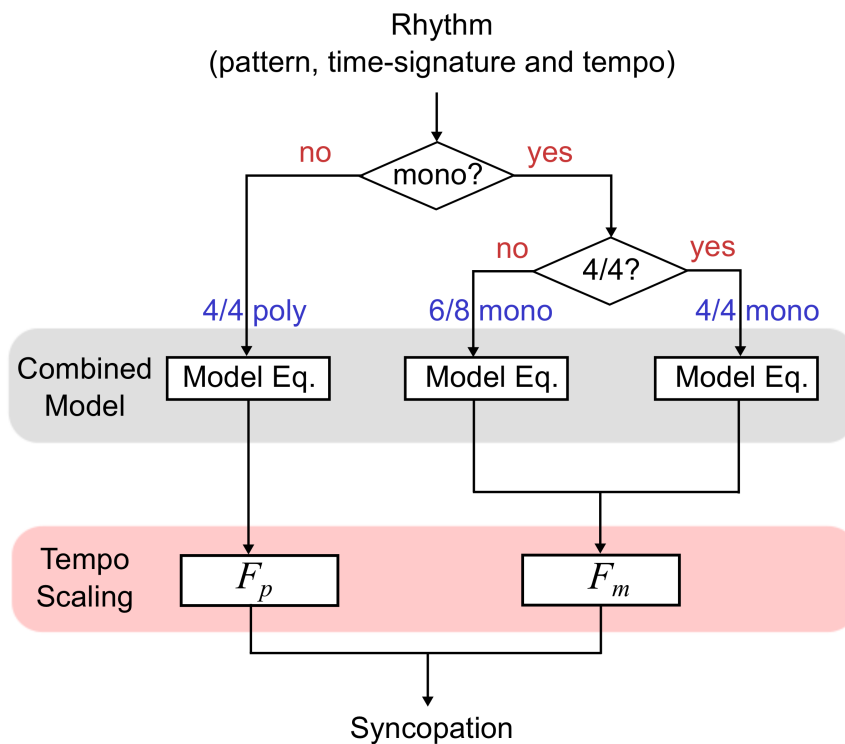


Figure 7.3: Flow chart of the overall algorithm for tempo-dependent combined models.

$$S_{\text{WMC}\sim\text{T}}(Y, \Upsilon) = \begin{cases} S_{\text{WMC}}(Y)F_m(\Upsilon), & \text{if monorhythms;} \\ S_{\text{WMC}}(Y)F_p(\Upsilon), & \text{if polyrhythms;} \end{cases} \quad (7.6)$$

## 7.5 Validation of tempo-dependent combined models for Dataset 2

In this section, we validate the three tempo-dependent combined models,  $\text{BSC}_2\sim\text{T}$ ,  $\text{BSC}_3\sim\text{T}$  and  $\text{WMC}\sim\text{T}$ , against Dataset 2. For each tempo-dependent combined model, the prediction of the model for a given stimulus at certain tempo was compared to the mean of the human ratings for that stimulus at the same tempo. The human ratings are not normally distributed, therefore we have calculated the Spearman's rank correlation coefficient between each model and perceptual data.

Figure 7.5 plots the predictions of the models as a function of the

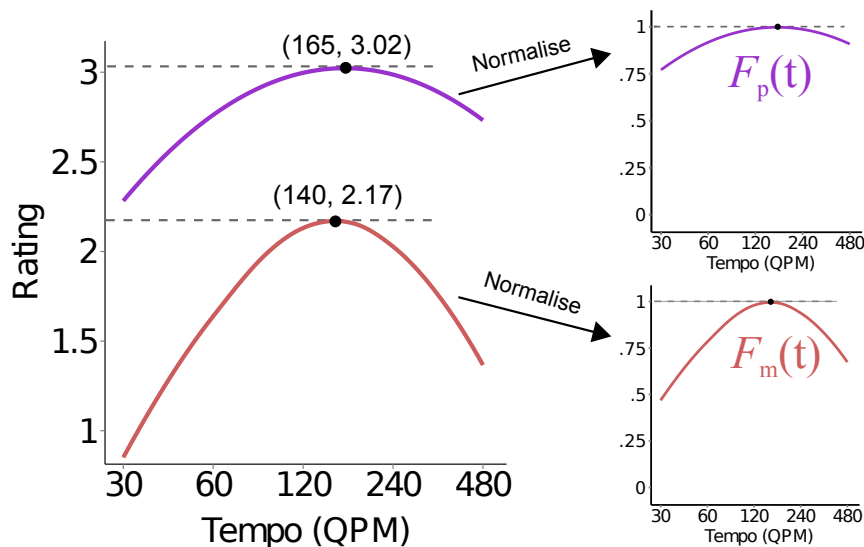


Figure 7.4: Separate tempo scaling functions for monorhythms and polyrhythms. Based on the quadratic functions fitted to the mean ratings of polyrhythms (purple) and monorhythms (red) given in Figure 6.6, we normalise these two curves (by their maxima), which turns into the scaling functions  $F_p$  for polyrhythms, and  $F_m$  for monorhythms of tempo  $\Upsilon$ .

perceptual data, including the regression line ( $\pm 95\%$  confidence intervals). The  $BSC_3 \sim T$  model performed remarkably better than the others ( $r = 0.89$ ,  $R^2 = 69.6\%$ ,  $F(1, 62) = 145$ ,  $p < 0.001$ ); the  $BSC_2 \sim T$  model shows advantage over the  $WMC \sim T$  model ( $BSC_2 \sim T$ ,  $r = 0.78$ ,  $R^2 = 61.0\%$ ,  $F(1, 62) = 99.71$ ,  $p < 0.001$ ;  $WMC \sim T$ ,  $r = 0.75$ ,  $R^2 = 45.9\%$ ,  $F(1, 62) = 54.38$ ,  $p < 0.001$ ).

In parallel to the validation result for Dataset 1, where the  $BSC_3$  model performs better than the  $BSC_2$  model (Figure 7.1), the  $BSC_3 \sim T$  model also performs better in predicting Dataset 2 than the  $BSC_2 \sim T$  model, and shows an even more obvious advantage. This may mean that  $BSC_2$  model is indeed under-fitted to Dataset 1, and the application of the tempo-dependent scaling functions to  $BSC_2$  have amplified this error.

Another interesting finding is that after applying tempo-dependent scaling to the combined models, the  $WMC$  model did not continue to retain the advantage over the  $BSC$  models in predicting Dataset 1 (Figure 7.1c-d), but performed a lot worse in predicting Dataset 2, especially



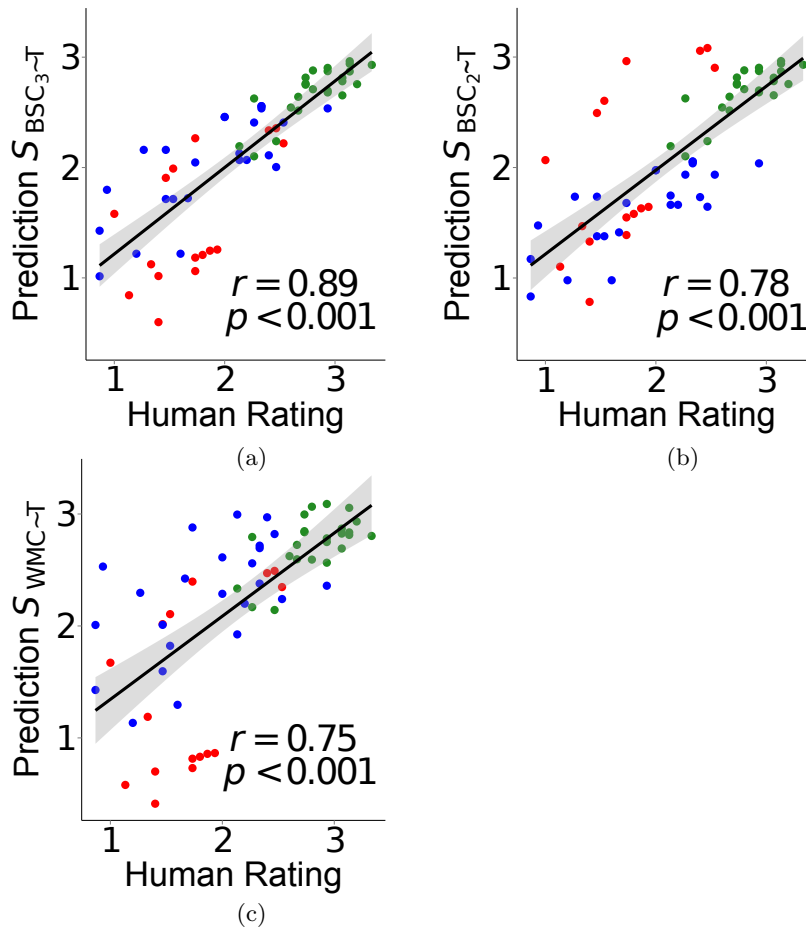


Figure 7.5: Predictions of tempo-dependent combined models for Dataset 2. The predictions of each model are plotted against mean human ratings. Red data points indicate 4/4 monorhythms, blue indicates 6/8 monorhythms and green indicates 4/4 polyrhythms. Spearman-rank correlation coefficients ( $r, p$ ) are given for each model. Linear regression lines (and 95% confidence interval) are plotted for illustration.

than the three-way BSC model (Figure 7.5). This further suggests that the multiple combined model is over-fitted to the data from Dataset 1, hence it does not generalise syncopation modelling to a data from a different paradigm (e.g. Dataset 2) and possibly a different sample of participants. To this end, the single combined model seems to be more robust than the multiple combined model.

We have also tested the performance of all the combined models without tempo adjustment (Equation 7.1–7.3) in predicting Dataset 2. The percentage of explained variance ( $R^2$ ) drops 32.7% on average comparing to the tempo-dependent combined models (BSC<sub>3</sub>,  $r = 0.74$ ,  $R^2 = 35.6\%$ ,  $F(1, 62) = 35.82$ ,  $p < 0.001$ ; BSC<sub>2</sub>,  $r = 0.47$ ,  $R^2 = 28.6\%$ ,  $F(1, 62) = 26.2$ ,  $p < 0.001$ ; WMC,  $r = 0.43$ ,  $R^2 = 14.1\%$ ,  $F(1, 62) = 11.32$ ,  $p < 0.01$ ). This demonstrates that the tempo-adjustment in combined models is effective in capturing Dataset 2.

## 7.6 Discussion

Generally, the combined modelling architecture has shown to be effective in predicting Dataset 1. By adding the tempo-dependence extension to this architecture, Dataset 2 is also well-captured. However, this approach does not directly refine the theory for modelling syncopation, instead, it searches for the best combinations of the elements in different models that optimise the fit to the data. It also points out two potential directions toward a more comprehensive mathematical model of syncopation: the first is to extend the best performing hierarchical models (e.g. PRS model) to capture polyrhythms and the second is to adapt the off-beat models to take metrical hierarchy into account.

In addition, the combined modelling architecture is also more difficult to interpret than an architecture with a single model representing a certain hypothesis. This is because the multiple parameters in the combined model need to be individually interpreted.

Another inherent limitation of the combined models is that by trained only to fit Dataset 1, they do not necessarily provide an equivalent improvement for predictions on different rhythms. For example, other time-signatures (that differ to 4/4 and 6/8) and different types of polyrhythms (other than 2:3 polyrhythms) may not be well predicted. In other words, these combined models may not be generalised enough to capture other aspects in rhythm that can contribute to syncopation. Therefore, the combined models require validation with datasets that these models are not fitted to.

To incorporate the tempo-dependence into syncopation models, we adopted log-quadratic regression model to generate the tempo-dependent scaling functions. Despite of the fact that this scaling function is simple and easy to interpret, fittings of tempo-dependent models to Dataset 2 may be further improved by optimising the scaling functions to capture Dataset 2. For example, we can extend Dataset 2 (which requires testing syncopation in more tempi conditions) and optimise the log-quadratic regression to a larger dataset; or we can try adopting different models (e.g. Gaussian regression or high-order polynomial regression) to the current Dataset 2.

## 7.7 Summary

In this chapter, we have provided two effective remedies to improve the current approaches for modelling syncopation. The first remedy is to combine the existing syncopation models that best suited to model each subset of the data. Three new combined models are generated, validated and all show good predictabilities. The second remedy is to apply tempo-dependent scaling functions which capture the tempo effects on syncopation found in Experiment 2, to syncopation models to make them tempo-dependent.

Generally, the new combined models, themselves and with the extension of tempo-dependence built in, can both capture the perception of syncopation better than the current state of the art. However, having highlighted their inherent limitations, these combined models require more validation with new datasets that incorporate broader aspects of rhythm.

# Chapter 8

## Conclusions

In this thesis our objective was to investigate the theory and perception of syncopation. We have reviewed the literature on the subject and gathered the current models together by introducing a unified mathematical framework. In order to test how well the theory and models explain the perception of syncopation we have conducted two main experiments to collect subjective ratings on perceived syncopation from musicians in response to rhythm-stimuli. Using the findings from these experiments, we have evaluated the previously existing models and built several new ones that capture the perception of syncopation better than the current state of the art.

### 8.1 Thesis contributions

This thesis makes a number of contributions to the understanding of syncopation both in terms of theory and perception. We have introduced new methods for collecting perceptual syncopation ratings and produced two new datasets using those methods.

#### **Theory**

We have reviewed various definitions and theories of syncopation in the existing literature and summarised them into four main schools of thought in Section 2.2. We have also examined seven existing models for syncopation, categorising their hypotheses, and consolidated them into a unified

mathematical framework. Based on this mathematical framework, we have implemented a syncopation model tool kit in Python [Son14].

We have evaluated the models against perceptual data from Dataset 1, and discussed the relative strengths and weaknesses of each model. Using these results, we have produced new combined models which out-perform the previously existing ones.

We have extended the theory by providing evidence to show that syncopation is a function of tempo. Using this observed relationship, we have extended our combined models so that they capture the tempo-dependent nature of syncopation.

## Method

We have conducted two experiments that investigate the perception of syncopation using psychophysical methods. In contrast to previous studies, our experiment provides the first direct investigation on the perception of syncopation.

## Data

We have collected two psychophysical datasets that include perceptual ratings of syncopation from trained musicians [Son14]. These datasets have been used to evaluate the existing models in this work. They can also be used in future studies that investigate a broad range of correlates of syncopation in multiple disciplines.

## 8.2 General discussion

In this section, we unify the theory on syncopation and the findings from our perceptual studies, and discuss what are the aspects captured in the theory, what are the aspects mentioned in the theory but not verified, and what are the missing elements in the theory.

All the theories share the consensus that syncopation is aroused by violating the regular beat salience defined in a certain meter structure [Ran86,

Ken94, Hur06, LHL84, HO06]. Our results from Experiment 1 in Chapter 4 supported this because we found that missing the down-beat, the most salient beat in a bar, had a strong effect on syncopation (Section 4.2.3). This theory finds further support in the evaluations in Chapter 5, because hierarchical models that take metrical weights into account were shown to perform better in predicting monorhythms than models from other categories.

Theories diverge on off-beatness, with some suggesting that only an off-beat event followed by an unfilled beat gives rise to syncopation [CM60, LHL84, HO06], while others suggest that any off-beat event will lead to syncopation [Kei91, Tou05, GMRT05]. The former notion is effectively a restatement of the violation of regular beat salience, and as such is supported by the results from Experiment 1 as discussed above. However, the latter proved to be unsupported because the models based on this theory (i.e. off-beat models TOB and WNBD) did not perform well in our evaluations (Section 5.2).

Many theorists treat polyrhythms as something completely separate from syncopation [Ran86, Ken94, LHL84, Lon04, CM60, HO06, Pre97], while some include polyrhythms as a category of syncopated rhythms [HO81, GMRT05]. The results of Experiment 1 strongly support this second school of thought with polyrhythmic patterns being given high syncopation ratings (Section 4.2.2).

Several elements have not been sufficiently considered in current theories or models. First and foremost, the effect of tempo on syncopation has rarely been addressed in the literature. Cooper and Meyer hypothesised a relationship between syncopation and tempo [CM60], and Sioros et. al [SMC<sup>+</sup>13] attempts to take account of tempo in the modelling by altering weights in their metrical hierarchy. However, until now, no direct investigation of the relationship between syncopation and tempo has been carried out. In Experiment 2 (Chapter 6), we directly tested this relationship and found that syncopation is a function of tempo. Our results are consistent with relationships found in studies between tempo and other rhythm phenomena such as tactus and meter [Duk89, Par94, vNM99].

In addition, theorists have not considered a link between time-signature

and syncopation. However, our results in Experiment 1 suggest time-signature has a possible effect on syncopation (Section 4.2.1). In Section 4.3.1, we speculated that such effect may be due to the duple subdivision of 4/4 being inherently less ambiguous than the triple subdivision of 6/8 [LJ83, PE85, Dra93, BT06]. On the other hand, the results from Experiment 2 did not show a significant difference between the two time-signatures in the tempo effects on syncopation (Section 6.3.4). Our evidence suggests that the tatum rate of stimuli (which was different for 4/4 and 6/8 rhythm-patterns in Experiment 1 but the same for both in Experiment 2) may provide an underlying explanation for this effect.

While we have gone some way towards unifying theory with perception, we must accept that our experiments have been limited to a small subset of western-oriented stimuli in only two isochronous time-signatures and note that our participants were all trained musicians with western musical backgrounds. Questions can be raised over how far our results can generalise across common rhythms from other music cultures, polyrhythms with various competing periodicities, and time-signatures (e.g. non-isochronous meter). However, our findings suggest that our method provides a good foundation for further investigation.

### 8.3 Future work

We conclude this thesis with a discussion of questions raised from our experiments that lead to possible areas for future work.

#### **Syncopation perception and meter induction**

In Chapter 4, we discovered that there were several rhythm-patterns in a time-signature of 6/8 that, while featuring missing down-beat or missing strong-beat, were not perceived to be particularly syncopated. This finding runs counter to most of the other results for patterns of this type and requires further investigation. Why should these particular patterns be different from the others? A plausible explanation could be that listeners may be adjusting their metrical interpretation to the rhythm-patterns

in order to reduce syncopation (Section 4.3.3). For example, rhythm-patterns JG and FG may be heard as 3/4 meter because the pattern of strong- and weak-beats in 3/4 would suggest lower syncopation than if they are heard in 6/8 meter. Listeners in our experiments had the freedom to interpret meter in this way because the given metronome was implied 6/8 with an accent only on the down-beat. It is possible that an explicit 6/8 metronome with accents on both first and fourth beats might have given different results by forcing a particular interpretation of the meter. This would be consistent with Povel and Essens's theory of meter induction [PE85], but still requires further verification.

Our hypothesis is, given an implicit metronome of 6/8 meter, a listener's interpretation of meter is chosen between 6/8 and 3/4 depending on which minimises the perceived syncopation. We propose two methods to test this hypothesis by collecting perceptual syncopation ratings of the same set of 6/8 rhythm-patterns as used in Experiment 1 but played against an explicit metronome, thereby forcing the metrical interpretation to be 6/8. We may use P&E's clock model [PE85] to predict which meter is in theory more likely to be chosen for a specific rhythm-pattern. If syncopation ratings for the rhythm-patterns that are believed likely to induce 3/4 meter are higher for the explicit metronome than for implicit metronome while ratings for the others remains unchanged then it suggests that listeners naturally select meter that helps with reducing syncopation.

Another method for exploring this hypothesis could use tapping to directly investigate meter interpretation. With the same set of rhythm-patterns played against the implicit metronome, we can ask listeners to tap out the perceived beats from the rhythm. If listeners tapping can be correctly predicted by P&E's clock model, then our hypothesis can be confirmed, because the clock model is designed to select the meter which minimise metrical contradiction between rhythm and meter.

If our hypothesis is verified, then existing syncopation models may be further improved by incorporating a meter induction step prior to calculating syncopation. So far the syncopation models measure syncopation against the notated time-signature, which is not necessarily the same as



the interpreted meter. Where metrical cues are ambiguous, a meter interpretation step can be applied to provide the syncopation model with the most-likely-perceived meter to measure against. The candidates for such a predictive model of meter induction are P&E's clock model [PE85] and Essens's model [Ess95].

### **Tatum rate and syncopation**

From Dataset 1 (Section 4.3.1) we observed that 4/4 and 6/8 meters elicited different syncopation ratings with 6/8 being the higher of the two. Later, in Section 6.4.6 we discovered that the tempo curves for these two meters were not significantly different, and that the difference between the ratings in Dataset 1 may actually be due to the tatum rate for the 4/4 and 6/8 rhythms being different rather than time-signature. From this we may hypothesise that the tempo effect on syncopation is affected by the tatum rate of the rhythm-pattern. To investigate this hypothesis, a new experiment can be carried out where rhythm-patterns with a fixed tempo (as defined by their metronome) but differing tatum rates can be rated for syncopation.

### **Transition of time-signatures**

As discussed in Section 2.2.3, another way in which syncopation can be produced is via a sudden transformation in the fundamental character of the meter [Ran86, Ken94] such as a change in time-signature or a horizontal hemiola. To investigate this aspect of syncopation, an experiment could be conducted with rhythm-stimuli that transition from one meter to another in order to characterise this relationship. The order in which the meters are presented can also be varied so that we may discover whether the perceived syncopation caused by such transitions is symmetrical or not. For example, would the transition from duple meter 4/4 to triple meter 3/4 be rated differently from the transition from 3/4 to 4/4?

### **Syncopation and rhythm-complexity**

In this work we have evaluated various models for syncopation against perceptual data collected in our two main experiments. Past studies [GTT07, SH07, Thu08] have instead tested models against perceptual data for rhythm-complexity but a question remains over precisely how this percept corresponds to syncopation. Some models for rhythm-complexity have also included syncopation as one factor in a larger calculation [SHG12].

Another area for future work is therefore to investigate the link between syncopation and rhythm-complexity further. To do so we propose an experiment using our method from Section 4.1 to collect ratings of syncopation for each of the rhythms in the datasets of rhythm-complexity [PE85, Ess95, SP00].

## Bibliography

- [Aka77] Hirotugu Akaike. *On entropy maximization principle*. Applications of Statistics, North-Holland, Amsterdam, 1977.
- [Bil93] Jeffrey A. Bilmes. Timing is of the essence: perceptual and computational techniques for representing, learning, and reproducing expressive timing in percussive rhythm. Master's thesis, MIT Masters Thesis, 1993.
- [Bro02] Warren Brodsky. The effects of music tempo on simulated driving performance and vehicular control. *Transportation Research Part F*, 4:219–241, 2002.
- [BT06] Tonya R. Bergeson and Sandra E. Trehub. Infants perception of rhythmic patterns. *Music Perception*, 23(4):345–360, 2006.
- [BZ06] Søren Bech and Nick Zacharov. *Perceptual Audio Evaluation: Theory, Method and Application*. Chap. 4. John Wiley & Son, 2006.
- [CH99] Clare Caldwell and Sally A. Hibbert. Play that one again: the effect of music tempo on consumer behaviour in a restaurant. *European Advances in Comsumer Research*, 4:58–62, 1999.
- [CH01] William G. Collier and Timothy L. Hubbard. Judgements of happiness, brightness, speed and tempo change of auditory stimuli varying in pitch and tempo. *Psychomusicology*, 17:36–55, 2001.
- [CM60] Grosvenor Cooper and Leonard B. Meyer. *The Rhythmic Structure of Music*. University of Chicago Press, 1960.

- [CPZ08] Joyce L. Chen, Virginia B. Penhune, and Robert J. Zatorre. Moving on time: brain network for auditory-motor synchronization is modulated by rhythm complexity and musical training. *Journal of Cognitive Neuroscience*, 20(2):226–239, 2008.
- [DGM88] Robert A. Duke, John M. Geringer, and Clifford K. Madsen. The effect of tempo on pitch perception. *Journal of Research in Music Education*, 36(2):108–125, 1988.
- [DH94] Peter Desain and Henkjan Honing. Does expressive timing in music performance scale proportionally with tempo? *Psychological Research*, 56(4):285–292, 1994.
- [Dix01] Simon Dixon. Automatic extraction of tempo and beat from expressive performances. *Journal of New Music Research*, 30(1):39–58, 2001.
- [Dra93] Carolyn Drake. Reproduction of musical rhythms by children, adult musicians, and adult nonmusicians. *Perception & Psychophysics*, 53(1):25–33, 1993.
- [Dra97] Carolyn Drake. Motor and perceptually preferred synchronisation by children and adults: binary and ternary ratios. *Polish Quarterly of Developmental Psychology*, 3:41–59, 1997.
- [Duk89] Robert A. Duke. Musicians' perception of beat in monotonic stimuli. *Journal of Research in Music Education*, 37(1):61–71, 1989.
- [Eck01] Douglas Eck. A positive-evidence model for rhythmical beat induction. *Journal of New Music Research*, 30(2):187–200, 2001.
- [Ess95] Peter Essens. Structuring temporal sequences: comparison of models and factors of complexity. *Perception and Psychophysics*, 57(4):519–532, 1995.

- [FR07] W. Tecumseh Fitch and Andrew J. Rosenfeld. Perception and production of syncopated rhythms. *Music Perception*, 25(1):43–58, 2007.
- [Fra63] Paul Fraisse. *Psychology of time*. New York: Harper, 1963.
- [Fra82] Paul Fraisse. *The Psychology of Music, “Rhythm and Tempo”*. Academic Press, New York, 1982.
- [GDPW04] Fabien Gouyon, Simon Dixon, Elia Pampalk, and Gerhard Widmer. Evaluating rhythmic descriptors for musical genre classification. In *Proceedings of the AES 25th International Conference*, pages 196–204, 2004.
- [GMRT05] F. Gómez, A. Melvin, D. Rappaport, and Godfried T. Toussaint. Mathematical measures of syncopation. In *BRIDGES: Mathematical Connections in Art, Music and Science*, pages 73–84, 2005.
- [Gou05] Fabien Gouyon. *A computational approach to rhythm description*. PhD thesis, Department of Technology of the University Pompeu Fabra, 2005.
- [GTT07] Francisco Gómez, Eric Thul, and Godfried T. Toussaint. An experimental comparison of formal measures of rhythmic syncopation. In *Proceedings of the International Computer Music Conference*, pages 101–104, 2007.
- [Han93] Stephen Handel. The effect of tempo and tone duration on rhythm discrimination. *Percept Psychophys*, 54(3):370–382, 1993.
- [HJ99] Karel Hrbacek and Thomas Jech. *Introduction to Set Theory*. Marcel Dekker, Inc., New York, 1999.
- [HL83] Stephen Handel and Gregory R. Lawson. The contextual nature of rhythmic interpretation. *Percept & Psychophys*, 34(2):103–120, 1983.

- [HLHW09] Henkjan Honing, Olivia Ladinig, Gábor P Hádén, and István Winkler. Is beat induction innate or learned? probing emergent meter perception in adults and newborns using event-related brain potentials. *Annals of the New York Academy of Sciences*, 1169:93–96, 2009.
- [HM90] Ira J. Hirsh and Caroline B. Monohan. Studies in auditory timing: 1. simple patterns. *Perception and psychophysics*, 47(3):215–226, 1990.
- [HO81] Stephen Handel and James S. Oshinsky. The meter of syncopated auditory polyrhythms. *Perception & Psychophysics*, 30(1):1–9, 1981.
- [HO06] David Huron and Ann Ommen. An empirical study of syncopation in american popular music, 18901939. *Music Theory Spectrum*, 28(2):211–231, 2006.
- [HSEK04] Erin E. Hannon, Joel S. Snyder, Tuomas Eerola, and Carol L. Krumhansl. The role of melodic and temporal cues in perceiving musical meter. *Journal of Experimental Psychology: Human Perception and Performance*, 30(5):956–974, 2004.
- [Hur06] David Huron. *Sweet anticipation: music and the psychology of expectation*. Cambridge, MA: MIT. Press, 2006.
- [Kei91] Michael Keith. *From Polychords to Pólya: Adventures in Music Combinatorics*. Vinculum Press, 1991.
- [Ken94] Michael Kennedy. *The Oxford Dictionary of Music*. Oxford University Press, second edition edition, 1994.
- [KR01] Peter E. Keller and Bruno H. Repp. Staying offbeat: sensorimotor syncopation with structured and unstructured auditory sequences. *Psychological Research*, 69(4):292–309, 2001.

- [Kre99] Harald Krebs. *Fantasy pieces: metrical dissonance in the music of robert schumann*. New York: Oxford University Press, 1999.
- [KS11] Peter E. Keller and Emery Schubert. Cognitive and affective judgements of syncopated musical themes. *Advances in Cognitive Psychology*, 7:142–156, 2011.
- [Lad09] Olivia Ladinig. *Temporal expectations and their violations*. PhD thesis, Institute for Logic, Language and Computation, Universiteit van Amsterdam, The Netherlands, 2009.
- [LCH06] Justin London, Ian Cross, and Tommi Himberg. The effect of tempo on the perception of anacrusis. In *The 9th International Conference on Music Perception and Cognition*, pages 1641–1647, Alma Mater Studiorum University of Bologna, 2006.
- [LeB81] Albert LeBlanc. Effects of style, tempo and performing medium on children’s music preference. *Journal of Research in Music Education*, 29(2):143–156, 1981.
- [Lew72] D. Lewin. *Theory and design of digital computers*. J. Wiley, Press, 1972.
- [LH78] H. C. Longuet-Higgins. The perception of music. *Interdisciplinary Science Review*, 3:148–156, 1978.
- [LH09] Olivia Ladinig and Henkjan Honing. Probing attentive and preattentive emergent meter in adult listners without extensive music training. *Music Perception*, 26(4):377–386, 2009.
- [LHL84] H. C. Longuet-Higgins and C. S. Lee. The rhythmic interpretation of monophonic music. *Music Perception*, 1(4):424–441, 1984.
- [LJ83] Fred Lerdahl and Ray Jackendoff. *A Generative Theory of Tonal Music*. Cambridge, Mass: MIT Press, 1983.

- [Lon04] Justin London. *Hearing in Time: Psychological Aspects of Musical Meter*. Oxford University Press, 2004.
- [Mad06] Guy Madison. Experiencing groove induced by music: consistency and phenomenology. *Music Perception: An Interdisciplinary Journal*, 24(2):201–208, 2006.
- [McA10] J. Devin McAuley. Tempo and rhythm. *Music perception*, pages 165–199, 2010.
- [MFD<sup>+</sup>01] Justine M. Mayville, Armin Fuchs, Mingzhou Ding, Douglas Cheyne, Lder Deecke, and J.A. Scott Kelso. Event-related changes in neuromagnetic activity associated with syncopation and synchronization timing tasks. *Human Brain Mapping*, 113(2):65–80, 2001.
- [Mil90] Alan J. Miller. *Subset Selection in Regression*. Chapman and Hall, London, 1990.
- [MJH<sup>+</sup>06] J. Devin McAuley, Mari Riess Jones, Shayla Holub, Heather M. Johnston, and Nathaniel S. Miller. The time of our lives: lifespan development of timing and event tracking. *Journal of Experimental Psychology: General*, 135(3):348–367, 2006.
- [MM04] Dirk Moelants and M McKinney. Tempo percepton and musical content: what makes a piece fast, slow or temporally ambiguous? In *Proceedings of the 8th International Conference on Music Perception and Cognition*, pages 558–562, 2004.
- [MMPR93] Jiří Mates, U. Müller, E. Pöppel, and Tomáš Radil. Stimulus anticipation disappears when following slow tonal sequences by finger tapping. *Homeostatis in Health and Disease*, 34:185–187, 1993.
- [Moe02] Dirk Moelants. Preferred tempo reconsidered. In *Proceedings of the 7th International Conference on Music Perception and Cognition*, pages 580–583, Sydney, 2002.



- [Moe12] Dirk Moelants. Conveying syncopation in music performance. In *Proceedings of the 12th International Conference on Music Perception and Cognition and the 8th Triennial Conference of the European Society for the Cognitive Sciences of Music*, pages 686–691, 2012.
- [MP01] Rosalee K. Meyer and Caroline Palmer. Rate and tactus effects in music performance. *Manuscript submitted for publication*, 2001.
- [MPF09] Daniel Müllensiefen, Martin Pfeiderer, and Klaus Frieler. The perception of accents in pop music melodies. *Journal of New Music Research*, 38(1):19–44, 2009.
- [MS99] J. Devin McAuley and Peter Semple. The effect of tempo and musical experience on perceived beat. *Australian Journal of Psychology*, 51(3):176–187, 1999.
- [MSD<sup>+</sup>13] Guy Madison, George Sioros, Matthew Davis, Marius Miron, Diogo Cocharro, and Fabien Gouyon. Adding syncopation to simple melodies increases the perception of groove. In *Proceedings of: Conference of Society for Music Perception and Cognition*, 2013.
- [OH78] James S. Oshinsky and Stephen Handel. Syncopated auditory polyrhythms: discontinuous reversals in meter interpretation. *The Journal of Acoustical Society of America*, 63(3):936–939, 1978.
- [Par94] Richard Parncutt. A perceptual model of pulse salience and metrical accent in musical rhythms. *Music Perception*, 11(4):409–464, 1994.
- [PE85] Dirk-Jan Povel and Peter Essens. Perception of temporal patterns. *Music Perception*, 2(4):411–440, 1985.

- [PK90] Caroline Palmer and Carol L. Krumhansl. Mental representations for musical meter. *Journal of Experimental Psychology: Human Perception and Performance*, 16(4):728–741, 1990.
- [PL93] Jeffrey Pressing and Peter Lawrence. Transcribe: a comprehensive autotranscription program. In *Proceedings of the 1993 International Computer Music Conference*, pages 343–345, 1993.
- [Pou89] E. C. Poulton. *Bias in Quantifying Judgement*. Lawrence Erlbaum Associates Ltd., East Sussex, U.K., 1989.
- [PRBH14] Maria Panteli, Bruno Rocha, Niels Bogaards, and Aline Honingh. Development of a rhythm similarity model for electronic dance music. In *AES 53rd International Conference, London, UK*, 2014.
- [Pre97] Jeffrey Pressing. Cognitive complexity and the structure of musical patterns. In *Proceedings of the 4th Conference of the Australian Cognitive Science Society*, 1997.
- [PT11] Olaf Post and Godfried Toussaint. The edit distance as a measure of perceived rhythmic similarity. *Empirical Musicology Review*, 6(3):164–179, 2011.
- [QW06] Sandra Quinn and Roger Watt. The perception of tempo in music. *Perception*, 35:267–280, 2006.
- [Ran86] Don Randel. *The Harvard Dictionary of Music*. Harvard University Press, 1986.
- [RD07] Bruno H. Repp and Rebecca Doggett. Tapping to a very slow beat: a comparison of musicians and nonmusicians. *Music Perception*, 24(4):367–376, 2007.
- [Rep03] Bruno H. Repp. Rate limits in sensorimotor synchronization with auditory and visual sequences: The synchronization

- threshold and the benefits and costs of interval subdivision. *Journal of Motor Behavior*, 35:355–370, 2003.
- [Rep08] Bruno H. Repp. Metrical subdivision results in subjective slowing of the beat. *Music Perception*, 26:19–39, 2008.
- [RWD02] Bruno H. Repp, W. Luke Windsor, and Peter Desain. Effects of tempo on the timing of simple musical rhythms. *Music Perception*, 19(4):565–593, 2002.
- [SC89] Karen C. Smith and Lola L. Cuddy. Effects of metric and harmonic rhythm on the detection of pitch alterations in melodic sequences. *Journal of Experimental Psychology: Human Perception and Performance*, 15(3):457–471, 1989.
- [SG11] George Sioros and Carlos Guedes. Complexity driven recombination of midi loops. In *Proceedings of the 12th International Society for Music Information Retrieval Conference*, pages 381–386, 2011.
- [SH93] Jasba Simpson and David Huron. The perception of rhythmic similarity: A test of a modified version of johnson-lairds theory. *Canadian Acoustics*, 21:89–90, 1993.
- [SH07] Leigh M. Smith and Henkjan Honing. Evaluating and extending computational models of rhythmic syncopation in music. In *Proceedings of the 2006 International Computer Music Conference*, pages 688–91, 2007.
- [SHG12] George Sioros, André Holzapfel, and Carlos Guedes. On measuring syncopation to drive an interactive music system. In *Proceedings of the 13th International Society for Music Information Retrieval Conference*, pages 283–288, 2012.
- [Sio11] George Sioros. Kinetic. gestural controller-driven, adaptive, and dynamic music composition systems. [https://http://smc.inescporto.pt/kinetic/?page\\_id=9](https://http://smc.inescporto.pt/kinetic/?page_id=9), 2011.
- [Sio14] George Sioros. Personal communication, January 2014.

- [SK01] Joel Snyder and Carol L. Krumhansl. Tapping to ragtime: Cue to pulse finding. *Music Perception*, 18(4):445–489, 2001.
- [Slo91] John A. Sloboda. Musical structure and emotional responses: some empirical findings. *Psychology of music*, 19:110–120, 1991.
- [SMC<sup>+</sup>13] George Sioros, Marius Miron, Diogo Cocharro, Carlos Guedes, and Fabien Gouyon. Syncopalooza: Manipulating the syncopation in rhythmic performances. In *International Symposium on Computer Music Multidisciplinary Research*, 2013.
- [Smi10] Leigh M. Smith. Rhythmic similarity using metrical profile matching. In *Proceedings of the 2010 International Computer Music Conference*, 2010.
- [Son14] Chunyang Song. C4DM syncopation dataset and toolkit. <https://code.soundsoftware.ac.uk/projects/syncopation-dataset>, 2014.
- [SP00] Ilya Shmulevich and Dirk-Jan Povel. Measures of temporal pattern complexity. *Journal of New Music Research*, 29(1):61–69, 2000.
- [Ste75] Stanley Smith Stevens. *Psychophysics: Introduction to its perceptual, neural, and social prospects. Chap. 1*. Wiley, New York, 1975.
- [Str06] Sebastian Streich. *Music complexity: a multifaceted description of audio content*. PhD thesis, Music Technology Group, The Universitat Pompeu Fabra, 2006.
- [Tay89] Eric Taylor. *The AB Guide to Music Theory, Part I*. Associated Board of the Royal Schools of Music, 1989.
- [Tem99] David Temperley. Syncopation in rock: a perceptual perspective. *Popular Music*, 18(1):19–40, 1999.

- [Tem01] David Temperley. *The cognition of basic musical structures*. The MIT Press, 2001.
- [Tho82] Joseph M. Thomassen. Melodic accent: experiments and a tentative model. *The Journal of the Acoustical Society of America*, 71(6):1596–1605, 1982.
- [Thu08] Eric Thul. Measuring the complexity of musical rhythm. (msc thesis). Master’s thesis, McGill University, 2008.
- [TK03] Michael H. Thaut and Gary P. Kenyon. Rapid motor adaptations to subliminal frequency shifts during syncopated rhythmic sensorimotor synchronization. *Human Movement Science*, 22(3):321–338, 2003.
- [Tou02] Godfried T. Toussaint. A mathematical analysis of african, brazilian, and cuban clave rhythms. In *Proceedings of BRIDGES: Mathematical Connections in Art, Music and Science*, pages 157–168, 2002.
- [Tou05] Godfried T. Toussaint. Mathematical features for recognizing preference in sub-saharan african traditional rhythm timelines. In *3rd International Conference on Advances in Pattern Recognition*, pages 18–27, 2005.
- [Tra07] Laurel J. Trainor. Do preferred beat rate and entrainment to the beat have a common origin in movement? *Empirical Musicology Review*, 2:17–21, 2007.
- [TS03] Petri Toivianinen and Joel S. Snyder. Tapping to bach: Resonance-based modelling of pulse. *Music Perception*, 21(1):43–80, 2003.
- [VL11] Marc J. Velasco and Edward W. Large. Pulse detection in syncopated rhythms using neural oscillators. In *Proceedings of the 12th International Society for Music Information Retrieval Conference*, pages 185–190, 2011.

- [vNM99] Leon van Noorden and Dirk Moelants. Resonance in the perception of musical pulse. *Journal of New Music Research*, 28:43–66, 1999.
- [VOP<sup>+</sup>09] Peter Vuust, Leif Ostergaard, Karen Johanne Pallesen, Christopher Bailey, and Andreas Roepstorff. Predictive coding of music brain responses to rhythmic incongruity. *Cortex*, 45:80–92, 2009.
- [VWOR11] Peter Vuust, Mikkel Wallentin, Leif Ostergaard, and Andreas Roepstorff. Tapping polyrhythms in music activates language areas. *Neuroscience Letters*, 494:211–216, 2011.
- [vZWvdB11] Marjolein D. vander Zwaag, Joyce H.D.M. Westerink, and Egon L. van den Broek. Emotional and psychophysiological responses to tempo, mode and percussiveness. *Musicae Scientiae*, 15(2):250–269, 2011.
- [WCW<sup>+</sup>14] Maria A. G. Witek, Eric F. Clarke, Mikkel Wallentin, Morten L. Kringelbach, and Peter Vuust. Syncopation, body-movement and pleasure in groove music. *PloS ONE*, 9(4):e94446, 2014.
- [WHL<sup>+</sup>09] István Winkler, Gábor P Hádén, Olivia Ladinig, István Sziller, and Henkjan Honing. Newborn infants detect the beat in music. *Proceedings of the National Academy of Sciences of the United States of America*, 106(7):2468–2471, 2009.
- [WK00] A. Wohlschläger and R. Koch. Synchronization error: an error in time perception. *Rhythm perception and production*, pages 115–127, 2000.
- [Yes76] M Yeston. *The stratification of musical rhythm*. New Haven, Conn: Yale University Press, 1976.